

# **Triboelectric Energy Generation**

**April 25, 2024**

**Joel Eckstrom**

**Flint Eller**

**Keston Holohan**

**Yashas Honnavalli**

**Ethan Shaw**

**Prof. Pratap Rao**, Primary Advisor

**Prof. Gregory Noetscher**, Project Co-Sponsor

**Justin Silva**, Project Co-Sponsor U.S. Army DEVCOM Soldier Center

Worcester Polytechnic Institute of  
Technology



US Army DEVCOM Soldier Center



## **Abstract**

In collaboration with the U.S. Army Combat Capabilities Development Command (DEVCOM) Soldier Center, this project seeks to investigate and improve upon the capabilities of triboelectric nanogenerators (TENGs) for future military use. TENGs passively produce electrical energy through the dynamic interaction of materials in the triboelectric series. This project focused on maximizing the power output of TENG designs through the selection of optimal triboelectric materials and the modification of contact surfaces. These TENGs were designed to be integrated into different types of military equipment such as boots, tents, and parachutes. The research of materials, textures, and contact modes improved the power output of the prototypes and informed the iterative development cycle. This project produced two final prototype designs, one boot-integrated and one wind-activated. These prototypes are capable of producing  $3.709 \times 10^{-6}$  Joules/step and 0.0002531 Joules/second, respectively, the latter providing enough power for running small sensors.

# Acknowledgments

This project was made possible by the contribution and support of others. The following individuals lent us their time, their expertise, and their advice.

- We would like to thank professors Pratap Rao and Gregory Noetscher, who served as advisors for this Major Qualifying Project. Their support, guidance, and feedback over the past year have been greatly appreciated. We also appreciate the access to and use of their lab space and materials in Atwater Kent.
- We would like to acknowledge the contributions of previous MQP teams who worked on this project. These teams consist of Aaron McCutcheon, Nancy Nguyen, Eric Scholz, Rebecca Serven, Spencer Tess (2020-2021), Peter Fagerholm, Kaleigh Hess, Caitlin Kean, Kyle Postans, Joshua Woodruff (2021-2022), Andrew Ferrecchia, Robert Hyers, Kyle MacPherson, and Katherine Morissette (2022-2023). Their research and effort over the past three years provided our team with the groundwork we needed to succeed.
- We would also like to thank the U.S. Army Combat Capabilities Development Command (DEVCOM) and the U.S. Army Natick Soldier Systems Center (NSSC), our sponsors, for providing our team with the opportunity funds to work on this project. In particular, we would like to thank Justin Silvia for his support and insight throughout the duration of the year.
- Additionally, we would like to thank Mrs. Barbara Furman, the Administrative Assistant of the Materials and Mechanical Engineering department, who assisted us in obtaining the necessary materials and funding for this project.
- Finally, we would like to thank Worcester Polytechnic Institute for the opportunity, spaces, and resources we used during this Major Qualifying Project

# Table of Contents

<b>Abstract.....</b>	<b>2</b>
<b>Acknowledgments.....</b>	<b>3</b>
<b>Table of Contents.....</b>	<b>4</b>
<b>List of Figures.....</b>	<b>8</b>
<b>List of Tables.....</b>	<b>12</b>
<b>Authorship.....</b>	<b>13</b>
<b>Chapter 1: Introduction.....</b>	<b>16</b>
<b>Chapter 2: Background.....</b>	<b>18</b>
2.1 TENG Introduction.....	18
2.1.1 First Instances.....	18
2.1.2 Harvesting in the Modern Era.....	18
2.2 How Triboelectricity Works.....	19
2.2.1 Physics of Triboelectricity.....	19
2.2.2 How TENGs work.....	19
2.2.3 Power Output.....	21
2.2.4 Motion.....	21
2.2.5 Configuration of TENGs.....	22
2.2.6 TENG Materials.....	23
2.2.7 Electrodes.....	25
2.2.8 Energy.....	27
2.3 Military Involvement.....	27
2.3.1 Military Interest.....	27
2.3.2 Current Military Systems.....	28
2.3.3 Military Potential.....	28
2.4 TENG Placement.....	29
2.4.1 Sock / Insole.....	29
2.4.2 Split Sole.....	30
2.4.3 Heel and Toe Configuration.....	31
2.4.4 Rucksack Placement.....	32
2.4.5 Parachute Placement.....	33
2.5 Surface Area Modifications.....	34
2.5.1 Purpose of Surface Area Modifications.....	34
2.5.2 Types of Surface Area Modifications.....	34
2.6 Previous Research.....	36

2.6.1 2020-2021 MQP.....	36
2.6.2 2021-2022 MQP.....	36
2.6.3 2022-2023 MQP.....	36
<b>Chapter 3: Objectives.....</b>	<b>38</b>
3.1 Higher Power.....	38
3.2 Ergonomics.....	39
3.2.1 Durability.....	39
3.2.2 Comfortability.....	39
3.3 Usefulness.....	40
3.3.1 Ease of Manufacturing.....	40
3.3.2 Cost.....	40
<b>Chapter 4: Circuit Design.....</b>	<b>41</b>
4.1 Load Circuit.....	41
4.2 Single Diode.....	42
4.3 Diode Bridge.....	44
4.4 Other Rectifying Circuits.....	46
<b>Chapter 5: Testing Methodology.....</b>	<b>48</b>
5.1 Drop Testing.....	48
5.1.1 Testing Procedure.....	49
5.1.2 Initial Testing Apparatus.....	49
5.1.3 Updated Testing Apparatus.....	50
5.2 Quantification of Results.....	51
5.2.1 Equipment Used.....	52
5.2.2 Open Circuit Voltage Test.....	55
5.2.3 Load Voltage Test.....	56
5.2.4 Ohm's Law to Understand Current and Power.....	57
<b>Chapter 6: TENG Material Testing.....</b>	<b>59</b>
6.1 Material Review.....	59
6.2 Material Testing.....	66
6.2.1 Testing Procedure: Round 1.....	66
6.2.2 Results: Round 1.....	67
6.2.3 Testing Procedure: Round 2.....	69
6.2.4 Results: Round 2.....	70
6.2.5 Testing Procedure: Round 3.....	73
6.2.6 Results: Round 3.....	73
6.2.7 Final Material Selection.....	75

<b>Chapter 7: Boot Prototype.....</b>	<b>76</b>
7.1 Boot Integration.....	76
7.1.1 TENG Design.....	76
7.2 Texturing.....	78
7.2.1 Texturing Methodology.....	78
7.2.2 Testing Methodology.....	79
7.2.3 Results.....	80
7.3 Springs.....	84
7.4 Final Iteration.....	86
<b>Chapter 8: Wind Prototype.....</b>	<b>88</b>
8.1 Wind TENG Introduction.....	88
8.2 Experimental Setup.....	88
8.2.1 Testing Procedure and Design.....	89
8.3 Testing Results.....	89
8.3.2 Capacitor Testing.....	92
8.3.3 Material Structure Testing.....	94
8.3.5 Freestanding Mode Testing.....	98
8.3.6 Wind Speed Testing.....	101
8.4 Final Design and Future Work.....	101
<b>Chapter 9: Applications.....</b>	<b>102</b>
9.1 Uses for Power.....	102
9.1.1 Battery Charging.....	102
9.1.2 Passive Sensors.....	103
9.2 Energy Comparison.....	106
9.3 Potential Military Uses.....	108
9.3.1 Parachute.....	108
9.3.2 Soft Structures.....	109
9.3.3 Patrolling.....	109
<b>Chapter 10: Broader Impact.....</b>	<b>111</b>
10.1 Engineering Ethics.....	111
10.2 Environmental Impacts.....	111
10.3 Economic Impacts.....	112
10.4 Societal and Technological Impacts.....	112
<b>Chapter 11: Conclusion.....</b>	<b>113</b>
11.1 TENG Improvements.....	113
11.1.1 Texturing.....	113

11.1.2 Components.....	114
11.1.3 Building Off of Feedback.....	114
11.2 Continuation.....	115
11.2.1 Integration with Soldier Equipment.....	115
11.2.2 PCB.....	115
11.2.3 Flexible Circuitry.....	116
11.2.4 Power Output.....	116
11.2.5 Sliding Testing.....	117
11.2.6 Surface Modifications.....	117
11.3 Final Remarks.....	118
<b>Bibliography.....</b>	<b>119</b>
<b>Appendix A: Supplemental Material Testing Graphs.....</b>	<b>123</b>

## List of Figures

Figure 1. Soldier Rucking Which is One Option for Generating Power [1].....	17
Figure 2. Soldier Parachuting Which is Another Option for Generating Power [2].....	17
Figure 3. Both sides of a basic TENG [3].....	20
Figure 4. Single electrode TENG structure [4].....	22
Figure 5. Freestanding TENG structure [5].....	23
Figure 6. Sock/Insole Boot TENG design [11].....	30
Figure 7. Split Sole Boot TENG design [12].....	31
Figure 8. Heel Toe Boot TENG design [13].....	32
Figure 9. Rucksack TENG placement [14].....	33
Figure 10. Examples of micro-texturing patterns, including lines (A), cubes (B) and pyramids (C) [18].....	35
Figure 11. The TENG circuit connected directly to the oscilloscope.....	42
Figure 12. The TENG circuit connected to a resistor.....	42
Figure 13. A visual of the semiconductor materials that make up a diode [19].....	42
Figure 14. A sine wave before being rectified [20].....	43
Figure 15. The output of the sine wave going through the circuit [21].....	43
Figure 17. The diode bridge [22].....	44
Figure 18. The output of a sine wave before and after rectification [23].....	44
Figure 19. The diode bridge with the colored sections being which diodes are active [24].....	45
Figure 20. The diode bridge with the colored sections being which diodes are active [25].....	45
Figure 21. The topology of a transformer [26].....	47
Figure 22. An example of the drop test setup.....	48
Figure 23. Structure of the TENGs used in the drop testing [27].....	49
Figure 24. The initial drop test apparatus.....	50
Figure 25. SolidWorks assembly of the updated drop testing apparatus.....	51
Figure 26. The updated drop testing apparatus.....	51
Figure 27. The DMM used in experiments [29].....	52
Figure 28. The way to measure both voltage and current [30].....	53
Figure 29. The DMM interface while measuring both voltage and current [31].....	53
Figure 30. The computer program view of the DMM.....	54
Figure 31. The oscilloscope used for experiments [32].....	55
Figure 32. The TENG materials connected to the oscilloscope through an open circuit.....	56
Figure 33. The TENG materials connected to the oscilloscope through a resistor.....	57
Figure 34. A close up of the circuit.....	57

Figure 36. PDMS from second round testing.....	62
Figure 37. Silicon rubber from second round testing.....	63
Figure 38. Nylon from second round testing.....	64
Figure 39. Graphene from second round testing.....	65
Figure 40. Polyurethane foam from second round testing.....	66
Figure 41. Graph comparing the TENGs made from PDMS during the first round of testing.....	68
Figure 42. Graph comparing the TENGs made from PTFE during the first round of testing.....	68
Figure 43. Graph comparing the TENGs made from silicone rubber during the first round of testing.....	69
Figure 44. Graph comparing the TENGs made from PDMS during the second round of testing.....	71
Figure 45. Graph comparing the TENGs made from PTFE during the second round of testing.....	71
Figure 46. Graph comparing the TENGs made from silicone rubber during the second round of testing.....	72
Figure 47. Voltage, current, and power produced by a PDMS TENG at different resistances.....	74
Figure 48. Voltage, current, and power produced by a Silicone Rubber TENG at different resistances.....	74
Figure 49. Solidworks model of the insole shape used to produce the boot-integrated TENG.....	77
Figure 50. The wooden pattern and examples of the insole shaped TENGs.....	77
Figure 51. The tools used to create the insole textures. From left to right, top to bottom, the tools are the knife, the sandpaper, the dremel wire brush, the clay cutter, and the cheese grater.....	79
Figure 52. The textured insole. From left to right, the insoles are the deep score, the shallow score, the dremel, the clay cutter, and the cheese grater textures.....	79
Figure 53. Graph comparing the voltage produced by different step counts in the single diode configuration across a 0.1 $\mu$ F capacitor.....	81
Figure 55. Graph comparing the voltage produced by the different textured insoles.....	83
Figure 56. Graph comparing the maximum voltage produced by the different textured insoles.....	83
Figure 57. Conical springs used in attempts to increase TENG power output.....	85
Figure 58. The final circuit.....	87
Figure 59. Wind TENG Testing setup.....	89
Figure 60. Wind Testing circuit setup.....	90
Figure 61. Baseline structure for the TENG (flapper).....	93
Figure 62. Two stranded structured TENG (flapper).....	94
Figure 63. Three slit structured TENG (flapper).....	95
Figure 64. 4 stranded structured TENG (flapper).....	96
Figure 66. Pinned tailed structured TENG (flapper).....	97
Figure 67. Diagram of freestanding mode wind TENG.....	98
Figure 68. Freestanding mode structured wind TENG.....	99

Figure 69. Graph comparison of TENG structured test results.....	100
Figure 70. The circuit diagram for an accelerometer [33].....	104
Figure 71. The specifications to run the accelerometer sensor [34].....	104
Figure 72. The ECG sensor and the data sheet for it [35].....	105
Figure 74. The specifications to run the temperature sensor [37].....	106
Figure 75. The specifications to run the UV sensor [38].....	106
Figure 76. A diagram of how piezoelectricity works [39].....	108
Figure 77. An example of what a PCB looks like [40].....	116
Figure A1. Graph showing the open circuit voltage of the TENG made from PDMS and graphene during the first round of testing.....	123
Figure A2. Graph showing the open circuit voltage of the TENG made from PDMS and polyurethane foam during the first round of testing.....	123
Figure A3. Graph showing the open circuit voltage of the TENG made from PDMS and nylon during the first round of testing.....	124
Figure A4. Graph showing the open circuit voltage of the TENG made from PTFE and graphene during the first round of testing.....	124
Figure A5. Graph showing the open circuit voltage of the TENG made from PTFE and polyurethane foam during the first round of testing.....	125
Figure A6. Graph showing the open circuit voltage of the TENG made from PTFE and nylon during the first round of testing.....	125
Figure A7. Graph showing the open circuit voltage of the TENG made from silicone rubber and graphene during the first round of testing.....	126
Figure A8. Graph showing the open circuit voltage of the TENG made from silicone rubber and polyurethane foam during the first round of testing.....	126
Figure A9. Graph showing the open circuit voltage of the TENG made from silicone rubber and nylon during the first round of testing.....	127
Figure A10. Graph showing the open circuit voltage of the TENG made from PDMS and graphene during the second round of testing.....	127
Figure A11. Graph showing the open circuit voltage of the TENG made from PDMS and polyurethane foam during the second round of testing.....	128
Figure A12. Graph showing the open circuit voltage of the TENG made from PDMS and nylon during the second round of testing.....	128
Figure A13. Graph showing the open circuit voltage of the TENG made from PTFE and graphene during the second round of testing.....	129
Figure A14. Graph showing the open circuit voltage of the TENG made from PTFE and polyurethane foam during the second round of testing.....	129
Figure A15. Graph showing the open circuit voltage of the TENG made from PTFE and nylon during the second round of testing.....	130
Figure A16. Graph showing the open circuit voltage of the TENG made from silicone rubber and	

graphene during the second round of testing.....	130
Figure A17. Graph showing the open circuit voltage of the TENG made from silicone rubber and polyurethane foam during the second round of testing.....	131
Figure A18. Graph showing the open circuit voltage of the TENG made from silicone rubber and nylon during the second round of testing.....	131
Figure A19. Voltage produced by a PDMS TENG at 510 $\Omega$ resistance.....	132
Figure A20. Voltage produced by a PDMS TENG at 1000 $\Omega$ resistance.....	132
Figure A21. Voltage produced by a PDMS TENG at 5100 $\Omega$ resistance.....	132
Figure A22. Voltage produced by a PDMS TENG at 10000 $\Omega$ resistance.....	133
Figure A23. Voltage produced by a silicone rubber TENG at 100 $\Omega$ resistance.....	133
Figure A24. Voltage produced by a silicone rubber TENG at 510 $\Omega$ resistance.....	133
Figure A25. Voltage produced by a silicone rubber TENG at 1000 $\Omega$ resistance.....	134
Figure A26. Voltage produced by a silicone rubber TENG at 5100 $\Omega$ resistance.....	134
Figure A27 Voltage produced by a silicone rubber TENG at 10000 $\Omega$ resistance.....	135

## List of Tables

Table 1. Material selection decision matrix.....	24
Table 2. Electrode type selection matrix.....	26
Table 3. Material selection decision matrix.....	60
Table 4. Table displaying the average voltages and peak to peak voltages found during the first round of testing.....	67
Table 5. Table displaying the average voltages and peak to peak voltages found during the second round of testing.....	70
Table 6. Table displaying the voltage, potential energy, and potential energy/step produced by different step counts in the single diode configuration across a 0.1 $\mu\text{F}$ capacitor.....	82
Table 7. A table comparing the voltage, potential energy, and potential energy/step produced by the different textured insoles.....	84
Table 8. The table for a 1 $\mu\text{F}$ capacitor prototype for energy per step.....	86
Table 9. The table for the final prototype for energy per step.....	86
Table 10. Single and Double Open circuit materials testing results.....	91
Table 11. The results of the 0.1 $\mu\text{F}$ capacitor test.....	93
Table 12. The results of the 1.0 $\mu\text{F}$ capacitor test.....	93
Table 13. The results of the 0.5 $\mu\text{F}$ capacitor test.....	93
Table 14. Results of Pinned Tailed structured TENG.....	98
Table 15. Chart comparison of TENG structured test results.....	100

## Authorship

Section	Author	Editor
Abstract	JE	ES
Acknowledgments	JE	ES
Chapter 1: Introduction	KH	JE
<b>Chapter 2: Background</b>		
2.1 TENG Introduction	KH	ES
2.2 How Triboelectricity Works	ES, FE	ES
2.3 Military Involvement	JE	JE
2.4 TENG Placement	ES	YH
2.5 Surface Area Modifications	JE	JE
2.6 Previous Research	KH	ES
<b>Chapter 3: Objectives</b>		
3.1 Higher Power	YH	ES
3.2 Ergonomics	YH	ES
3.3 Usefulness	ES	YH
<b>Chapter 4: Circuit Design</b>		
4.1 Load Circuit	YH	ES
4.2 Single Diode	YH	ES

4.3 Diode Bridge	ES	JE
4.4 Other Rectifying Circuits	ES	JE
<b>Chapter 5: Testing Methodology</b>		
5.1 Drop Testing	JE	KH
5.2 Quantification of Results	ES	JE
<b>Chapter 6: TENG Material Testing</b>		
6.1 Material Review	KH	JE
6.2 Material Testing	JE	KH
<b>Chapter 7: Boot Prototype</b>		
7.1 Boot Integration	JE	KH
7.2 Texturing	JE	KH
7.3 Springs	KH	JE
7.4 Final Iteration	ES	KH
<b>Chapter 8: Wind Prototype</b>		
8.1 Wind TENG Introduction	YH, FE	YH, FE
8.2 Experimental Setup	YH, FE	YH, FE
8.3 Testing Results	YH, FE	YH, FE
8.4 Final Design and Future Work	YH, FE	YH, FE
<b>Chapter 9: Applications</b>		

9.1 Uses For Power	ES	KH
9.2 Energy Comparison	ES	KH
9.3 Potential Military Uses	KH	JE
<b>Chapter 10: Broader Impact</b>		
10.1 Engineering Ethics	KH	FE
10.2 Environmental Impacts	FE	KH
10.3 Economic Impacts	FE	KH
10.4 Societal and Technological Impacts	FE	KH
<b>Chapter 11: Conclusion</b>		
11.1 TENG Improvements	ES, JE	JE
11.2 Continuation	ES, JE	JE
11.3 Final Remarks	KH	JE

# Chapter 1: Introduction

As the human race pursues more technological advancement, the need for a reliable yet sustainable source of energy only grows. In recent years, the weaknesses of non-renewable energy sources have become clear. They are finite, harmful to the environment, and contribute towards the degradation of human safety. Researchers around the world have studied ways of harnessing renewable energy as a more reliable energy resource. From using the sun's energy to converting wind into power, even reaching as far as possible fusion reactors, the world has stopped at nothing to pave the way for a cleaner and more efficient future of energy.

In 2012, Professor Zhong Lin Wang of Georgia Institute of Technology became the first person in the world to harvest mechanical energy using a triboelectric nanogenerator, or a TENG. Professor Wang and his team discovered that by creating a charge potential between oppositely-charged materials, the flow of electrons can be captured by an electrode and converted into electricity. Movement, whether it is in the form of sliding materials against each other or vertical compression, where the materials are separated by a vertical distance and then brought back together, are both viable methods to capture as much energy as possible. This makes this method of harvesting energy incredibly versatile, being able to be used in multiple different applications. Any form of motion, whether it comes from wind, kinetic, or another energy source can be harvested and turned into a reliable source of electrostatic energy. The separation of the materials is the key component, as the separation of the charges is what generates static electricity. It can collect energy from motion that didn't used to be a viable source of energy. This technology creates an opportunity for a countless number of energy sources around the globe.

With support from the U.S. Army Combat Capabilities Development Command (DEVCOM) Soldier Center, this project's goal is to further investigate the capabilities and potential of TENGs and their use in the future of the US Army. We aim to create a renewable source of energy that can be used in multiple different applications for soldiers to be able to rely on. The ability to power both existing technology and future technology is crucial to supporting the success of the US Army, whatever its needs may be.



Figure 1. Soldier Rucking Which is One Option for Generating Power [1].



Figure 2. Soldier Parachuting Which is Another Option for Generating Power [2].

# Chapter 2: Background

## 2.1 TENG Introduction

Triboelectric nanogenerators were first created in 2012 in order to harvest mechanical energy from various activities. In terms of renewable energy, TENGs have unlimited potential in their future development. Any activity involving mechanical energy, such as walking, air flowing past a material, or friction between two surfaces has the opportunity to be harvested. The process of exactly how this works will be discussed in this chapter along with how we can use this knowledge to build a better TENG.

### 2.1.1 First Instances

At first when Professor Zhong Lin Wang and his team of engineers created and applied a triboelectric nanogenerator, it was only able to harness small scale, low frequency mechanical energy. However, in recent years of study and research, the TENG has been transformed into a reliable generator that can be placed in a variety of scenarios. For instance, TENGs have been used to harvest energy from waves, wind, mechanical vibration, and human motion. The TENG is known for being highly efficient in energy harvesting, even at low levels of operation frequency. The construction of a TENG is both low cost, and the required materials can vary for applications, with most materials being readily available.

### 2.1.2 Harvesting in the Modern Era

As previously mentioned, TENGs are among the most versatile and reliable sources of energy harvesting. In 2018, it was recorded that just 6 years after TENGs were invented, there were 195 patents, and that number has not stopped increasing. Previous MQP groups have studied using TENGs in places outside the human body. Parachutes have been one application, or placing TENGs on the top of tents, both placements harvesting wind energy. When parachuting in the air, the wind speeds are extremely high, and since TENGs rely on the separation and contact of the materials, doing this at high wind speeds means that there will be a lot of contact being made, allowing us to theoretically harvest more energy. Recently, engineers

have developed a method of energy collection using waves. TENGs can be used in any location where there is a source of friction, meaning the potential for energy harvesting is unlimited.

## 2.2 How Triboelectricity Works

This section will focus on understanding triboelectricity, and how we can use this understanding to benefit in this project. Additionally understanding material properties, and how we can engineer them to work better for our scenario.

### 2.2.1 Physics of Triboelectricity

In looking for a way to create electricity from motion, we must consider the movement of electrons. The movement of electrons drives electric potential and therefore electricity. A more basic way of thinking about triboelectricity is contact electrification which is electrons transferring surfaces when two opposite electric potential surfaces come in contact. For example, when static electricity is built up on your hand and you touch a doorknob, contact electrification means that the charge is transferred on touch. Using this phenomenon, our goal is to create a way of transferring electrons by repeated contact of materials to generate electricity.

### 2.2.2 How TENGs work

A TENG is a generator built specifically to induce the transfer of electrons when touched or moved around. The problem is that each time the electrons are transferred, only an extremely small electric potential is generated. To increase the efficiency and overall power output of these devices, there are a few variables we can control. One way we can do this is by choosing the optimal materials. The amount of charge a TENG is able to transfer largely depends on the charge of the material used. Different materials have different electron affinities, which means they tend to either collect or give away electrons with varying strengths. By carefully choosing two materials on opposite sides of the spectrum, we can increase the amount of charge being transferred with each contact. After the electrons have transferred surfaces, they need to continue to be moved throughout the circuit. That is why in a TENG's structure, the triboelectric materials have an electrode on the back which gathers all the new charges and feeds them into a wire to

complete the circuit and finally harvest the electricity. An example of the layers can be seen on the next page in Figure 3.

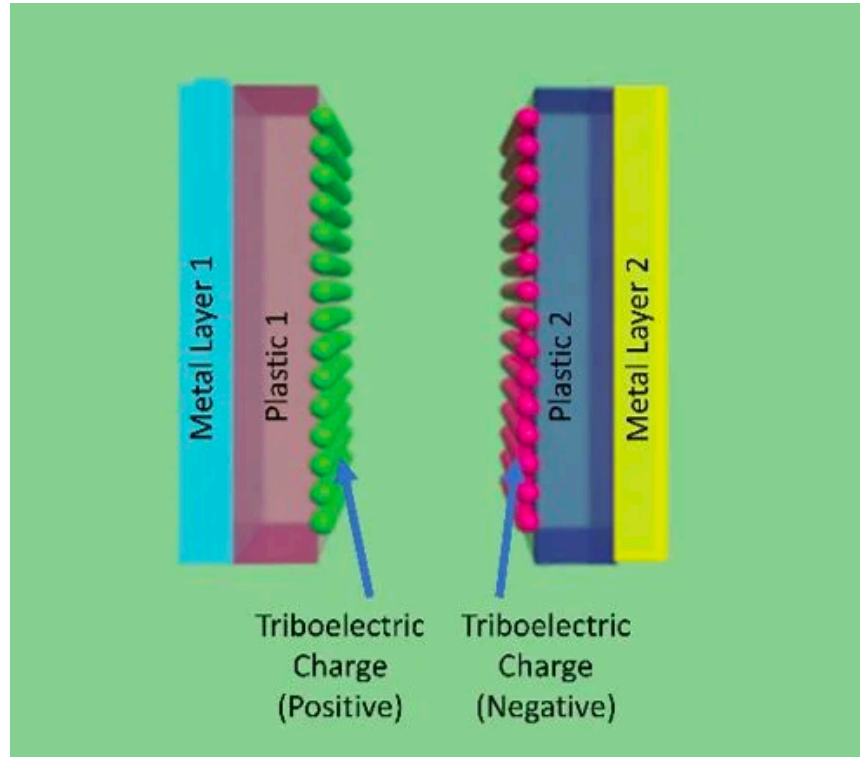


Figure 3. Both sides of a basic TENG [3].

Now that a basic understanding of a TENG's structure has been solidified, we will look mathematically at what variables we can influence to increase the voltage of our TENG. A system that periodically charges up and then discharges can be modeled as a capacitor. A capacitor is governed by the equations:

$$C = q/V$$

$$C = \epsilon_0 A/d$$

These result in an equation for voltage as follows:

$$V = qd/\epsilon_0 A$$

This tells us that by maximizing our charge differential ( $q$ ) and separation distance between the layers ( $d$ ) we can increase the voltage ( $V$ ). We will attempt to use this information in designing our TENG to get the best results possible.

### 2.2.3 Power Output

Ever since its inception, more efficient and higher power output has been the primary goal of TENG research. A critical step in this research is accurately and effectively benchmarking all types of TENGs. While benchmarking TENGs is notoriously difficult there are some ways to do it. Power density is often the easiest way, but to do this you need an accurate power measurement. Energy stored in a capacitor is given by the first equation below, where C is the capacitance and V is the voltage:

$$E = 0.5CV^2$$

$$P = ET$$

To get power, if applicable, energy can be multiplied by time as seen in the second equation above. To be able to power passive sensors, we need the energy output of the system to be equal to or higher than the required wattage to run the sensor. However, the power that the TENG creates cannot exceed the limitations of the sensors, because this would cause damage to the sensor, and most likely give inaccurate readings, overheat, or break. The sensor with the most desire to see from the engineers at the soldier center is an accelerometer, which tracks acceleration. This is important to track movement, steps taken, posture, and for detecting falls. The specifications to run an average accelerometer are 2V to 3.6V for the operating voltage, and the supply current is between 100 $\mu$ A to 300 $\mu$ A. This gives an estimate for power consumption to be around 0.2mW to operate this sensor. As long as the power generated by the TENG is greater than the necessary power, the values chosen for the resistor and the capacitor will be able to alter the voltage and current to reach these values.

### 2.2.4 Motion

There are actually two types of TENGs that use very different types of motion to transfer electrons. The first is the vertical separation method. This method involves lifting the two layers away from each other so there is an air gap between them, and then bringing them back together. The force applied when they are brought together should be maximized to increase the voltage. The second method is called the horizontal sliding method where the materials slide past each

other horizontally. There is no need to separate them; they simply slide past and overlap each other. With the horizontal sliding method, the sliding speed should be maximized to increase voltage. These two types of motion make TENGs very versatile and gives us the ability to engineer one to our specific needs. This could mean different parts of a system might use different TENGs based on their type of motion.

### 2.2.5 Configuration of TENGs

Although there are two main methods for TENGs to fall under, lifting and sliding, there are lots of types of TENGs with different configurations. Variables like type of motion (sliding vs. lifting), electrode placement, circuitry choices, number of layers, and more can all be explored to create new types of TENGs. Some of the more unique types of TENGs are single electrode and free standing. A single electrode TENG only uses one electrode and one triboelectric material, it can be seen in Figure 4. The charge is built up in the electrode and the other side is grounded which means there is a charge differential. The free standing TENG or FTENG is where there is one free standing, stationary layer in the middle and two moveable layers above and below it. These layers could be any order of triboelectric material and electrode and can be seen on the next page in Figure 5. These are a couple of types of TENGs that use slightly different setups. By carefully examining the aspects of different types of TENGs, we can find the most optimal version for our use.

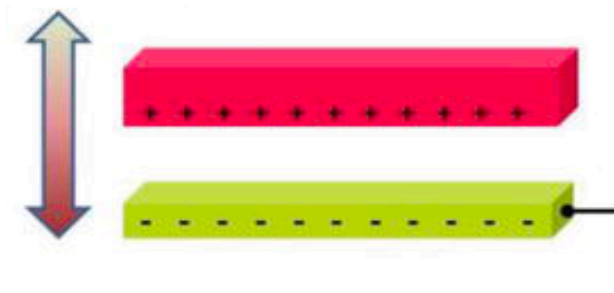


Figure 4. Single electrode TENG structure [4].

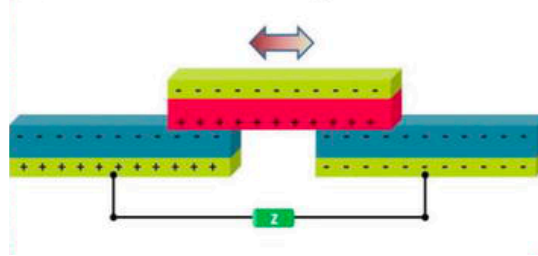


Figure 5. Freestanding TENG structure [5].

### 2.2.6 TENG Materials

The type of material used in a TENG has been proven to be a critical factor in the amount of power output a TENG can produce. That is why our main focus was on finding materials with the highest difference in electronegativity. For instance, kapton and PTFE are two great matchups, because of the difference in electronegativity. Durability, cost of materials, manufacturability, and availability are factors we are aware of, but our main focus for our group is to get the most amount of power possible. Table 1 shows our rating of how well each material scores in four categories. The higher the number the better the score. The negatively charged materials have a negative sign next to them, and the positive materials have a positive sign.

Materials	Manufacturability	Availability	Cost (1=High cost)	Charge potential	Total Score
PTFE(-)*	9	9	4	9	31
PDMS(-)*	9	9	5	8	31
PET(-)	9	8	4	9	30
Teflon(-)	5	7	7	9	28
Silicone Rubber(-)*	7	9	7	10	33
Rayon(-)	6	7	6	8	27
Nylon (+)*	8	10	9	7	34
Kapton (+)	8	8	7	7	30
Graphene(+)*	7	8	8	9	32
Polyurethane Foam (+)*	6	9	8	8	31

Table 1. Material selection decision matrix.

The score for each material is based out of 40, 40 being the best possible score for a material to achieve. Based on this decision matrix, we can conclude that the top materials for us

to focus on would be silicone rubber, nylon, graphene, PTFE, and PDMS. Once we begin testing, we are going to primarily use these materials, since they have the most potential out of all the materials we have looked at.

### 2.2.7 Electrodes

Electrodes are a basic component in energy harvesting to convert energy to electricity. It acts as a conductor between a metal and a nonmetal. In this case, as well as many others, the metal part is a wire, and the nonmetal part is whatever material that we decide to do testing on, as talked about in section 2.2.5. When choosing an electrode, there are many factors that come into play. Below is a chart of the different options that were looked at when choosing electrodes.

Electrode Materials	Conductivity (x4)	Electronegativity (x5)	Price (x2)	Durability (x1)	Totals
Aluminum	9	10	9	8	112
Copper	10	7	10	8	103
Silver	10	7	6	6	93
Stainless Steel	5	8	6	10	82
Nickel	5	8	8	10	86
Polyacetylene	2	5	4	4	45

Table 2. Electrode type selection matrix.

In this table the categories are ranked based on four categories: conductivity, electronegativity, price, and durability. Electronegativity is the most important for an electrode to have so its score is considered the most heavily. Conductiveness is the second most important category, followed by price, and then durability. Electronegativity is a crucial factor, as it determines the voltage potential for maximum power output as well as dictates how much electrons move through the material. As for Conductivity, the higher the value, the better the flow of charge is. This chart helps us decide which electrodes are most important to test, even though most likely, all will be tested.

### 2.2.8 Energy

The triboelectric materials will be layered with electrodes, which is how energy transforms from mechanical energy to electrical energy. The placement of the electrodes is talked about later in section 2.5. After being transformed, the negative charged electrode will begin to move the electrons towards the positive charged electrode. However, before it reaches the positive electrode, the electrons travel through the circuitry that will be designed to efficiently rectify and smooth out the signal. This is where the power travels into the sensors, to turn on and then keep the sensors running. This process will continue as long as there is constant movement or friction applied to the TENG. The circuitry will make use of resistors, capacitors, and diodes, to smooth out the signal to a constant output voltage. The specifics of the circuitry will be talked about in Appendix A.

### 2.3 Military Involvement

The DEVCOM Soldier Center in Natick, Massachusetts has sponsored this project for the past several years. Their input and interest represents the United States Army as a whole. Therefore, it is important to understand how the TENGs will fit into the current dismounted soldier power ecosystem.

#### 2.3.1 Military Interest

In the 20th and 21st centuries, the United States Army has grown to rely on powered devices such as radios, night vision goggles (NVGs), advanced combat optical gunsights (ACOGs), and sensors. These devices give soldiers an edge on the battlefield, but they also come with a logistical price. Despite efforts at standardization, many of the devices in service today rely on different power sources. A soldier's NVGs and ACOGs, for example, might run on replaceable lithium ion AA batteries, while most tactical radio systems built in batteries that must be recharged by outside power sources. This means that soldiers must carry pounds of extra batteries, power supplies, and chargers while on patrol. On particularly long operations, batteries must be included in resupply considerations, along with other essentials such as food, water, and

fuel. In order to simplify this burden, the Army (and other branches of the military) has a vested interest in passive energy generation, harvesting, and storage.

### 2.3.2 Current Military Systems

The military uses many different batteries, but the most common are commercial lithium ion batteries of various sizes, device integrated batteries that vary by manufacturer and device, and the conformal wearable battery (CWB). The CWB is a flexible pack of lithium ion batteries 7.6” wide, 8.7” tall, and 0.7” thick that can be worn behind a plate or fighting load carrier. With a 148Wh power capacity, the CWB acts as a lightweight, flexible, and durable battery that integrates into many of the programs and systems used by the modern day soldier. These systems include the Nett Warrior (NW) system and the Squad Power Manager (SPM) [6].

The NW system is a tactical and situational awareness kit utilized by many of today’s soldiers. The system includes an end user device (EUD), typically a phone, several sensors, and software systems. NW links individual soldiers into a larger tactical network that allows for enhanced tactical capabilities. The whole system runs off of a CWB [7].

The SPM is another critical part of the Army’s power infrastructure. The SPM works as an intermediary between many of the Army’s systems. The SPM can draw power from or supply power over 200 types of vehicles, batteries, solar blankets and panels, and other systems to lower the logistical burden of the Army’s many powered systems. With 6 ports, the SPM can simultaneously charge and deliver power across multiple systems, including radios, GPS, phones, tablets, laptops, power tools, batteries like the CWB, and other pieces of equipment [8].

### 2.3.3 Military Potential

Part of the issue with the current power infrastructure is that all of these various batteries must be actively charged or replaced on a regular basis. TENGs, on the other hand, offer a passive energy option. In a recent discussion about the potential of TENGs, representatives from DEVCOM Soldier Center stated that many sensors and other powered systems are excluded from fielded items because of their reliance on batteries [9]. If a soldier forgets to charge or change a battery, it could lead to a loss of combat effectiveness and hinder planning and

operation success. With passive power generation integrated into equipment, this risk could be mitigated, allowing for enhanced soldier capabilities.

Some of the examples discussed included passive sensors integrated into equipment like parachutes or boots. Altimeters, accelerometers, thermometers, heart rate sensors, and other sensors would give valuable insights into equipment and soldier health, leading to decreases in equipment failure, dehydration, and other debilitating issues. Linking sensor systems to the NW system would make this information available to both soldiers in the field and commanders in tactical operations centers, leading to enhanced planning capabilities. In addition, making the TENGs compatible with the SPM system would allow it to power other systems, such as lithium ion batteries and the CWB.

Equipment like parachutes could provide shorter bursts of high intensity production, as wind causes large amounts of movement in both chute material and the straps connecting the soldier to the chute. High altitude drops last for as long as 45 minutes, leading to consistent power generation. Including TENGs in boots and rucksacks, however, would provide much lower production over a longer period of time. Patrols utilizing this type of equipment can last for weeks or even months, with each step passively generating power [10].

## 2.4 TENG Placement

The placement of our TENG will be towards the end of the project, but it is still one of the most important aspects. Once we have our TENG that can give a constant high power output, the next step is to manufacture a way to implement that into a working prototype. That means that the placement of our TENG is vital to make sure that the power output stays high, as well as the surfaces be comfortable and safe. The options that have been researched are talked about in the following subsections.

### 2.4.1 Sock / Insole

This option has the TENG materials that were talked about earlier as the Sock and the Insole inside of the boot. The negative material would be the sole while the positive material would be the sock. Below is a diagram of what those materials would look like.



Figure 6. Sock/Insole Boot TENG design [11].

The electrode touching the electropositive material would be a part of the sock. This design would have the best contact, but there are many other problems with this design. This includes easier damage to rain or other weather, as well as having to have a wire attached to a sock.

#### 2.4.2 Split Sole

This design has the sole of the shoe in 2 parts, one half touches just the outsole and the other half would touch the foot or sock. This option has the TENG material as both halves of the sole, the direction can be either the positive or negative material on top. Below is a diagram that shows potentially what that could look like.

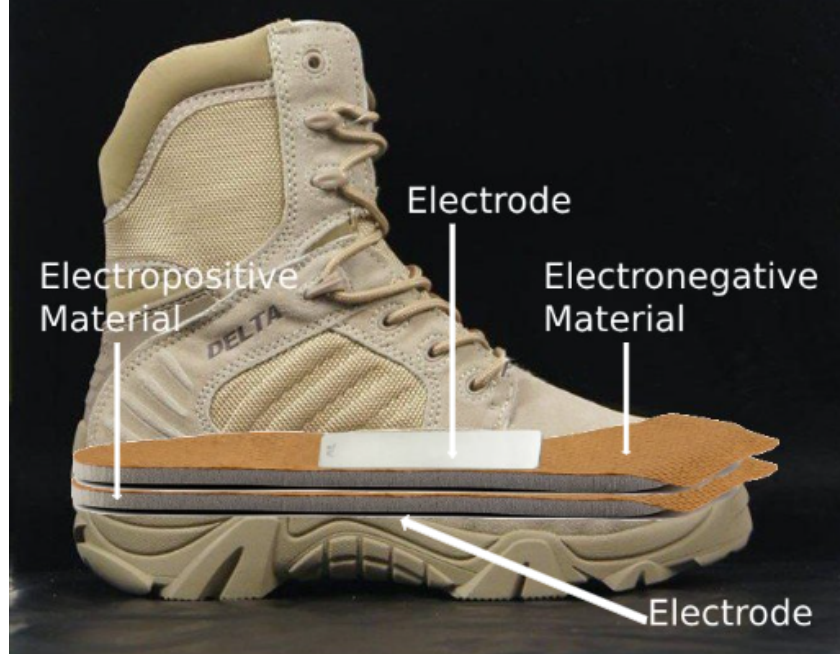


Figure 7. Split Sole Boot TENG design [12].

This option has the most data from other years, so it has been proven to work. However in the tests, it has its drawbacks, as there would be less friction than the other options. Meaning less power.

#### 2.4.3 Heel and Toe Configuration

This design uses a different type of motion than the previous two designs. This one uses sliding motion that was talked about more in depth in section 2.2.4. The electronegative triboelectric material, rather than being on the sole, is in the front and back of the shoe where the heel and toe would make contact. This sock in this case would be electropositive material. The electrodes would be between the boot and the electronegative material; below is a diagram that would show how this would look.



Figure 8. Heel Toe Boot TENG design [13].

This option makes use of a different motion than the rest, which has less research based on it. However the benefits of this would be an increase in friction because of the sliding nature, and a possible negative is there is much less surface area, so less places to get contact.

#### 2.4.4 Rucksack Placement

This design uses the sliding motion similar to the design talked about in section 2.5.3, however the placement of the TENG is not a part of the shoe at all. Rather the TENG is placed on the straps on the rucksack, where the rucksack is the backpack the military uses. The materials would be placed on the outside of the uniform where the straps would be placed, as well as having the other material on the strap itself. This could be the shoulder straps, the hip strap or both. Below is a diagram of what this could look like.



Figure 9. Rucksack TENG placement [14].

The image on the right is the straps of the rucksack. The electronegative material will be used on the side of the strap that touches the chest of the soldier. The electrode is placed directly behind the material. The picture on the right is the uniform. The electrode is attached directly to the uniform, and the electropositive material is placed over the electrode, where the straps sit on the soldier. This option makes use of different areas that have previously had no testing done. The potential positives that can come from this design is the increase in power due to more sliding, therefore more friction. The potential issues could be from the environment, as this is a common place that could be damaged by water, sweat, and dirt.

#### 2.4.5 Parachute Placement

This option explores something very dissimilar to the others. The TENG is not placed on the soldier directly, but rather the parachute. The triboelectric effect is still applicable in this scenario since the parachute itself flaps in the wind, which would make material come into contact with each other. The TENG would be placed in between the cells of the parachute, which would allow us to generate a great amount of power due to the high velocity of the wind causing a large amount of contact which would in theory produce more energy. Another possible location for TENG placement on parachutes would be on the slider. The slider is a rectangular piece of

fabric that is attached to the parachute cords. At some point during the deployment of the parachute, the slider will slide down the cords towards the parachuter, which forces the cords to open up the parachute, allowing the parachute to effectively slow the descent of the parachuter. This motion of sliding from the slider produces a large amount of friction on the cords, offering another option for energy harvesting. However, this motion only occurs once per parachute deployment, so it is a limited energy output.

## 2.5 Surface Area Modifications

As discussed in Section 2.2, TENGs take advantage of the triboelectric effect producing a charge during the contact and separation of materials. One of the ways to increase the amount of voltage generated in this way is to modify the contact surface area of the TENG, as described below.

### 2.5.1 Purpose of Surface Area Modifications

The triboelectric effect is dependent on multiple factors, including the amount of surface area of the materials involved. Generally, TENGs that use a larger contact surface area generate more electricity per a pass, all other factors remaining equal. To this end, it can often be beneficial to physically modify the surface roughness of the materials utilized in a TENG in such a way as to increase the surface area.

### 2.5.2 Types of Surface Area Modifications

There are many different methods that can be used to modify the surface roughness of a material. Some methods can be as simple as manual abrasion utilizing coarse grit sandpaper or a wire wheel. Quick and repetitive passes of these abrasive tools over a surface removes material at an uneven rate, leading to an increase of surface roughness and overall surface area. Abrasion is a simple, cheap way to increase surface area without requiring complex machinery or hours of training. However, these methods also produce less consistent results than other types of surface area modifications, which often used advanced machines to create specific micro-textures on the surface of a material.

Micro-texturing is a more complex process than simple abrasion, but offers a level of consistency and control that sandpaper and other simple hand tools lack. There are many methods of micro-texturing, each utilizing a different medium with unique benefits and drawbacks. Reactive Ion Etching (RIE), plasma etching, and dry etching, for example, all utilize various types of high energy plasma to cut away surface material. Laser Surface Texturing (LST), meanwhile, utilizes a localized laser to melt and evaporate material in a precise pattern. Photolithography, a process commonly used in the microchip industry, uses UV exposure to erode at susceptible materials while a resistant mask creates a specific pattern. Abrasive jet machines such as water jets bombard parts with fine particles of sand and other abrasives in a liquid medium [15]. Molds used in injection molding can be manufactured with micro-textures, allowing for a high throughput of textured parts. High precision nano-3D printing machines can be utilized to produce additively manufactured parts with nanometer precision micro-texturing [16]. Specialized inkjet printers can also be used to create micro-textures with a variety of inks that provide different material properties for products like electronics and photovoltaics [17].

Using precision micro-texturing methods, specific patterns can be created on a surface in order to maximize contact surface area. Examples of these patterns include channel-like lines, cubic protrusions, and pyramidal (and inverse pyramidal) patterns. Examples of these patterns are pictured below in Figure 10.

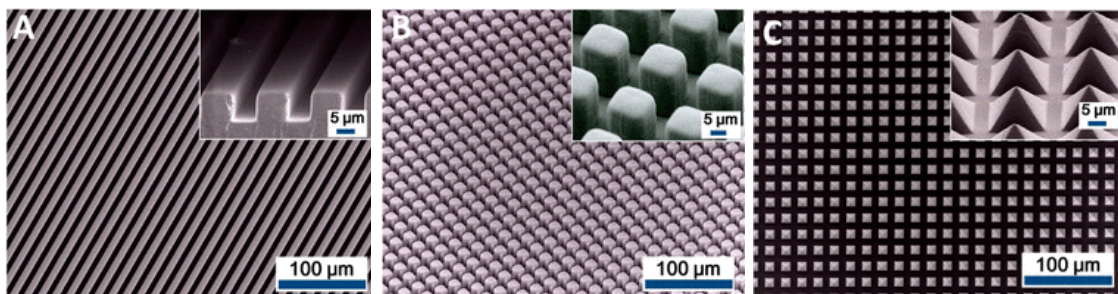


Figure 10. Examples of micro-texturing patterns, including lines (A), cubes (B) and pyramids (C) [18].

## 2.6 Previous Research

Analyzing what previous years' groups have done will help us not only learn what they were working to discover, but also give us an idea as to what needs to be improved in the current TENG design. A good understanding of the background of the TENG development and technology is critical in our success for our own goals with the project.

### 2.6.1 2020-2021 MQP

The 2020-2021 MQP group were the pathfinders for this project. Their job was to create a functioning TENG that could be applied to several different applications and produce energy for the US Army. To complete this task, this group began by studying what materials maximized energy output. They tested From there, they determined that the sole of the boot had the highest amount of friction of the locations on the body. Combining this research with their material research, they created a prototype of a TENG integrated with the sole of the boot. This allowed them to get the most amount of energy output while also harnessing energy every step.

### 2.6.2 2021-2022 MQP

The 2021-2022 MQP team decided to take what the previous group had, and they worked to refine the placement and the design of the TENG. To start, they began with the placement of the TENG, experimenting with different locations within the boot, and also focusing on the shape of the TENG, and the effects different shapes had on efficiency and power output. This group also studied various configurations of the TENG, such as adding layers. They found that layered TENGs generate more power than TENGs without layers. Their final product included both a layered TENG to increase power output and placement to maximize efficiency from each step.

### 2.6.3 2022-2023 MQP

The 2022-2023 MQP group took what the previous two groups did, and they decided to research more uses of the TENG. This group studied how placing TENGs on tents or parachutes, both of which would harvest wind energy, and how effective those placements would be. They

did research more ways to increase the TENGs power generation and versatility as well, continuing with the layered TENGs and developing different circuits for the TENGs energy to be harvested through. They experimented with different types of circuits, with a variety of configurations to best convert any energy that is collected.

## Chapter 3: Objectives

In this chapter we will discuss the overall goals and objectives for this project. This is done in consideration from our project advisor and our sponsor. As a result of setting goals for the project our advisor and sponsor will understand what is expected for the outcome of this project.

For our project we are developing two portable TENGs. One that is compatible with a standard issue army boot, while the other is compatible with a standard issued parachute. The TENG is to be used as a portable source of energy that can be attached to biometric sensors to monitor a soldier's health. With all this in consideration the following objectives were created were

- Increase TENG voltage and current output
- Be able to rectify output from the TENG so it can power biometric sensors directly without the use of a battery
- Design the TENG to be durable in different environments as well as comfortable for users to wear.
- Affordable and simple manufacturability
- TENG should be user friendly

### 3.1 Higher Power

As mentioned before, one of our main objectives of this project is to enhance power output from the TENG so we are able to provide consistent power to the biometric sensors, without the use of a battery. When rectifying the output we need to make sure that we supply sufficient enough power making sure it's not too high nor too low. This can be achieved by amplifying the current output of the TENG as well as the output voltage, since power is directly proportional to current, and voltage.

$$P=VI$$

Previous years were able to get decent voltage output however failed to get a decent current output. We plan on using the research and resources from previous years and improve the output of the TENG.

## 3.2 Ergonomics

### 3.2.1 Durability

In addition to achieving a higher power output we want to make sure the TENG is durable so that it is able to withstand diverse environments such as jungles, forest, deserts, and tundras. These environments are very difficult to navigate through so it is essential the TENG can withstand the soldiers' impact from these environments. The Soldier Center in Natick, Massachusetts has a shoe lab that we can utilize to test different impact scenarios. For the wind TENG, the TENG should be able to withstand different environmental scenarios like the boot, as well as withstand high wind speed, since it will be utilized on a parachute.

### 3.2.2 Comfortability

While durability is an important factor, we also have to take into account comfortability. Since the TENG is going to be placed within a standard issued army boot it is crucial that the boot is comfortable for the soldier. Soldiers spend most of their time in the standard boot, and are placed in harsh environments. Therefore it is crucial the boot is comfortable with the TENG placed inside so that it does not hinder a soldier's movement. Or if the decision is to go with an alternative other than the boot, having comfortable straps on the uniform, as in section 2.4.4. It is just as important to not interfere with the way the soldier uses their upper body.

For the wind TENG, the TENG should not hinder the performance of the parachute, and not weigh it down too much. Like the boot TENG, it should be comfortable and not hinder soldier movement.

### 3.3 Usefulness

This section talks about the objective of making the TENG useful for the purposes of military use as well as general uses. It needs to be easily used in everyday scenarios or else the system that is designed won't be worth the effort of implementing.

#### 3.3.1 Ease of Manufacturing

Having a system that is easy to make is vital for having a useful product. There are roughly 60,000 people that are in the army and could use a system like this implemented, so having a product that is difficult to make, will make it less likely to be implemented. Also, this project has a deadline of only 6 months, so to be able to get the most testing done, the materials that are chosen have to be easily manufacturable or this project won't be able to be completed in that time.

#### 3.3.2 Cost

As this is a project sponsored by the United States Military, there is a limited budget. Since one of the goals of this product is to implement this in as many soldiers as possible, while being cost effective. Having a high price will most likely mean that there will be a limit to the amount of TENG's that will be manufactured and as a result many soldiers that will not have access to the product.

#### 3.3.3 Easy to Use

To have this system work in the military it is going to need to be integrated into a soldier's daily routine. To implement something that is complicated, or takes a lot of time to do means that this is not a very useful tool. So making this system easy to use is vital to the goal of this project.

## Chapter 4: Circuit Design

Circuits act as the middle ground between the TENG and the load that requires the power that is generated. The waveform of power generated is a nonstandard wave, so to have any practical use, we needed to create a circuit to manipulate the waveform into usable power. This section will cover the different stages of circuits that we made to visualize and understand the power of the TENG. Unlike years past, we did not model this based on what we guessed a soldier would walk like, rather we spent our time testing and finding which option was the most practical.

### 4.1 Load Circuit

The first circuit we used for testing, although simple, was incredibly effective at understanding the output voltages and power a TENG could achieve. This circuit had the TENG connected to an oscilloscope with either no load or different values of resistance as the load. Our initial round of testing was measuring the open circuit voltage. The first step involved connecting the positive and negative terminals of the TENG to the oscilloscope, as illustrated in Figure 11, below. This allowed us to observe the best possible voltage output to determine which combination of materials we should work with.

Additionally, we placed different values of a resistor in parallel with the oscilloscope. This way, we would be able to find the voltage across the resistor and be able to calculate the current and therefore power generated by the TENG. A diagram of what this would look like is shown in Figure 12. However, there is an issue with this setup. Since the TENGs voltage swings positive to negative, having negative values for current can't occur since powering a device can only flow in one direction. A battery or a capacitor won't be able to charge if current is traveling against the polarity.

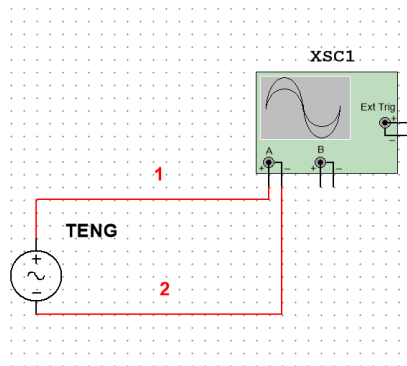


Figure 11. The TENG circuit connected directly to the oscilloscope.

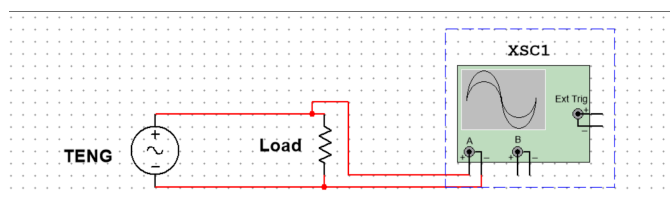


Figure 12. The TENG circuit connected to a resistor.

#### 4.2 Single Diode

To address this issue, we connected a diode in series with the TENG and the capacitor. A diode is an electrical component that only allows current to flow in one direction. A diode consists of an anode and cathode where the anode is made up of a P-type material while the cathode is made up of an N-type material as shown in Figure 13.

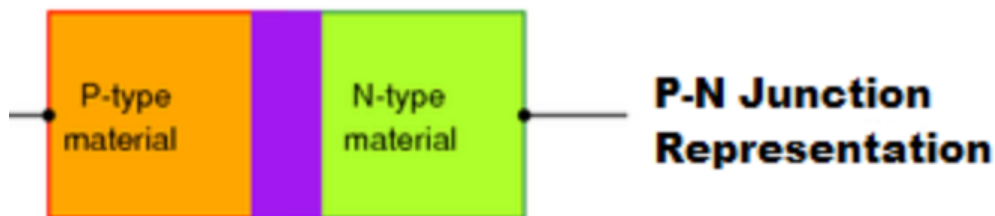


Figure 13. A visual of the semiconductor materials that make up a diode [19].

When the diode allows current to flow, it's known as forward bias, and when the diode blocks current flow, it's known as reverse bias. Therefore, by adding the diode in series with the capacitor and TENG only the positive portion of the voltage will go through and block the negative voltages. However, it is important to note that there is a voltage drop across a diode

which can range between 0.3-0.7V depending on the type. This allows for the capacitor to be able to hold a charge and not be damaged by negative voltages. Below is what a sine wave would look like going through a diode.

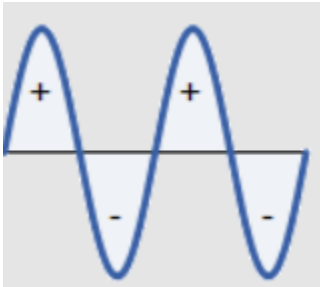


Figure 14. A sine wave before being rectified [20].

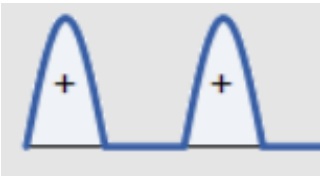


Figure 15. The output of the sine wave going through the circuit [21].

In our case, the TENG is connected to the anode, while the cathode is connected to the capacitor.

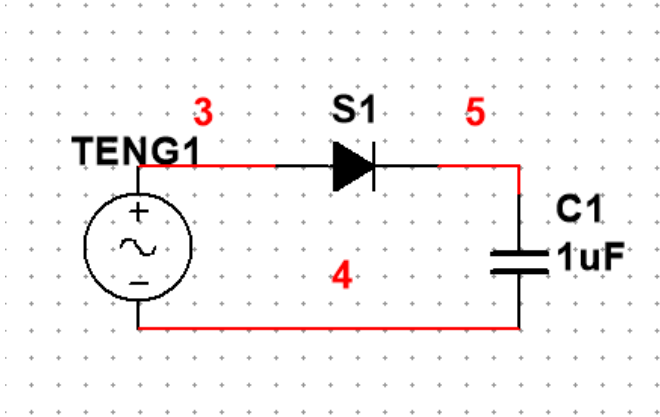


Figure 16. Half-wave rectifier circuit

This circuit has its benefits, however, because we are getting rid of the negative voltages, we are reducing the TENG's efficiency since we are essentially getting rid of half the energy. To improve efficiency, we built a diode-bridge talked about in the section below.

### 4.3 Diode Bridge

Unlike the single diode, the diode bridge contains four diodes arranged in a bridge circuit that allows the negative portions of AC Current to be mirrored across the X-axis and be positive. Below is an image of what the Diode Bridge looks like, and what a sine wave looks like after it goes through the diode bridge.

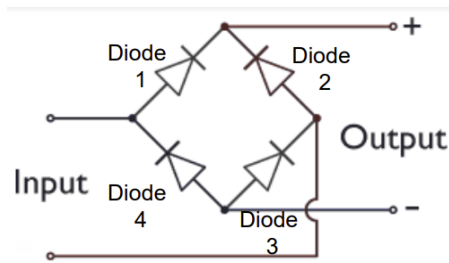


Figure 17. The diode bridge [22].

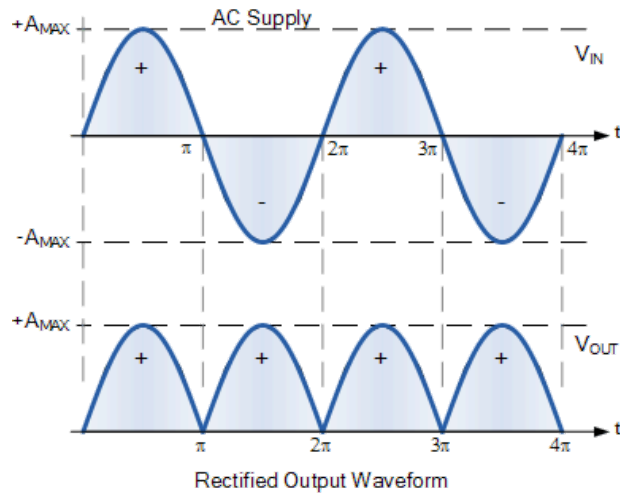


Figure 18. The output of a sine wave before and after rectification [23].

When the input voltage is positive, it travels through the Input on the far left and goes through Diode 1, it will then go through whatever load is connected to the positive Output, then

go through the negative output, through Diode 3, and then back to the input through the right side of the Input.

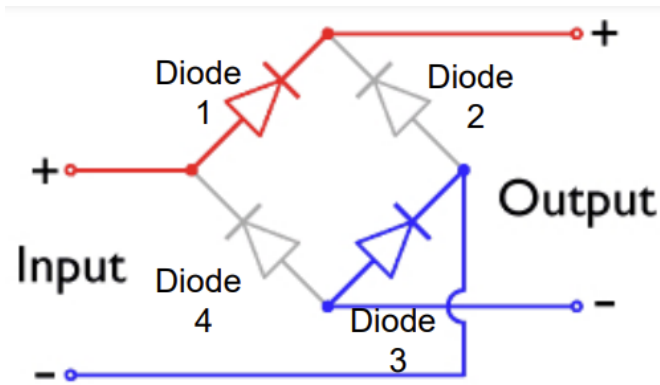


Figure 19. The diode bridge with the colored sections being which diodes are active [24].

When the voltage is negative, it travels through the right side of the Input, through Diode 2 to the positive Output. Then it goes through the negative Output, through Diode 4, back to the other end of the Input.

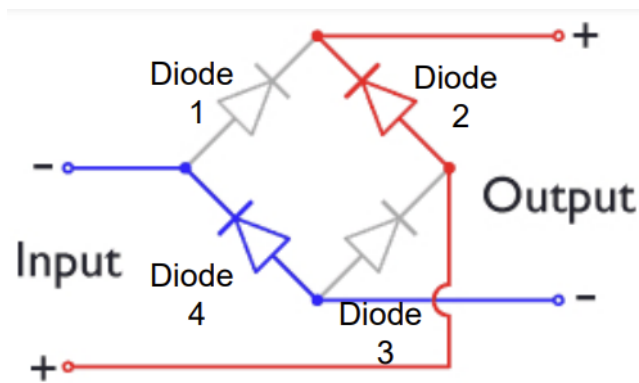


Figure 20. The diode bridge with the colored sections being which diodes are active [25].

Diodes are electronic switches that only allow electricity to flow in one direction. So, when voltage is positive, 2 diodes are in forward bias and 2 are in reverse bias, and vice versa when voltage is negative. This results in only a positive waveform. Allowing for negative voltage will result in problems for the capacitor or battery connected to this circuit causing dielectric breakdown, leading to short circuits or permanent damage.

One possible downside of a diode bridge is the increase of lost voltage due to the diodes since there is a voltage drop of 0.337V for each diode. This means that 0.674V is lost for every impulse that is recorded. However, in our case, this was still the best option going forward, as the negative values for voltage were significant, so rectifying them was worth the 0.674V loss. Below is a visual to show before and after the rectification.

#### 4.4 Other Rectifying Circuits

As talked about in previous year's MQP reports, there are many types of rectifier circuits that can take an unusable waveform and transform it into something useful. However there are issues with each of the models that they recommended, so as a team, we did not spend time researching and testing these, as they are not practical for military application. Some of the options make use of a transistor, either a MOSFET or a Bipolar Junction Transistor (BJT), which acts as an electrical switch similar to a diode. They offer benefits like controlling the flow of energy by being ON or OFF providing advanced control and stabilizing output voltage.

However, they require external power to run them, so it would require a battery or other power supply to run to have the ability to charge a battery; which is counterintuitive. Examples of this include the Fractal Switch Capacitor Converter, Parallel Switch Circuit, Series Switch Circuit, Active Full Wave Rectifier, and Universal Management Circuit. Additionally, last year's group looked into an Inductive Transformer, which would require a magnetic core with inductive wires around 2 sides of the core. These are often bulky and potentially dangerous in a prototype like we are making. Since they are not perfect, there will be energy lost as heat.

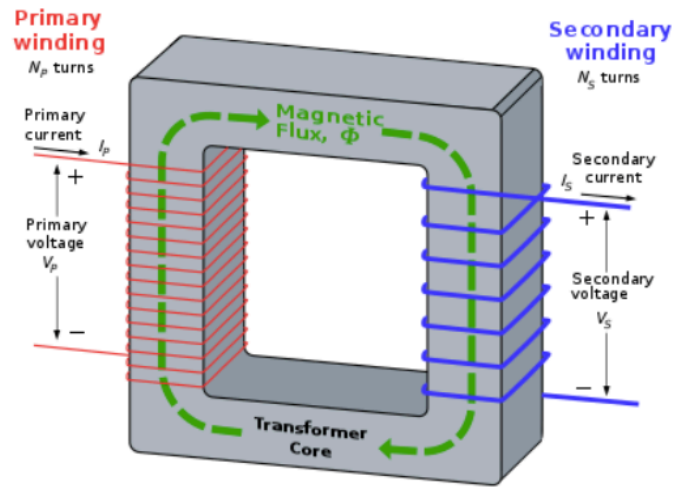


Figure 21. The topology of a transformer [26].

So in a prototype like a shoe where there is no ventilation, the risk of fire is high. Additionally, since the person is so close to the transformer, the human body can interfere with the magnetic field created by the transformer.

## Chapter 5: Testing Methodology

This chapter discusses the testing procedure, apparatuses, and evaluation techniques used during the first joint testing stage of this project. Before splitting off into boot-integrated- and wind-activated TENG groups, the full team performed impact based material testing to ensure common understanding, reliable testing methodology, and the production of usable results. Many of the lessons learned from this initial testing period are reflected in later portions of the project.

### 5.1 Drop Testing

The drop test, shown in Figure 22, was used to evaluate material performance and TENG structural integrity during repetitive and consistent impacts. This test allowed the group to determine which materials would maximize TENG power output and durability during repetitive low to medium impact situations. This test had the following goals:

- Develop methods of measuring the output voltage, current, and power of a TENG.
- Develop metrics to assist in the comparison of TENG performance using the methods of measurement developed.
- Compare the performance of different triboelectric materials and electrodes in a controlled environment.

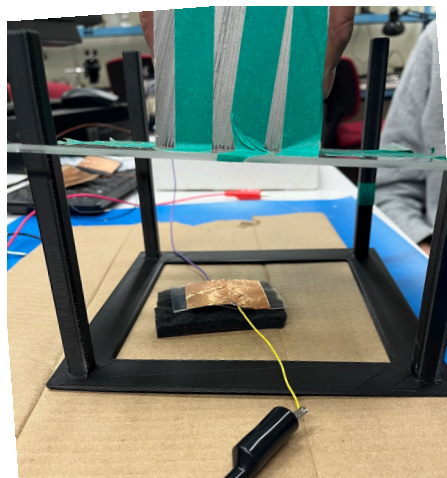


Figure 22. An example of the drop test setup.

### 5.1.1 Testing Procedure

Testing was conducted on a series of 2" x 2.5" and 7" x 4" TENGs, each consisting of a positively charged triboelectric material, a negatively charged triboelectric material, and two electrodes. One electrode was placed on each material, which were then placed in contact with each other, as shown by Figure 23. A weight of 4.95 lbs was then dropped from several predetermined heights a total of 10 times. The weight was isolated from the TENG and evenly distributed by an acrylic plate. Each material combination was tested a total of three times. The resulting methodology of measuring TENG output is discussed in section 5.2, while the result of the material tests are discussed in section 6.1.

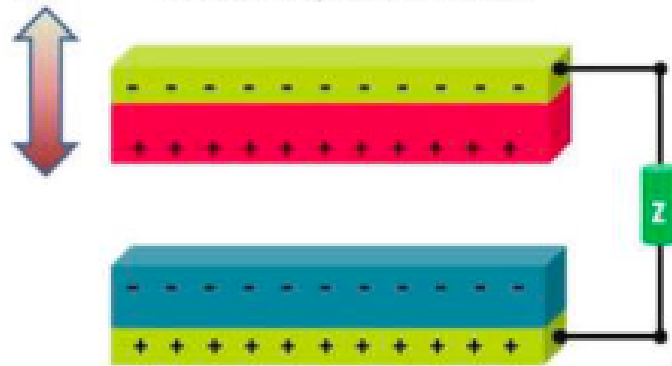


Figure 23. Structure of the TENGs used in the drop testing [27].

### 5.1.2 Initial Testing Apparatus

Initially, the drop test was performed using apparatus left behind by the 2020-2021 Triboelectric Energy Generation group. This testing apparatus included a PLA base and a single acrylic plate. The base stand was 210mm x 210mm x 162mm and was 3D printed. The base plate included four vertical guiding rails that allowed the plate to be dropped. The plate was 210mm x 210mm x 3.18mm and was laser cut. Four holes in the plate fit on the guiding rails of the base with a clearance of 0.6mm [28]. Figure 24 shows the apparatus.

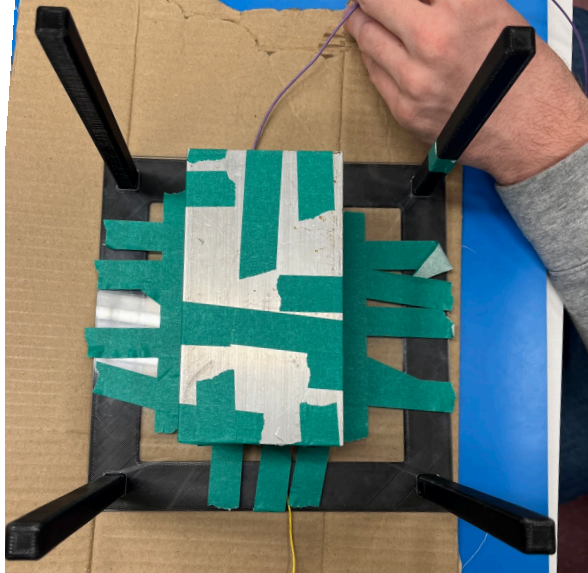


Figure 24. The initial drop test apparatus.

This initial testing apparatus, while functional, had several operational flaws. The base was hollow in the center to save material, which led to uneven distribution of force and cracking of the acrylic plate. The guide rails had no method of ensuring consistent drop height, and their square shape led to the plate getting stuck. These flaws impacted the first several rounds of testing and led to the iteration and development of the new testing apparatus discussed in section 5.1.2.

### 5.1.3 Updated Testing Apparatus

The updated testing apparatus was designed using SolidWorks with three separate components: A base, a plate, and four separate guide rails, as shown in Figure 25. The base stand was 8.25" x 8.25 " x ¼" and was made by laser cutting wood. The base included four holes for the guide rails and four additional holes to bolt the base down, securing it during testing. The acrylic plate was 8.25" x 8.25 " x ⅛" and was made by laser cutting acrylic. The design remained largely unchanged from the initial plate. Finally, the guard rails were each ¼" x ¼" x 4" and had holes cut at ½" intervals. Dowel rods could be inserted through these holes to create consistent drop heights. These guiding rails were machined from aluminum. The completed testing apparatus is pictured in Figure 26.

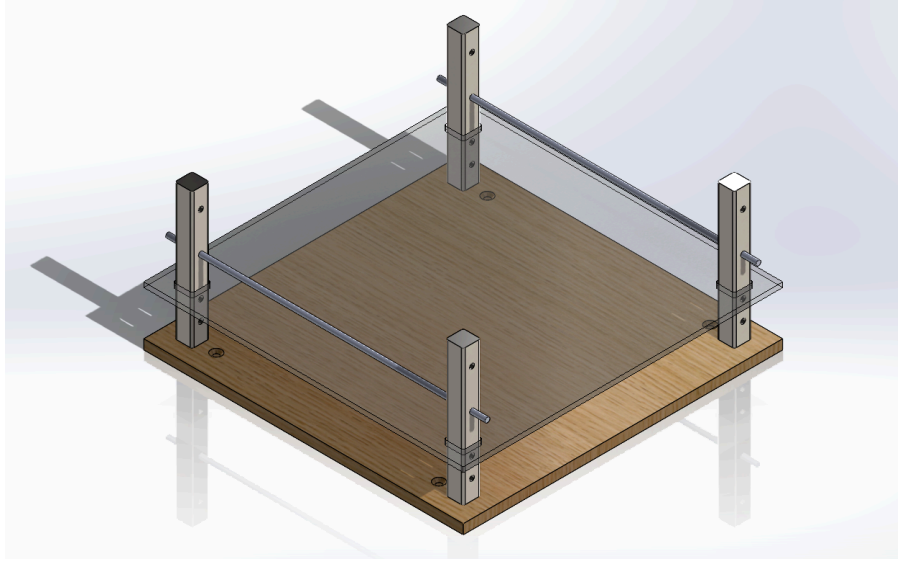


Figure 25. SolidWorks assembly of the updated drop testing apparatus.

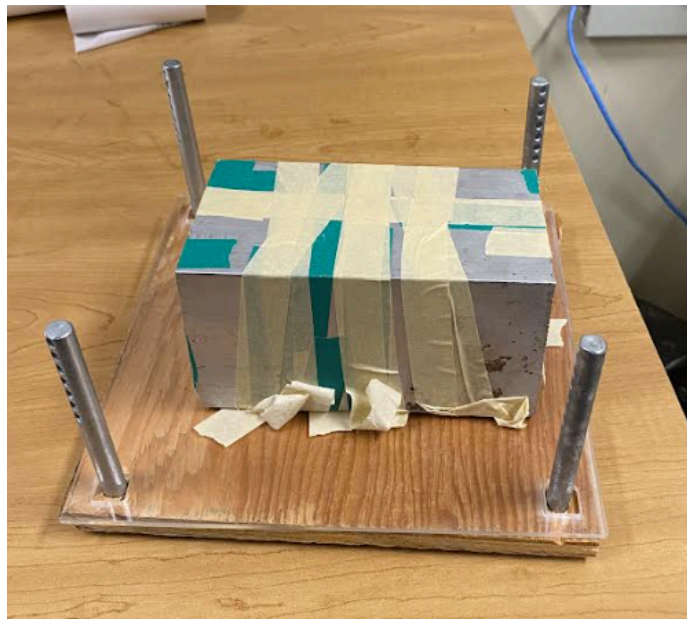


Figure 26. The updated drop testing apparatus.

## 5.2 Quantification of Results

After designing the drop test, a way of measuring the effectiveness of our TENG was needed. We needed a tool to measure the power that was generated from each material

combination. This section will talk about what equipment we used to record, as well as the results from these initial material tests.

### 5.2.1 Equipment Used

As for measuring equipment, we needed a tool to record the results based on the following criteria:

- Could accurately measure Voltage
- Could accurately measure Current
- Had a high enough sampling rate to record all of the values measured during the test
- Could translate the data onto our devices to be processed
- Within our budget

After looking at many options, we settled on the Digital Multimeter (DMM) that the laboratories in Atwater Kent already had. It had all of the options we needed with the addition of a customer support engineer who would keep in contact to answer our questions. This model was the Keysight EDU34450A 5½ Digit Digital Multimeter.



Figure 27. The DMM used in experiments [29].

This model appealed since it had the option of measuring both voltage and current, which would give an almost perfect measurement of the power generated. Below in Figure 28 is how to

place the probes of the oscilloscope to get both a voltage and current reading and in Figure 29 is what the screen looks like when measuring voltage and current simultaneously.

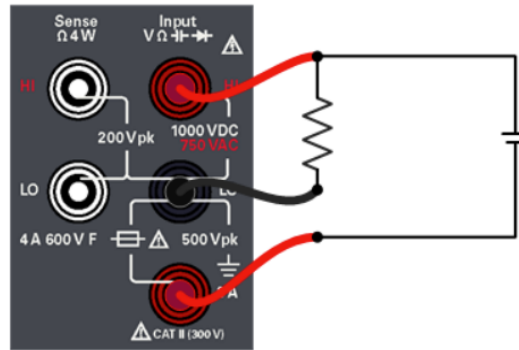


Figure 28. The way to measure both voltage and current [30].



Figure 29. The DMM interface while measuring both voltage and current [31].

In addition, this multimeter can connect to a laptop through a program called Keysight PathWave BenchVue Digital Multimeter. It allows for computer control of the multimeter, to set the sampling rate, when to start, stop, and save the data. In Figure 30 it shows what this program looks like when it is connected to the DMM.



Figure 30. The computer program view of the DMM.

However, these 2 features do not work in conjunction with each other. When I reached out to the support, they informed me this was a heavily requested feature, and that they will make it so they can both work at the same time eventually. For next year, this could be a good option to check if it's working.

There was also an issue in the sampling rate of voltage to begin with. After many tests of using the DMM, there were some voltage peaks that didn't line up with the others even though all the other conditions of the test were standardized. This resulted in us choosing to switch to the Keysight InfiniiVision DSOX1204A/G Oscilloscope. The sampling rate increased to a maximum of 2 GSa/s, whereas the DMM only had a maximum of 100 KSa/s, however, this would result in the software crashing. With the increase in sample size, it was less likely to lose data points, so the primary method of data recording once materials were chosen was the oscilloscope.

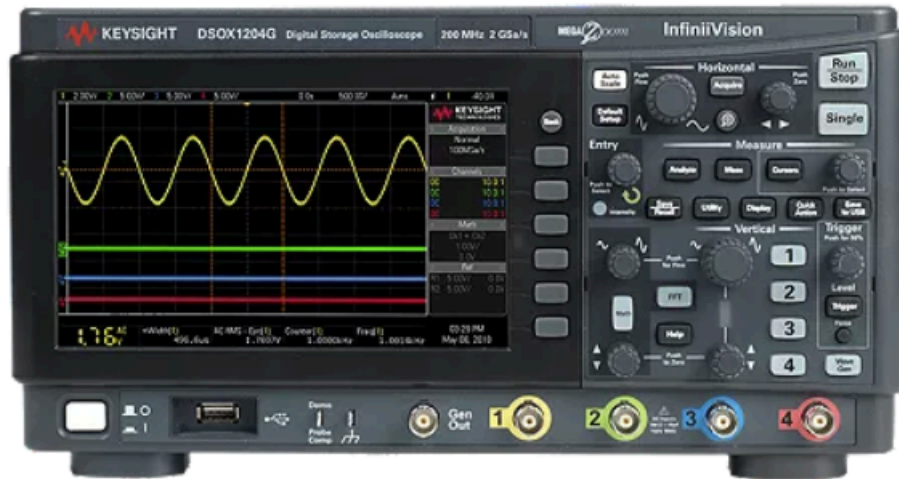


Figure 31. The oscilloscope used for experiments [32].

This Oscilloscope met all of the criteria, with it being able to interface with our computers through a USB stick. Additionally, it was also in the laboratories at Atwater Kent, so it was convenient for us to do our testing. It however could not measure current, but that ended up being okay as talked about in section 5.2.4.

### 5.2.2 Open Circuit Voltage Test

The first way we decided to measure the initial tests was to take the TENG and connect it directly to the probes on the oscilloscope. The internal resistance of the DMM is  $10\text{ M}\Omega$ , so not exactly an open circuit, but very high, so current should be close to  $0\text{ A}$ . The goal of this test is to see the maximum voltage that is achieved without anything else interfering with the circuit. This will allow us to compare all of the voltages from each test and compare their peak-to-peak values and average values.

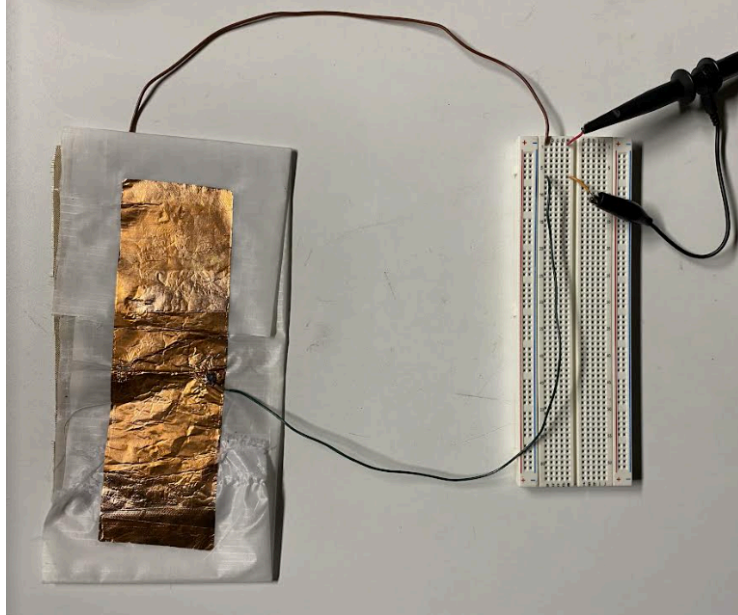


Figure 32. The TENG materials connected to the oscilloscope through an open circuit.

### 5.2.3 Load Voltage Test

The load voltage test is another important test we ran to understand which materials would give the best results except this one had an additional component of a resistor in parallel with the DMM. This allows for current to flow throughout this circuit, so voltage would be lower and current would be higher than the open circuit test. The value of the resistor is changed from a  $100\text{k}\Omega$ ,  $51\text{k}\Omega$ ,  $10\text{k}\Omega$ ,  $5.1\text{k}\Omega$ ,  $1\text{k}\Omega$ ,  $510\Omega$ ,  $100\Omega$ ,  $51\Omega$ , and finally a  $10\Omega$ . This way we can measure the changes from all the different values of the load and see which combination gives the best power output.

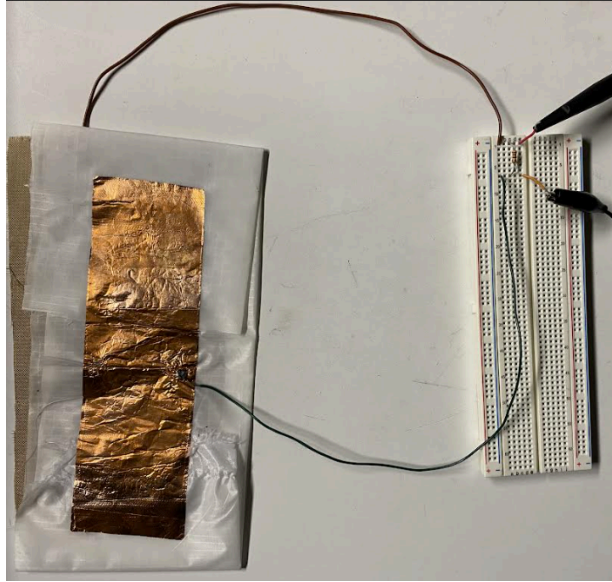


Figure 33. The TENG materials connected to the oscilloscope through a resistor.

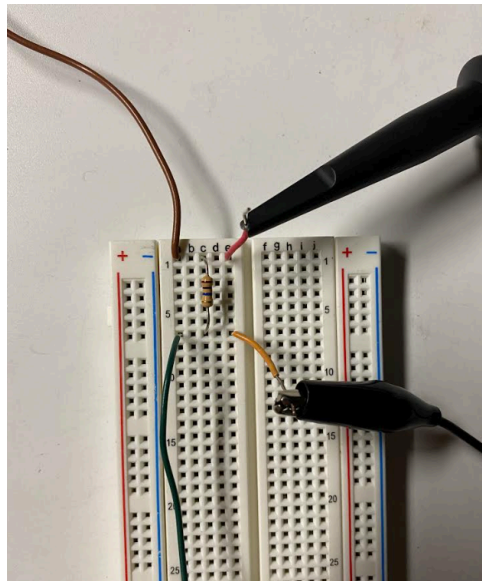


Figure 34. A close up of the circuit.

#### 5.2.4 Ohm's Law to Understand Current and Power

In the previous two sections, the only thing that was measured was voltage, however, voltage is not the same as power, which is what we want to generate. Therefore we used the laws

of Electrical Engineering to understand the power that goes through the circuit. In this case, we only need to use Ohm's law, since we have a voltage and a resistor, so using the formula  $V=I \cdot R$ , we can calculate the current. By calculating current, we can use the formula  $P=V \cdot I$  to calculate power. These allow us to get a calculation of power based on the measured results of voltage. The reason we couldn't measure current and voltage at the same time is because of the issues with the sampling rate in the Keysight DMM program. We had two computers connected to the same circuit, with one measuring current in the circuit and the other measuring voltage. However, even though both computers started taking data at the same time and ended at the same time with all the same sampling settings, the number of samples taken was significantly off. If we tried to get power based on these values, the power would be wrong since the values are not lined up to the correct time. To try and correct this, we would need to downsample the current since it is recorded 180 times per second, whereas voltage is recorded only 50 times a second. Downsampling is an issue since we would get rid of good data points to try and make the times match each of each data point, but even that would not be 100% accurate.

## **Chapter 6: TENG Material Testing**

This chapter discusses the material testing conducted during the first joint testing stage of this project. Using the testing methodologies established in chapter 5, the group narrowed down the number of conductive triboelectric materials, settling on just three to use for prototypes going forward into the next stages of the project.

### **6.1 Material Review**

To maximize the power generated by our TENGs, we evaluated the material performance of multiple popular triboelectric conductors during repetitive and consistent impacts. This allowed the group to determine which materials would be most likely to increase TENG power output and durability during the repetitive low to medium impact situations that the devices would be expected to operate in. These tests also tested and proved the validity of the methodology established in chapter 5.

The first step in deciding what materials we were planning on using in our design was to prioritize the aspects of the different materials. As discussed in section 2.2.6, we prioritized the electronegativity of a material, while also considering characteristics like manufacturability, practicality, availability, cost, and durability. We created a decision matrix based on these criteria to help us determine which materials we wanted to test, as seen in Table 3.

Materials	Manufacturability	Availability	Cost (1=High cost)	Charge potential	Total Score
PTFE(-)*	9	9	4	9	31
PDMS(-)*	9	9	5	8	31
PET(-)	9	8	4	9	30
Teflon(-)	5	7	7	9	28
Silicone Rubber(-)*	7	9	7	10	33
Rayon(-)	6	7	6	8	27
Nylon (+)*	8	10	9	7	34
Kapton (+)	8	8	7	7	30
Graphene(+)*	7	8	8	9	32
Polyurethane Foam (+)*	6	9	8	8	31

Table 3. Material selection decision matrix.

Expensive materials were given a low cost score, giving low cost materials a positive impact on the overall score. We determined that we were going to test with materials that scored

31 or higher in this decision matrix. This meant that we would test PTFE, PDMS, and silicone rubber as the negatively charged triboelectric material, and nylon, graphene, and polyurethane foam for the positively charged material.

PTFE was a material we found after researching options for prior TENGs. Polytetrafluoroethylene is an engineered polymer that is used in several applications, such as an anti-stick coating for cookware, electrical applications as an insulator, and gaskets in different wiring equipment. PTFE is known for being chemically resistant, to the point where no known chemical solution can dissolve PTFE at room temperature.



Figure 35. PTFE from second round testing.

PDMS is another engineered polymer that we had researched thoroughly. Many triboelectric experiments before ours had concluded it was one of the best materials available to use for TENGs. It is commonly used in lithography, and inside microfluidic chips because of its physical properties and ease of manufacturing. It would be a reliable option for our TENG usage, and still have the ability to produce large amounts of electrostatic energy.



Figure 36. PDMS from second round testing.

Silicon Rubber is a synthetic rubber elastomer, similar to an engineered polymer. It had the highest potential electrostatic charge out of all the materials. It is a similar material to PDMS, however, it is not as durable or rigid as PDMS. It was easy to get our hands on, and it is commonly used in most aspects of life, from home repairs, to apparel, to automotive uses.



Figure 37. Silicon rubber from second round testing.

Nylon is a material that has thousands of uses. It can be found in everyday objects, and is widely used by the military in tents, parachutes, and straps. Nylon also has a high potential electrostatic charge, and because of its durability and versatility, it would be a good material to incorporate into our TENG.



Figure 38. Nylon from second round testing.

Graphene was a material we did not originally plan on testing, but we were surprised by how well other TENG tests did when using graphene. Graphene is a positively charged material, however it is also known for being fragile. It is not a durable material, especially when used in the sole of a shoe. We had hopes for the potential output, so we decided to test it with the other materials.



Figure 39. Graphene from second round testing.

Polyurethane foam had a very high potential electrostatic charge. The positive material is commonly used in packaging and furniture. As for durability, it does not hold up to stress as much as nylon or PDMS, however it is more durable than materials such as graphene. Using polyurethane foam in the sole for a TENG might produce good amounts of electrostaticity, however it may not function well under that much stress.



Figure 40. Polyurethane foam from second round testing.

## 6.2 Material Testing

To select the most effective materials, the drop test was conducted on each combination of materials. Between tests, circuitry was updated and independent control variables were altered to test how TENGs operated under different conditions. Each round of testing is discussed in detail below

### 6.2.1 Testing Procedure: Round 1

During the first round of material testing, each combination of positive and negative materials was combined together into a TENG and then subjected to the drop test detailed in section 5.1. Two 2" x 2.5" rectangles were cut from each material. Each square was then connected to an electrode made of either copper or aluminum tape. Each electrode was then soldered to a wire which could be connected to the DDM as discussed in section 5.2. By producing the TENGs in this way, each material/electrode combination could be exchanged for another quickly and efficiently. Each positive material/negative material/electrode combination

was subjected to the drop test. These tests were run with the open circuit configuration, creating higher average and peak to peak voltages for the ease of comparison.

### 6.2.2 Results: Round 1

During this round of testing, each negative triboelectric material was combined with each of the positive materials and an electrode. It became immediately obvious that the copper tape made a much better electrode, as the aluminum tape was fragile and ripped easily, making it unsuitable for the tests. Therefore, we formed the rest of our electrodes throughout this process out of copper tape.

As each material combination was tested, the resulting data was recorded in a voltage/data point graph. These graphs were then combined, as shown in Figures 41, 42, and 43, while the graphs of each individual material combination can be found in Appendix A. The average voltage and highest peak to peak voltage instance of each test was recorded. The highest peak to peak voltage was also marked on the graphs. These two metrics were then compared to the other combinations in a table, shown in Table 4.

Material	PDMS (-)	PTFE (-)	Silicone Rubber (-)
Graphene (+)	$V_{avg} = 0.49 \text{ V}$ $V_{pk-pk} = 8.70 \text{ V}$	$V_{avg} = 0.86 \text{ V}$ $V_{pk-pk} = 5.46 \text{ V}$	$V_{avg} = 1.78 \text{ V}$ $V_{pk-pk} = 13.71 \text{ V}$
Polyurethane Foam (+)	$V_{avg} = 1.08 \text{ V}$ $V_{pk-pk} = 15.45 \text{ V}$	$V_{avg} = 0.55 \text{ V}$ $V_{pk-pk} = 5.60 \text{ V}$	$V_{avg} = 0.50 \text{ V}$ $V_{pk-pk} = 3.16 \text{ V}$
Nylon (+)	$V_{avg} = 1.34 \text{ V}$ $V_{pk-pk} = 13.02 \text{ V}$	$V_{avg} = 0.70 \text{ V}$ $V_{pk-pk} = 8.65 \text{ V}$	$V_{avg} = 0.86 \text{ V}$ $V_{pk-pk} = 10.62 \text{ V}$

Table 4. Table displaying the average voltages and peak to peak voltages found during the first round of testing.

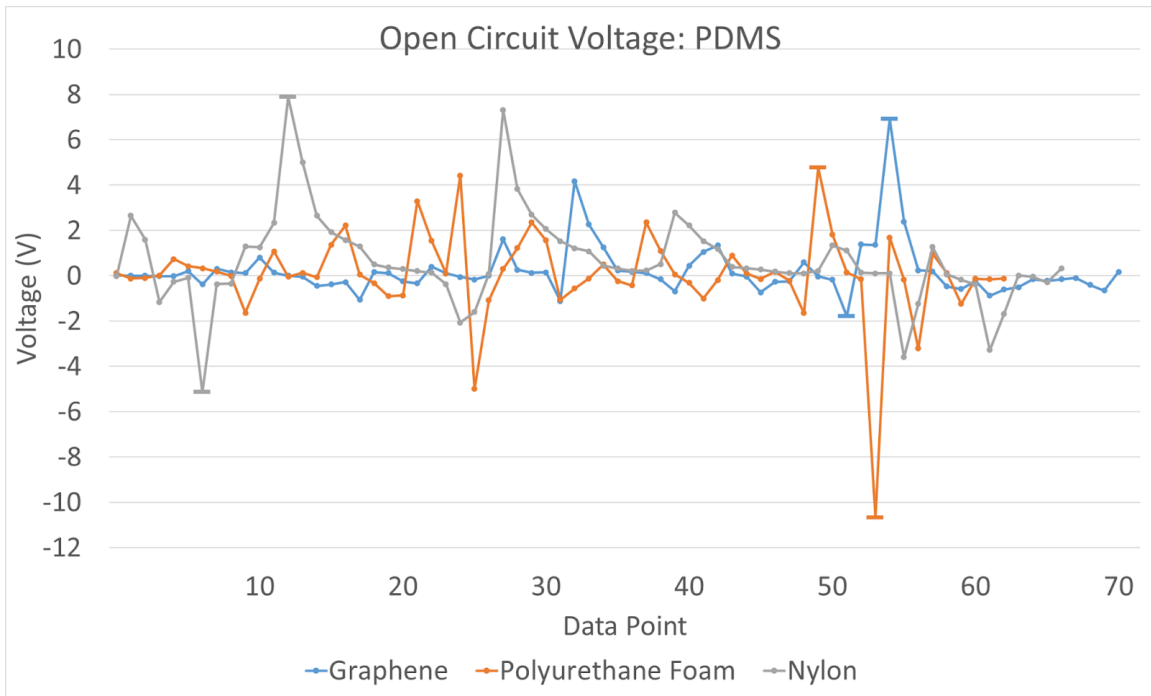


Figure 41. Graph comparing the TENGs made from PDMS during the first round of testing.

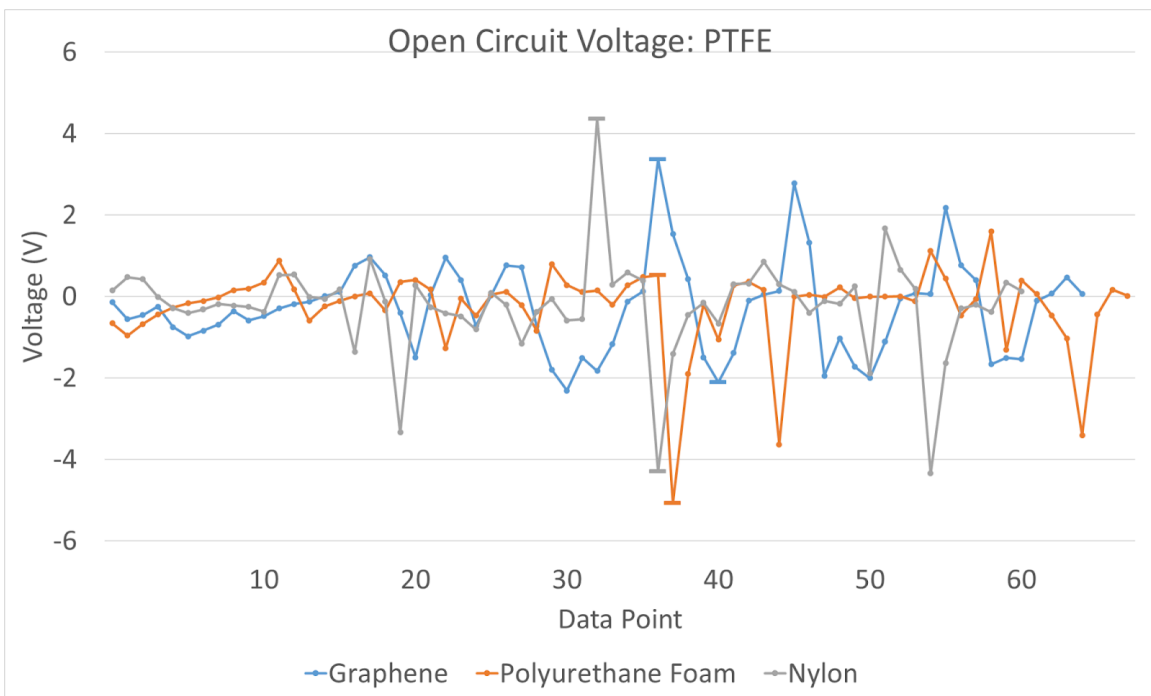


Figure 42. Graph comparing the TENGs made from PTFE during the first round of testing.

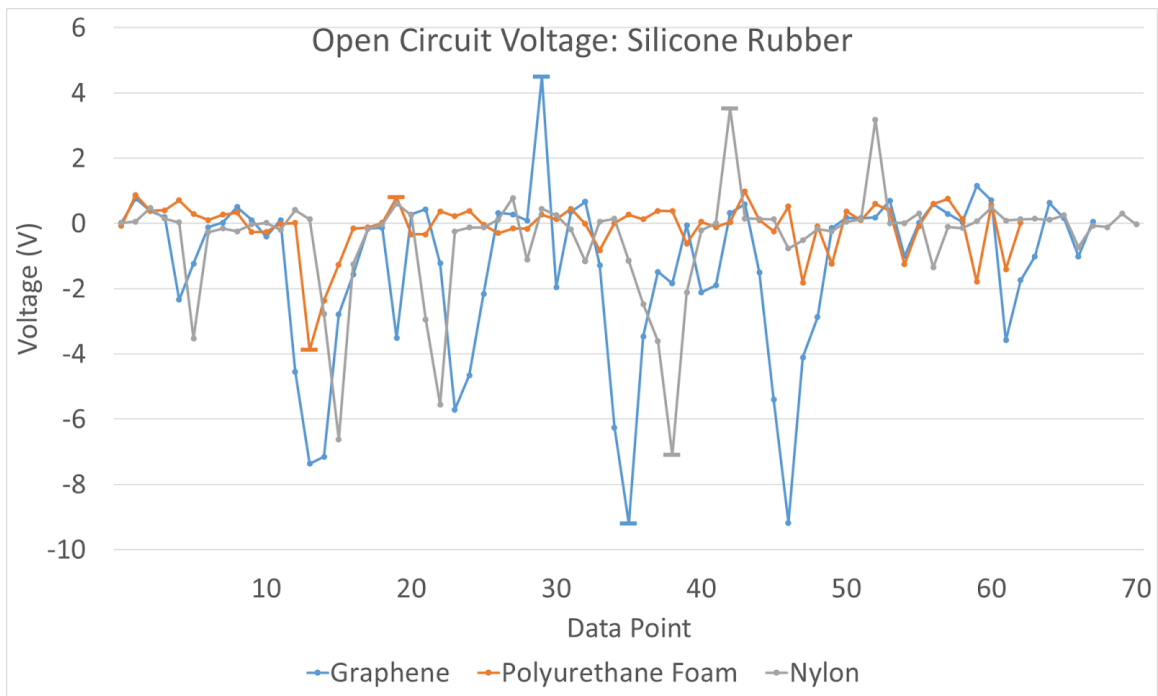


Figure 43. Graph comparing the TENGs made from silicone rubber during the first round of testing.

These tests quickly began to reveal that both PDMS and silicone rubber both acted extremely well as negative triboelectric materials, while all three of the positively charged materials showed promise in at least one configuration. Graphene and nylon reacted well more universally, while polyurethane foam produced the single highest peak to peak drop when combined with PDMS.

### 6.2.3 Testing Procedure: Round 2

While the first round of testing began to narrow down which materials acted as effective combinations, further evidence was required before deciding which materials to eliminate. To this end, the second round of testing increased the size of the materials to 7" x 4" rectangles. This test, therefore, provided an idea as to which materials would scale their energy production better with an increase in size. In addition, the higher surface area TENGs produced more voltage, clearly highlighting the differences in the materials. As with round 1, each material combination was subjected to the drop test in the open circuit configuration.

### 6.2.4 Results: Round 2

Much like the first round of testing, the results of the second round of testing were graphed and tabulated for easy comparison. The graphs can be seen in Figures 44, 45, and 46, while the graphs of each individual material combination can again be found in Appendix A. Table 5 shows the final tabulated results.

Material	PDMS (-)	PTFE (-)	Silicone Rubber (-)
Graphene (+)	$V_{\text{avg}} = 1.16 \text{ V}$ $V_{\text{pk-pk}} = 13.83 \text{ V}$	$V_{\text{avg}} = 1.91 \text{ V}$ $V_{\text{pk-pk}} = 17.08 \text{ V}$	$V_{\text{avg}} = 1.49 \text{ V}$ $V_{\text{pk-pk}} = 13.82 \text{ V}$
Polyurethane Foam (+)	$V_{\text{avg}} = 2.03 \text{ V}$ $V_{\text{pk-pk}} = 17.81 \text{ V}$	$V_{\text{avg}} = 0.91 \text{ V}$ $V_{\text{pk-pk}} = 6.00 \text{ V}$	$V_{\text{avg}} = 2.88 \text{ V}$ $V_{\text{pk-pk}} = 17.77 \text{ V}$
Nylon (+)	$V_{\text{avg}} = 2.82 \text{ V}$ $V_{\text{pk-pk}} = 15.77 \text{ V}$	$V_{\text{avg}} = 1.31 \text{ V}$ $V_{\text{pk-pk}} = 10.37 \text{ V}$	$V_{\text{avg}} = 4.07 \text{ V}$ $V_{\text{pk-pk}} = 22.32 \text{ V}$

Table 5. Table displaying the average voltages and peak to peak voltages found during the second round of testing.

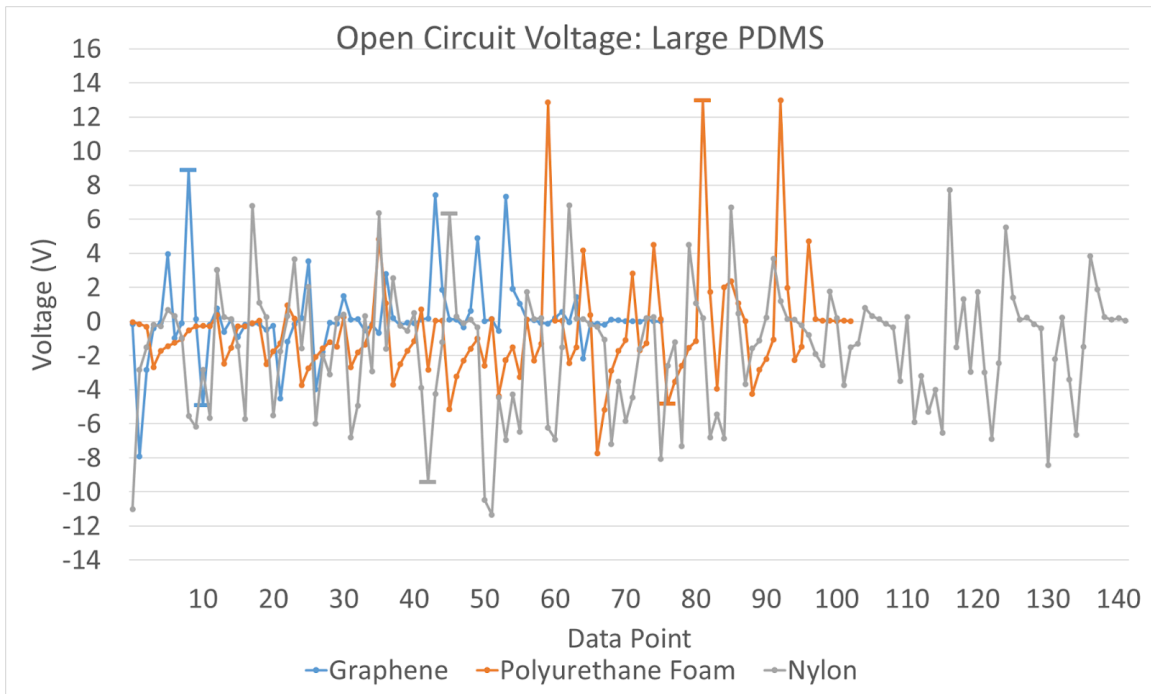


Figure 44. Graph comparing the TENGs made from PDMS during the second round of testing.

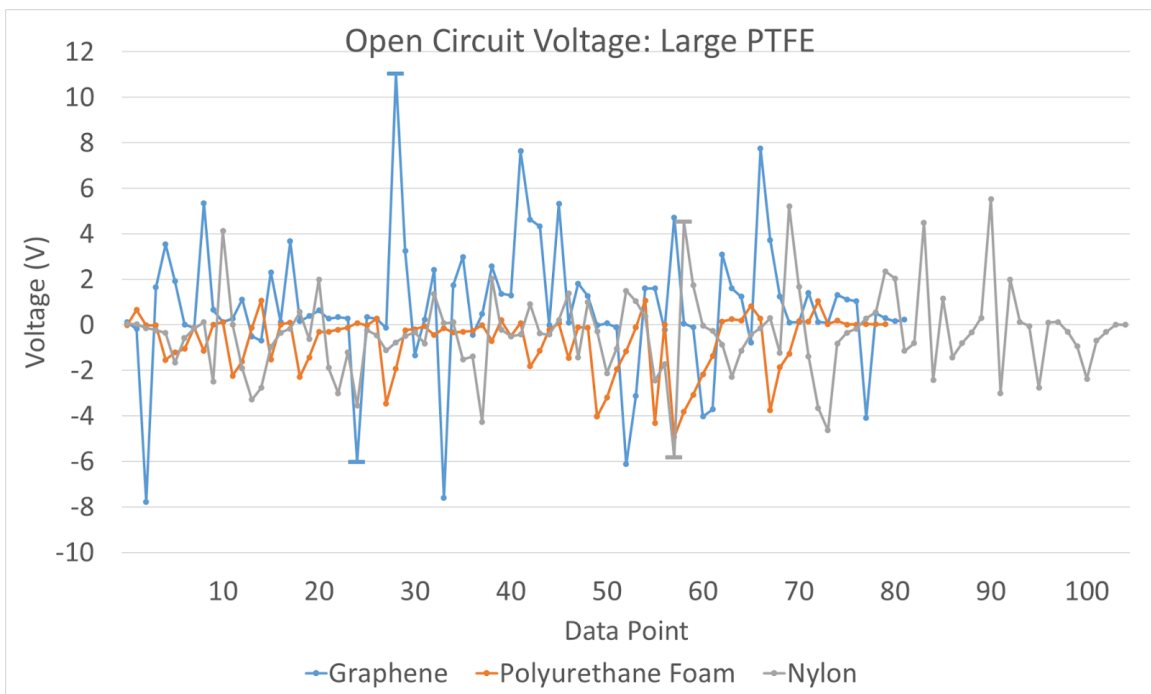


Figure 45. Graph comparing the TENGs made from PTFE during the second round of testing.

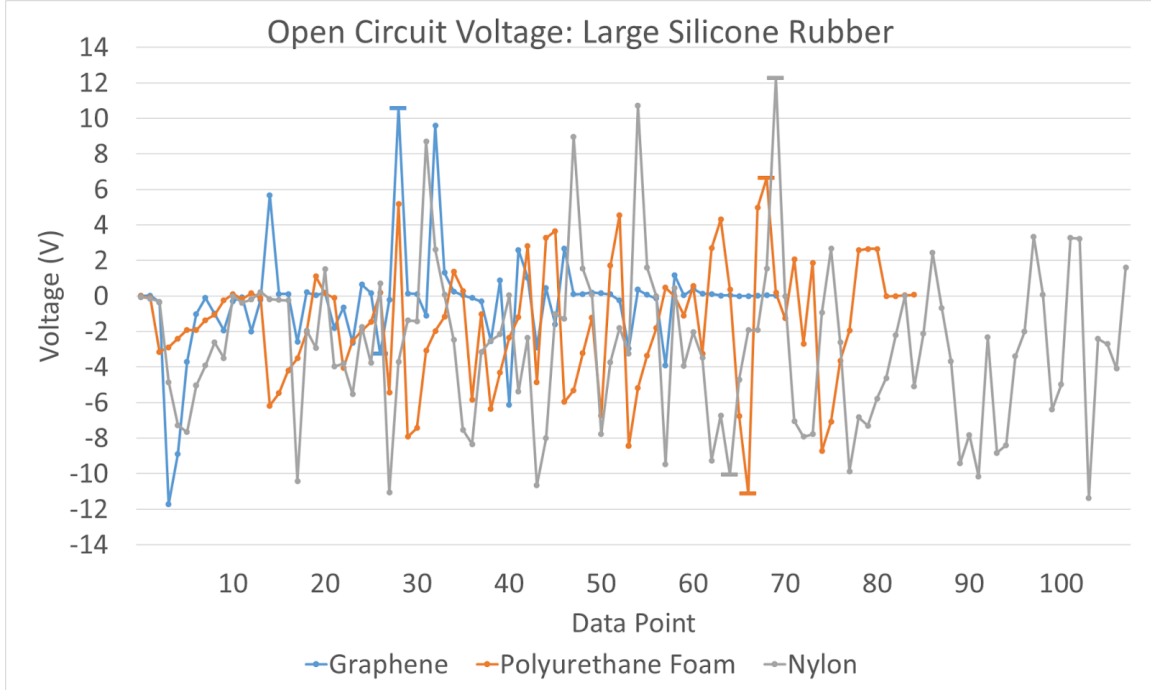


Figure 46. Graph comparing the TENGs made from silicone rubber during the second round of testing.

During this round of testing, PDMS and silicone rubber continued to outperform PTFE as negative triboelectric materials. It was at this point that the group decided to officially eliminate PTFE from further trials. Likewise, nylon clearly performed the best average voltage metric while generating comparative peak to peak voltage to polyurethane foam. The fact that nylon was much easier to work with and structurally resilient than the foam, in conjunction with its competitive performance metrics, made it the clear choice going forwards.

The increase in size from the 2.5" x 2" TENGs to the 7" x 4" TENGs led to a surface area increase of 460%, while the average voltage changed drastically depending on the material. For example, silicone rubber and graphene actually decreased by 0.29 V (a 16.3% decrease) while silicone rubber and polyurethane increased by 2.35 V (a 476% increase). However, discluding outliers, the increase in surface area led to an average increase in voltage of 101.6%.

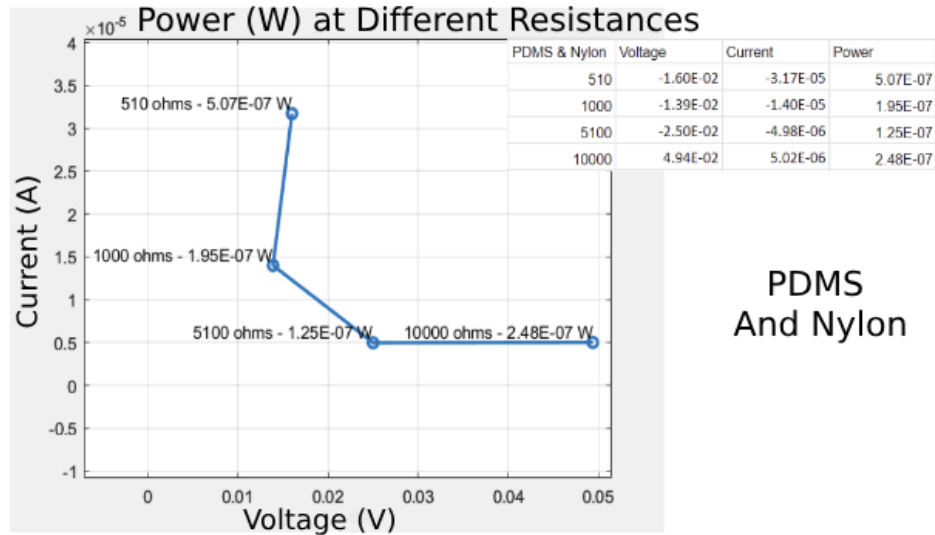
### 6.2.5 Testing Procedure: Round 3

Finally, the third round of testing confirmed how the materials would perform when there was a load in the circuit. This load allowed for the calculation of current, and therefore power, where the open circuit configuration only measured voltage, as mentioned in section 5.2. Untextured insole shaped TENGs, the design of which is discussed in section 7.1, were subjected to the drop test. However, instead of being connected directly to the DDM in the open circuit configuration, they were instead connected to a circuit with a resistor. The test was run multiple times, using 10k $\Omega$ , 5.1k $\Omega$ , 1k $\Omega$ , 510 $\Omega$ , and 100 $\Omega$  resistors. By doing so, the tests revealed which loads would lead to the optimal combination of voltage and current, maximizing the power produced.

For these tests, a layered nylon material was introduced. Four layers of nylon sheet were cut in the shape of the insoles and sewed together using nylon thread. This design change added to the durability of the nylon. Single sheet nylon TENGs were also tested to see if layering nylon would increase the output of the TENGs.

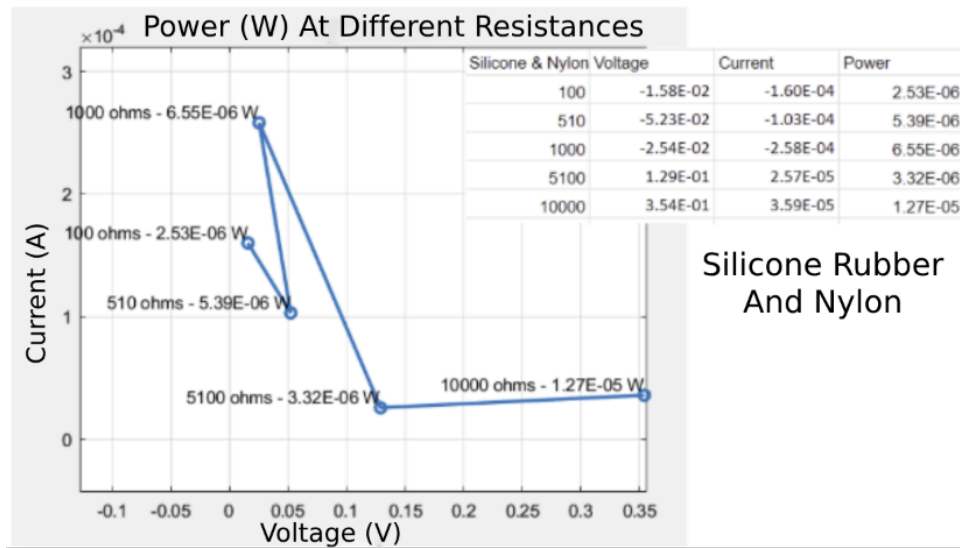
### 6.2.6 Results: Round 3

After measuring the voltage produced by a circuit with a known load, Ohm's law can be used to calculate current and power. This relationship was critical, as the project aims to maximize the power output of the TENGs. In aiming to optimize the combination of voltage in current, the graphs shown in Figure 47 and Figure 48 were produced.



PDMS  
And Nylon

Figure 47. Voltage, current, and power produced by a PDMS TENG at different resistances.



Silicone Rubber  
And Nylon

Figure 48. Voltage, current, and power produced by a Silicone Rubber TENG at different resistances.

Outside the outlier of the silicone rubber TENG tested at 1kΩ, the tests showed that the power produced was highest with a 510Ω resistor acting as a load, and that the silicone rubber TENGs generally provided a higher output than the PDMS TENGs. However, this test revealed another critical discovery. This third round of testing was the first involving the insole shaped TENGs. The thin silicone rubber insoles did not hold up well in this shape, while the PDMS insoles had no such struggles. This led the group to the conclusion that the minor increase in

power output was large enough to justify the less durable material, especially as half the group moved into boot integration and surface texturing, which would only weaken the material further.

#### 6.2.7 Final Material Selection

The final TENG materials used in the project were heavily influenced by the results of the test results described above. The tests showed that PDMS was the most viable material for several reasons. Both PDMS and silicone rubber outperformed PTFE. The potential output for both materials was similar, however, PDMS was much easier to work with. Silicon rubber did not adhere well to the electrode and was less durable when it came to testing. Repairs were often required after each test. Furthermore, PDMS was both cheaper and more readily available than silicon rubber. Nylon was chosen as the positive material because it produced the highest potential output. It also was the cheapest material and the easiest to work with. Layers of nylon could be sewed together with nylon thread to further increase the durability of the TENG. Copper tape would be used as the electrode due to its durability and superior adhesive.

## Chapter 7: Boot Prototype

This chapter discusses the design, texturing, and testing of the boot-integrated TENG produced by the project. This TENG is intended to be slipped into the standard Army combat boot and worn during long-distance patrols, taking advantage of the repetitive impacts of walking while under combat load.

### 7.1 Boot Integration

One of the major design choices faced by the boot-integrated TENG portion of the team was the physical integration of the TENG with the Army combat boot. The boots are specifically designed with weight, comfort, and durability in mind, and changing that design can impact the efficacy of the boots in the field.

#### 7.1.1 TENG Design

Army combat boots are manufactured by several different companies. While each company has their own take on the boot, they all must comply with a set of standards as defined by the Army. One of the standard features shared by all boots is the removable insole boot. These insoles allow the boot to dry faster and are replaceable, increasing the lifetime of the boot. The replaceable insoles of the Army boot provided the basis for the design of our boot-integrated TENG. Removing the insole of the boot creates space in which the TENG can fit into the boot without expanding the boot or adding a large amount of weight. Inserting the TENG in this way is also an extremely simple process and utilizes the largest possible surface area.

To design these TENGs, the insole of a size 10.5 boot was modeled in CAD, as shown in Figure 49. This model was then used to program a laser cutter and produce a wooden pattern. This pattern enabled the quick and accurate production of triboelectric materials in the same shape as the original insole. The wooden pattern and an example of these insole shaped TENGs are shown in Figure 50.

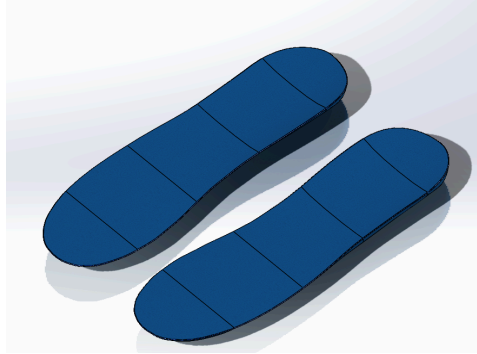


Figure 49. Solidworks model of the insole shape used to produce the boot-integrated TENG.



Figure 50. The wooden pattern and examples of the insole shaped TENGs.

As discussed in section 6, the positive triboelectric material for these TENGs was nylon. Sheets of nylon were sewn together for durability, attached to a copper electrode, and then taped to the original boot insole. This tape both kept the nylon from bunching up and ensured that the nylon stayed fixed to the bottom of the boot, creating the separation distance required for the TENG to function. The negative triboelectric materials, PDMS and silicone rubber, were

likewise cut to shape and attached to a copper electrode before being placed inside the boot. Both electrodes were attached to long wires so that the TENGs could be placed on the floor during testing while still reaching the DDM. These wires were then wrapped around electromagnets to absorb the electromagnetic interference from the other electrical components in the lab.

The TENGs sat on top of the original insole while inserted in the boot. While the TENG was originally intended to replace the insole entirely, it was found that the thin nylon sheets lacked the structure to be placed in the boot without the support of the insole. This cut down on the amount of space available in the boot, but the TENG still achieved the separation distance required to function. The TENG rested on top of the insole rather than underneath to preserve the thin wiring, which otherwise risked being crushed or torn by the close fit of the original insole.

## 7.2 Texturing

As discussed in section 2.5, TENGs often benefit from the addition of texturing to the surfaces of the triboelectric materials. This texturing increases the surface roughness and available contact area of a TENG without increasing its overall dimensions. While this project lacked the qualification and machinery required for many of the more complex micro-texturing methods, various abrasive macro-textures were added to the boot-integrated TENGs to increase efficiency and power output.

### 7.2.1 Texturing Methodology

The group used the wooden pattern to produce multiple insole TENGs, and each was given a different texture. A total of five textured insole TENGs were produced, each with a unique pattern to the textures applied. Various abrasive tools were used to produce these textures, including a knife, a dremel wire brush, clay cutters, and a cheese grater. These tools are pictured in Figure 51, and the insoles they produced are pictured in Figure 52.

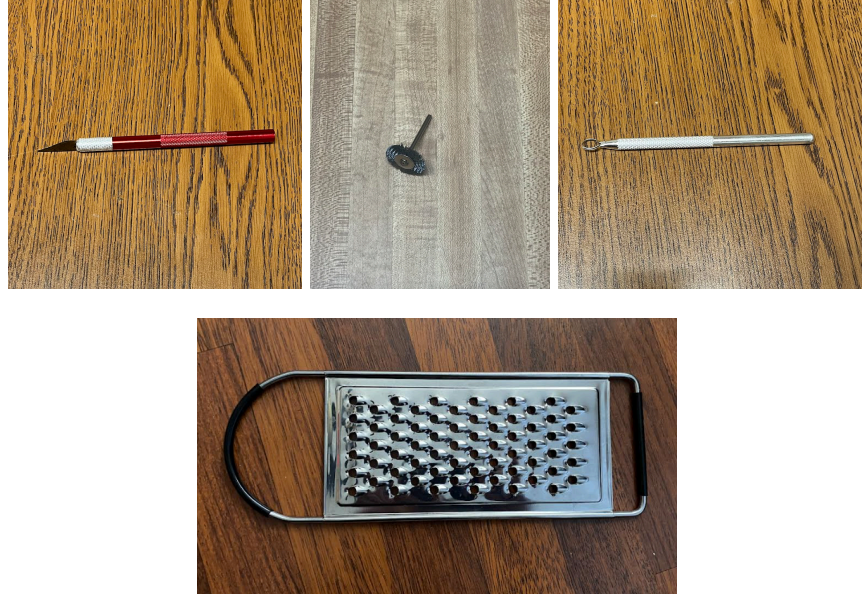


Figure 51. The tools used to create the insole textures. From left to right, top to bottom, the tools are the knife, the sandpaper, the dremel wire brush, the clay cutter, and the cheese grater.



Figure 52. The textured insole. From left to right, the insoles are the deep score, the shallow score, the dremel, the clay cutter, and the cheese grater textures.

The knife produced the deep score and shallow score textures, while the other tools each produced one texture, which was named for the corresponding tool.

### 7.2.2 Testing Methodology

The group tested the effects of the texturing by running the same tests they used for testing materials, but instead of switching out materials, they swapped out PDMS soles. Each

sole had a different type of texturing on the surface that was in contact with the nylon. The idea behind texturing the surfaces was to increase the amount of surface area in contact at a given moment.

The testing circuitry for these tests was different from the tests run in section 6. We used the single diode rectifier, discussed in section 4.2, and the diode bridge rectifier, discussed in section 4.3, to measure the energy generated across different-sized capacitors. With an understanding of the energy stored in the capacitor, we can calculate the energy per step, and with an estimate of how many steps someone takes per second, can calculate the power generated by each TENG.

To test out these different textures, we took 20 steps and then discharged the capacitor by connecting the probes of the oscilloscope to the capacitor. We then recorded the peak voltage on the oscilloscope after each step count test. This was repeated for each of the microtextures to see which was the best-performing TENG to move forward with.

### 7.2.3 Results

During the first tests of the boot-integrated insoles, the test circuitry utilized a single diode as a rectifier and a 0.1  $\mu\text{F}$  capacitor. Different numbers of steps were taken to judge the effect of the length of charging on the overall voltage produced per step. The graphs comparing the voltage produced can be seen in Figures 53 and 54.

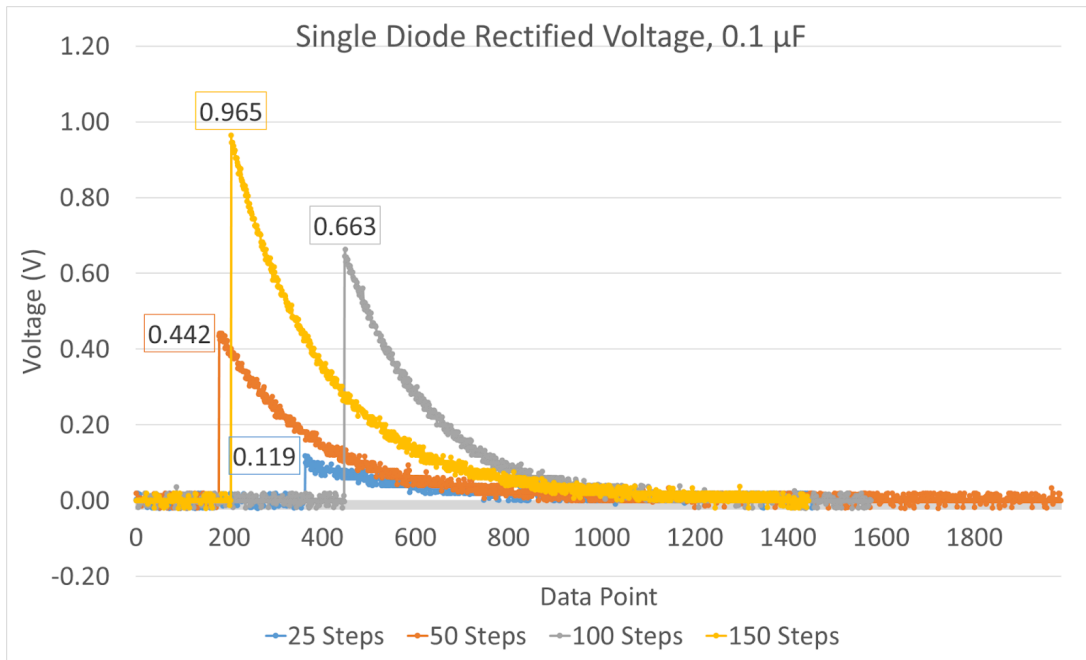


Figure 53. Graph comparing the voltage produced by different step counts in the single diode configuration across a 0.1  $\mu$ F capacitor.

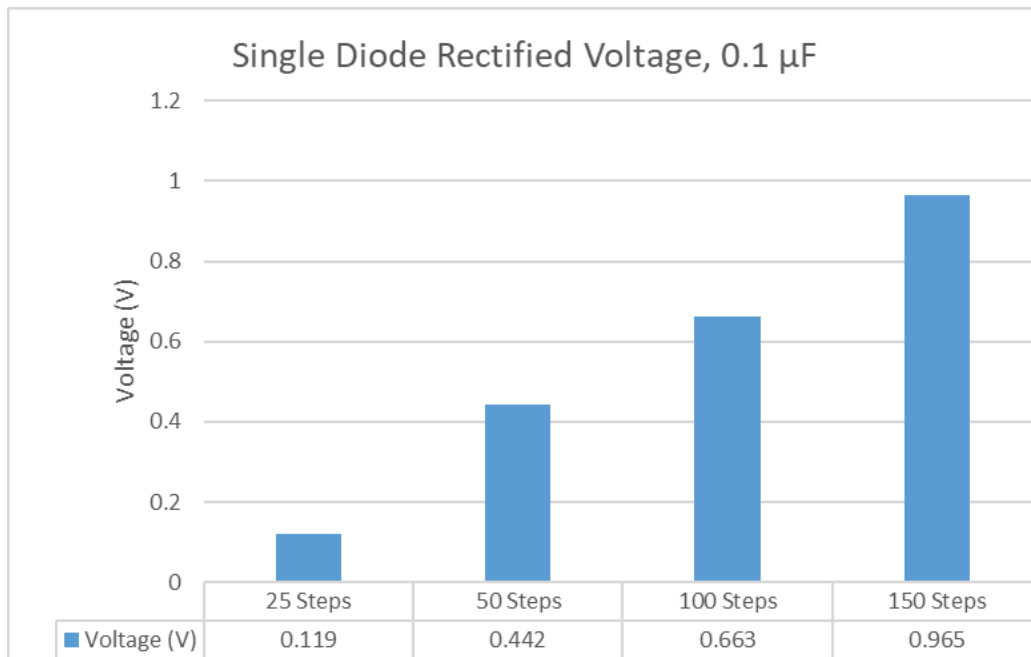


Figure 54. Graph comparing the maximum voltage produced by different step counts in the single diode configuration across a 0.1  $\mu$ F capacitor.

Once the voltage produced by the TENGs was measured, the energy stored in the capacitor in joules could be calculated using the equation

$$E = \frac{1}{2}CV^2$$

where U equals the potential energy stored in the capacitor and C equals the capacitance. This potential energy could then be divided by the number of steps taken to find out the amount of energy each individual step was producing. The results of these calculations are shown in Table 6.

Number of Steps	25	50	100	150
Voltage (V)	0.119	0.442	0.663	0.965
Potential Energy (J)	$7.04 \times 10^{-10}$	$9.78 \times 10^{-9}$	$2.20 \times 10^{-8}$	$4.66 \times 10^{-8}$
Potential Energy/Step (J)	$2.82 \times 10^{-11}$	$1.96 \times 10^{-10}$	$2.20 \times 10^{-10}$	$3.10 \times 10^{-10}$

Table 6. Table displaying the voltage, potential energy, and potential energy/step produced by different step counts in the single diode configuration across a 0.1  $\mu$ F capacitor.

Encouragingly, the amount of energy produced by each individual step tended to increase as the number of steps increased. While this trend would likely plateau at some point, it points towards improved results during a charging period with as many steps as a day's patrol. However, larger step counts like this are impractical in a lab setting, and so further tests with consistent step counts utilize a lower step count in favor of testing throughput.

The next test run utilized a diode bridge rather than a single diode to rectify the voltage produced by the TENGs. This diode bridge led to a large increase in the amount of voltage collected in the capacitor, as explained in section 4.3. This increase in measurable voltage resulted in more definitive test results when comparing the textured TENG materials, as shown in Figures 55 and 56.

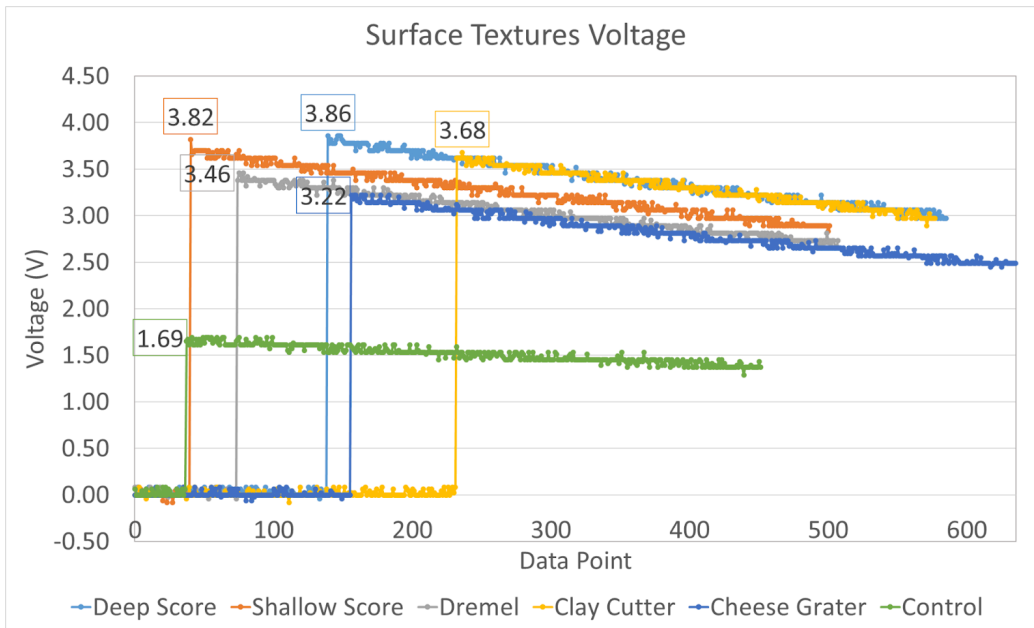


Figure 55. Graph comparing the voltage produced by the different textured insoles.

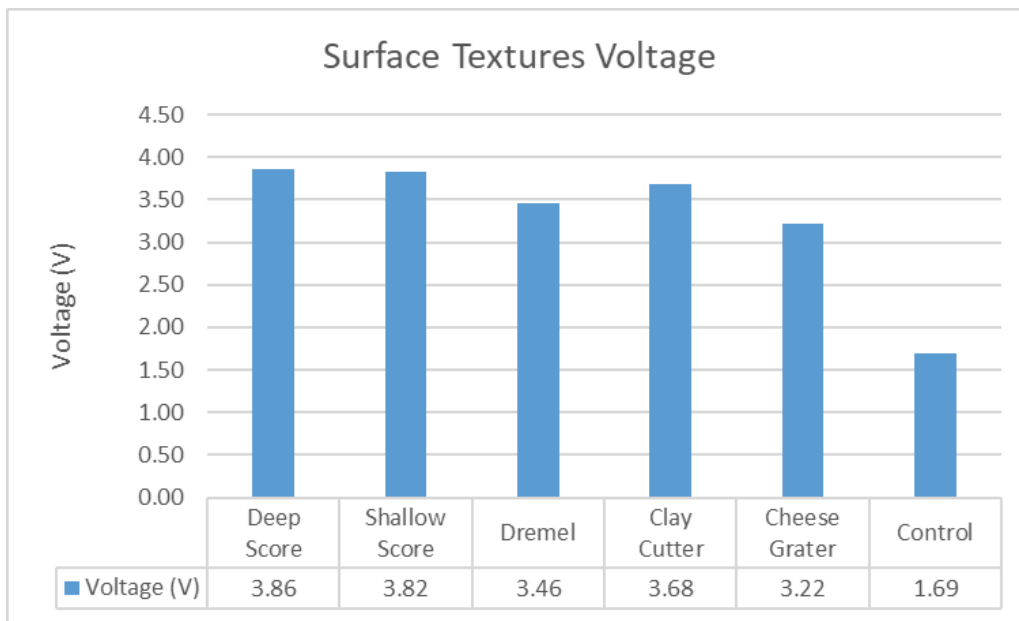


Figure 56. Graph comparing the maximum voltage produced by the different textured insoles.

Once again, the maximum voltage recorded during the test was then converted to potential energy using the formula

$$E = \frac{1}{2}CV^2$$

as shown in Table 7. The higher calculated energy per step corresponds to the higher voltages of the diode bridge.

Texture	Deep Score	Shallow Score	Dremel	Clay Cutter	Cheese Grater	Control
Voltage (V)	3.86	3.82	3.46	3.68	3.22	1.69
Potential Energy (J)	$7.45 \times 10^{-6}$	$7.30 \times 10^{-6}$	$5.99 \times 10^{-6}$	$6.77 \times 10^{-6}$	$5.18 \times 10^{-6}$	$1.43 \times 10^{-6}$
Potential Energy/Step (J)	$3.72 \times 10^{-7}$	$3.65 \times 10^{-7}$	$2.99 \times 10^{-7}$	$3.39 \times 10^{-7}$	$2.59 \times 10^{-7}$	$7.14 \times 10^{-8}$

Table 7. A table comparing the voltage, potential energy, and potential energy/step produced by the different textured insoles.

The score patterns, both deep and shallow, performed the best in this test, with the deep score pattern producing 3.86 V over 20 steps (a 128% increase). However, when compared to the untextured control insole, all of the texture patterns drastically increased the voltage produced, with an average voltage increase of 113.5%. This proves that increased surface area texturing provided is critical for increasing TENG output.

### 7.3 Springs

In an attempt to improve power output, we thought of implementing springs into the TENG. The idea behind this was to increase separation between the materials when they were not being pushed together. This would theoretically increase the charge between the materials by forcing the materials to separate further, subsequently increasing the electrostatic charge between them. To test this, we took disc springs made of stainless steel that were 1 ½ inches in diameter, and conical aluminum springs that were 1 inch in height and incorporated them into the TENGs.

Looking into the stainless steel disc springs, we found that they were a much sturdier option than the conical springs. Disc springs are meant to withstand extreme loads for long periods of time, which made them perfect for our use. While testing the disc springs, we found that they did too good of a job keeping the materials separated. There wasn't enough weight to force the spring to compress enough to allow the materials to touch. As a result, we decided to drop the disc springs from the project.



Figure 57. Conical springs used in attempts to increase TENG power output.

We chose aluminum springs in an attempt to help increase the positive charge, since aluminum has a slight positive charge. We took 4 springs and spread them out in between the positive and negative materials, trying to concentrate more springs at locations that bore more weight, such as the heel. The locations that had the most weight were the locations that needed extra resistance to separate the two materials. At first, the springs were too tall, so we cut the spring height down to  $\frac{1}{2}$  of an inch. This seemed to have more of an effect than the 1 inch, however, the overall change in electrostatic charge was negligible. When the textured TENGs and the springs were used in conjunction, they performed worse than the normal TENGs with no springs or surface modifications. As a group, we found that the springs did not make a big enough impact to pursue the idea anymore, and decided to drop the idea from the TENGs.

#### 7.4 Final Iteration

After completion of all the material, surface modifications, and spring tests, we concluded that the best material combination was the four layers woven together of nylon with the PDMS that had the deep scoring. After finding this to be the best selection for a practical prototype, we continued to run tests on it to see the best results that it could produce. Doing the test of letting the capacitor charge with each step taken and then discharging the capacitor once we took the desired number of steps we measured the data in the tables below. To note, this is the circuit that contains the diode bridge and just a single capacitor across the load.

For the 1.0 uF capacitor:

Number of Steps	20	50	75
Voltage (V)	5.427136	7.819095	7.58794
Energy (J)	0.0000147269025812	0.0000305691233095	0.0000287884167218
Energy per Step (J/step)	$7.3634512906 \times 10^{-7}$	$6.1138246619 \times 10^{-7}$	$3.8384555629 \times 10^{-7}$

Table 8. The table for a 1 uF capacitor prototype for energy per step.

For the 0.1uF capacitor:

Number of Steps	20	50	75
Voltage (V)	30.753769	60.904523	64.1
Energy (J)	0.0000472897153853	0.000185468046093	0.0002054405
Energy per Step (J/step)	$2.3644857693 \times 10^{-6}$	$3.7093609219 \times 10^{-6}$	$.27392066667 \times 10^{-6}$

Table 9. The table for the final prototype for energy per step.

The best choice moving forward would be to have the 0.1uF capacitor in the final circuit because the average energy per step was higher for all the number of step counts. To have this be

in a final prototype, a battery would then be in parallel with the capacitor across a diode shown in Figure 58. This would allow proper charge and storage of the energy without it reaching the max capacity of the capacitor which happened between 50 and 75 steps. Although having the battery in place would affect the voltage and energy generated from the TENG, it was never tested how much it would affect, ideally it would have no change or just a small voltage drop across the diode.

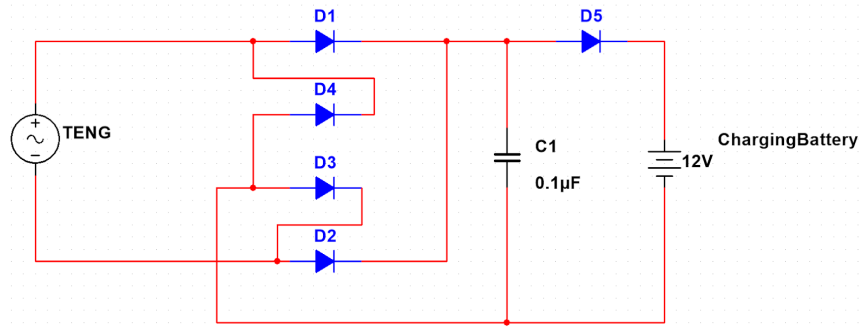


Figure 58. The final circuit.

# Chapter 8: Wind Prototype

## 8.1 Wind TENG Introduction

The boot TENG converts the energy used in walking into electrical power. Besides walking, there are many other types of energy to harvest energy from, and one prominent example of this is wind. The wind is a renewable source of energy that is commonly harnessed, with a wind turbine. What if we could use triboelectricity to harvest this wind energy? This chapter will explore our attempts to create a TENG to capture wind. Our goal was to test the viability of using the triboelectric effect to capture energy from the wind and generate the highest power output. Additionally, we could build on the knowledge and results from the drop and boot testing to inform us best how to build, test, and measure a wind powered prototype. From there we tried to improve our model, testing different TENG designs to try and increase our power output.

## 8.2 Experimental Setup

For our experimental testing setup we created a testing apparatus out of a wooden platform, and two rods standing up with string in between them shown below in Figure 59. The two rods had holes every inch, so we were able to vary the height of our design. As mentioned earlier there were two main wind TENG designs. The design, as shown in Figure 59, consisted of two triboelectric materials. One laid flat on the wooden board, we called that the stator. And the other material is held by the leading edge a small distance above the platform to create some separation to allow air to enter, which we call the flapper.



Figure 59. Wind TENG Testing setup.

### 8.2.1 Testing Procedure and Design

Since we were trying to compare the two different TENGs to see which was better, it was important to have a consistent testing procedure that could be easily reproducible. We also needed to make sure we could have a one to one comparison with the boot TENG so we could accurately and confidently say which model is more efficient. In order to do this, we created a standardized testing procedure similar to the boot TENG.

First, the size of the wind TENG was 3x11 inches which is the same size as the boot TENG. Next we attach our flapper to the wire which is 1 inch above the stator. Finally we used a hairdryer, and placed it as close as possible and blew cold air at a constant speed into the TENG and recorded our results using the oscilloscope.

### 8.3 Testing Results

In this part we will discuss testing several different aspects of the wind TENG; material and electrode placement testing, capacitor testing, material structure testing, free-standing mode tests, and wind speed tests.

#### 8.3.1 Materials and electrode Selection

We started off with the same six materials as for the boot TENG, three positive and three negative. The positive materials were nylon, graphene and polyurethane foam. And the negative materials were PTFE or Teflon, PDMS or neoprene, and silicone rubber. However, only some can flap effectively, the flappers are nylon(positive), PTFE(negative), and silicone

rubber(negative). While the stators are graphene(positive), polyurethane foam(positive), and PDMS(negative). Since each TENG design needs to have one positive and negative material, as well as a flapper and stator the possible pairing for each tests whereas followed nylon and PDMS, Graphene and PTFE, silicone rubber and graphene, PTFE and polyurethane foam, and silicone rubber and polyurethane foam. We also tested two different electrode setup, single electrode and double electrode as shown below in Figure 60. For the single electrode setup we used copper tape on the bottom side of the stator, while the flapper had no electrode as seen below. For the double electrode setup we tapped the electrode to both the flapper and the stator. For the material of the electrode we decided to only use copper, since that was what the boot group was using, and found to have had the most success with. We then measured the open circuit voltage of the setups to gather a baseline, and see which combination of materials and electrode setup would output the highest amount of voltage.

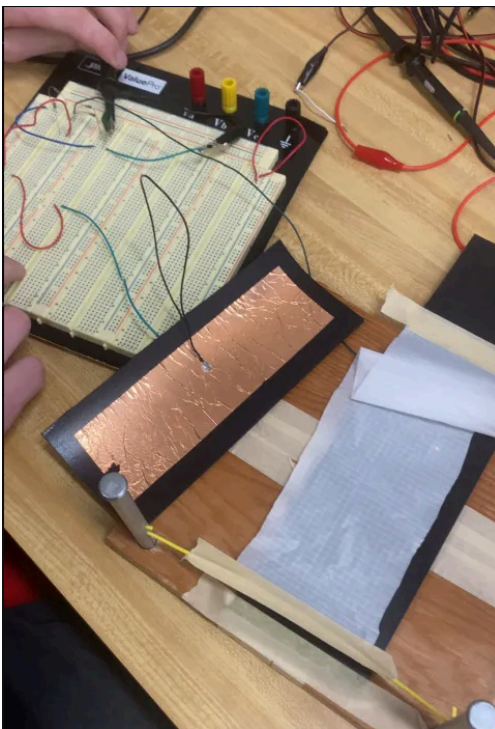


Figure 60. Wind Testing circuit setup.

The results for our materials and electrode testing in the form of open circuit voltages is shown below in Table 10.

Material (Flapper)	Material (Stattor)	Electrode	Single or Double electrode	Peak Positive Voltage	Peak Negative Voltage	Average Positive voltage	Average Negative Voltage
Nylon (+)	PDMS (-)	Copper	Single	5.16V	-5.06V	3.09V	-3.16V
Nylon(+)	PDMS(-)	Copper	Double	2.51V	-2.07V	0.32V	-0.49V
PTFE(-)	Graphene(+)	Copper	Single	2.2V	-3.08V	0.583V	-0.918V
PTFE(-)	Graphene(+)	Copper	Double	1.63V	-1.73V	0.406V	-0.400V
Silicone Rubber (-)	Graphene(+)	Copper	Single	4.3V	-3.84V	1.44V	-1.23V
Silicone Rubber (-)	Graphene(+)	Copper	Double	1.03V	-3.4V	0.75V	-0.78V
PTFE(-)	Poly Foam(+)	Copper	Single	1.32V	-1.27V	0.33V	-0.39V
PTFE(-)	Poly Foam(+)	Copper	Double	2.11V	-1.79V	0.64V	-0.65V
Silicone Rubber (-)	Poly foam (+)	Copper	Single	6.53V	-5.13V	1.89V	-1.81V
Silicone Rubber (-)	Poly Foam (+)	Copper	Double	3.07V	-2.79V	0.77V	-0.74V

Table 10. Single and Double Open circuit materials testing results.

In every test, the double electrode has much lower voltage output in terms of peaks, as well as averages. We believe the reason for this is because of the extreme reduction in frequency of flaps. The copper tape electrode caused the flapper to be much much stiffer, negating one of nylon's biggest advantages, causing it to flap less and therefore produce much less voltage. Additionally, copper tape is much less durable than nylon. From the table, we decided to use Nylon and PDMS double electrodes as it had the highest output within the double electrode setups. The reason for using the double electrode compared to the single electrode even when the single electrode outputted a higher open circuit voltage was because, when placing it into the full-wave rectifier we needed to have a return path, and this was not possible without having a double electrode.

### 8.3.2 Capacitor Testing

Now that we had a working model, we were looking for a way to measure power, not just voltage. Since the output of the TENG is just a bunch of impulses both positive and negative, we needed a way to rectify the negative voltages, and provide a smooth DC output. To do this we created a full-wave rectifier circuit. The full wave-rectifier will allow us to rectify the negative voltages, from there we then connect a capacitor to store the charge. After we build up charge, we discharge the capacitor and measure the voltage. We tested 3 different capacitors as well as 3 different time intervals. We measured the voltage, and since we know the voltage we are able to calculate the energy in the capacitor which is

$$E = (1/2) * C * V^2$$

which is then divided by time to get power. However, because the TENG output's, extremely low current, we had to use the (insert diode name) diodes, since they are meant for low current applications. However while doing our tests we noticed that the leading edge where the flapper is held does not flap very much. We then started reducing the amount of copper tape that we covered the flapper in so that only the leading edge has about one inch of copper tape on it as seen below. Originally we never tried this because we didn't think the electrons would be able to travel that far and still be captured. After trying this, we saw flapping behavior very similar to the single electrode test. Meaning our new model was flapping extremely fast, and could charge a capacitor.

0.1 uF capacitor

Time (sec)	5	10	20
Voltage(V)	73	149	240
Energy(J)	0.0002662299505	0.00111005	0.002885429821
Energy/sec(watts)	0.00005324599009	0.000111005	0.000144271491

Table 11. The results of the 0.1uF capacitor test.

1.0 uF capacitor

Time (sec)	5	10	20
Voltage(V)	10.4	15.379397	21.5
Energy(J)	0.00005360546397	0.000118262926	0.0002313411255
Energy/sec(watts)	0.00001072109279	0.0000118262926	0.00001156705628

Table 12. The results of the 1.0uF capacitor test

0.5 uF capacitor

Time (sec)	5	10	20
Voltage(V)	17.5	24.7	33.6
Energy(J)	0.00007649655671	0.0001528764462	0.0002817843161
Energy/sec(watts)	0.00001529931134	0.00001528764462	0.0000140892158

Table 13. The results of the 0.5uF capacitor test.



Figure 61. Baseline structure for the TENG (flapper).

The tables above show the results of the capacitor testing, and based on these results there is one capacitor that stood out. The 0.1  $\mu$ F capacitor had voltage and energy levels much much

higher than any of the other capacitors. The reason we were able to charge the capacitor to such high voltages is because the current is very minute, which means there is not much wattage being stored.

### 8.3.3 Material Structure Testing

Now that we realized we didn't need tape spanning the length of the material, it was possible to change the shape of the flapper. We tested these shapes by charging a 0.1uF capacitor for 10 seconds. Our baseline to compare these shapes to is the capacitor test with the same 0.1uF capacitor and 10 second interval which yielded a whopping 149 volts, and its shape is pictured just below. We tried six different shapes, each with a few variations. They will be discussed in the order of increasing levels of power output.

Firstly we created the two-stranded TENG. It is a sheet of nylon with one big cut in it and can be seen below. Note there was a copper tape electrode during testing, however, it had to be recycled for subsequent tests. With a voltage output of 31.1 volts or  $4.83 * 10^{-6}$  watts, this shape was not worth keeping.

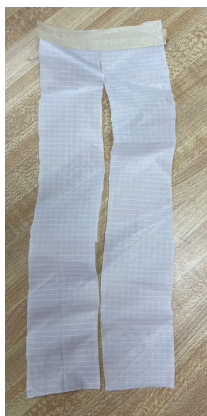


Figure 62. Two stranded structured TENG (flapper).

Second, is a TENG with three equally spaced slits spanning the width of the TENG, that is, perpendicular to the wind direction. We thought this might allow for more fluttering action, however this did not work as intended. Instead, the slits allowed air to leave the cavity below the

TENG without really pushing on it, meaning the TENG only produced about 40 volts or  $8.08 * 10^{-6}$  watts. This shape can be seen below, the slits have been emphasized for readability.



Figure 63. Three slit structured TENG (flapper).

Next is a shape similar to the first one, with some interesting results. The third worst shape was the four-stranded TENG. The four-stranded TENG produced about double the power as the two stranded with 61.7 volts and  $1.91 * 10^{-5}$  watts.

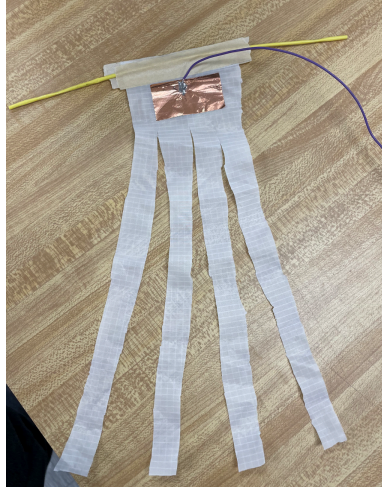


Figure 64. 4 stranded structured TENG (flapper).

The next shape is interesting because it was made to have some opposite properties to our baseline TENG shape. Our baseline has a shape that is slightly wider at the leading edge and somewhat tapers off towards the tail. This seemed to create an almost whip-like effect with the tail, so the logic was that it would create more power if we did the opposite and put the heaviest part on the tip of the whip. However, this did not really work and this shape only produced about 88 volts or  $3.91 * 10^{-5}$  watts, still well below baseline.



Figure 65. Inverted triangle structured TENG (flapper).

The next shape is a little more complicated than the 2D geometry, and it takes advantage of one of nylon's best aspects. This test involves taping the tip of the tail down to the testing platform as shown in Figure 66. This motion creates a standing wave effect that makes the flapper flutter extremely quickly. It's fairly difficult to measure the frequency of this TENG for a few reasons. Not only are the waves fast and hard to see even with a high speed camera, but it is extremely nonuniform, there are multiple waves and flaps and collisions per flap

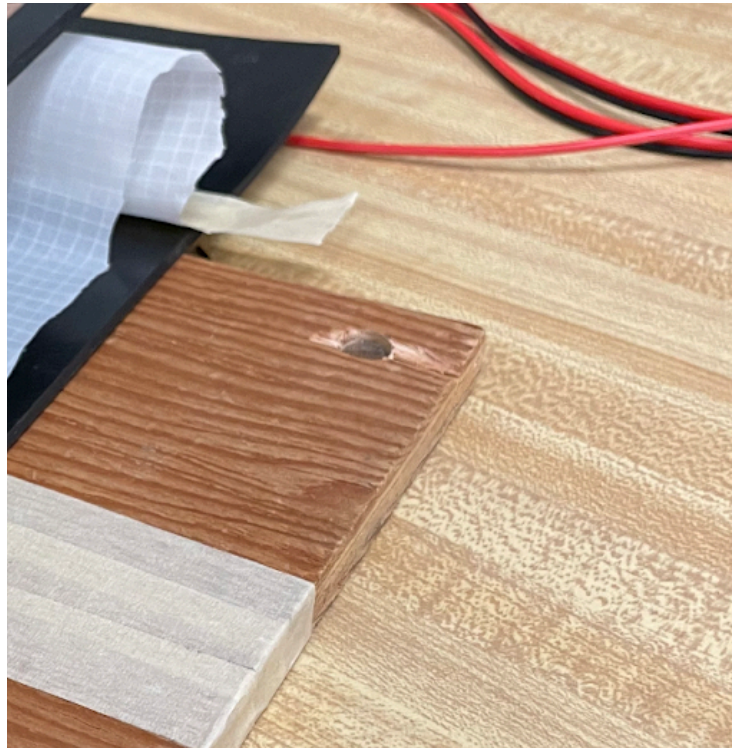


Figure 66. Pinned tailed structured TENG (flapper).

So without a way to measure the frequency we had only the produced voltage to test different locations for taping(pinning) the tail. Changing the distance changes how loose the flapper is, and the shape of the flap. We tested six distances from 0.3 inches to 5.6 inches. Their results are below in order of output.

Pinning Distance (in.)	Peak Voltage	Peak Energy (Watts)	Peak Energy (Joule)
Tail Pinned ~0.5"	74.4	$2.77 \times 10^{-5}$	0.000276558678
Tail Pinned ~0.3"	109	$5.89 \times 10^{-5}$	0.0005890760598
Tail Pinned ~2.75"	128.76885	$8.29 \times 10^{-5}$	0.0008290708365
BASELINE	149	$1.11 \times 10^{-4}$	0.00111005

Table 14. Results of Pinned Tailed structured TENG.

As you can see, this is the point where we were able to actually improve the output from the original design. This was a huge breakthrough although a somewhat confusing one. There did not seem to be much of a trend towards one exact spot. While we may not have optimized this aspect completely we still felt good about the results because we tested such a wide range of values and some of them were actually very successful.

### 8.3.5 Freestanding Mode Testing

At this point we had improved the voltage output a substantial amount. However, objectively there was still a lot of flapping energy not being harnessed to be stored in the capacitor. We were capturing all of the slaps on the way down using the stator, and none of the flaps on the way up. The final structural design change was editing the type of TENG we used. Below is an illustration of this type of TENG called a Freestanding TENG.

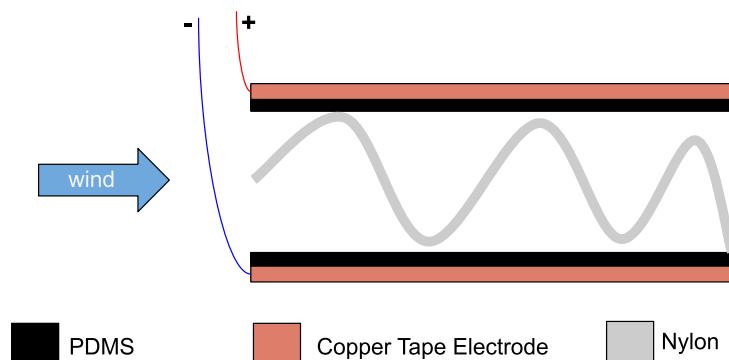


Figure 67. Diagram of freestanding mode wind TENG.

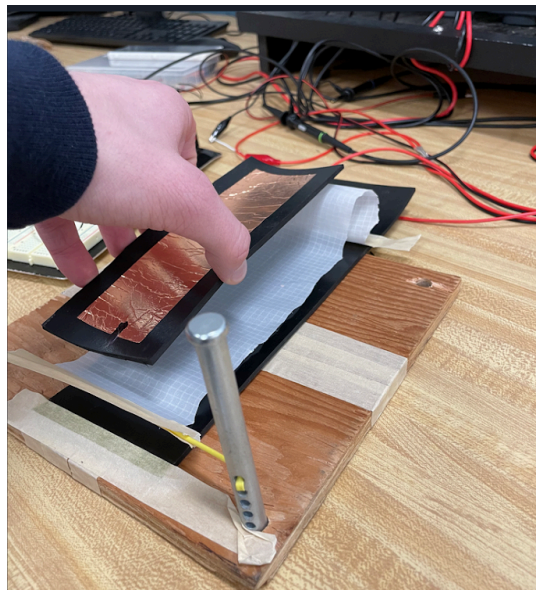


Figure 68. Freestanding mode structured wind TENG.

This design captures the energy from the motion of both flapping down as well as flapping up. We thought that this would massively increase the efficiency and total output, and we were right. We combined the best pinning distance of 5.6 inches with the extra layer creating the freestanding TENG. Our initial results yielded an immediate jump in voltage, with 493 volts and then 594 volts stored in just 10 seconds, and  $1.21 * 10^{-3}$  watts and  $1.76 * 10^{-3}$  watts.

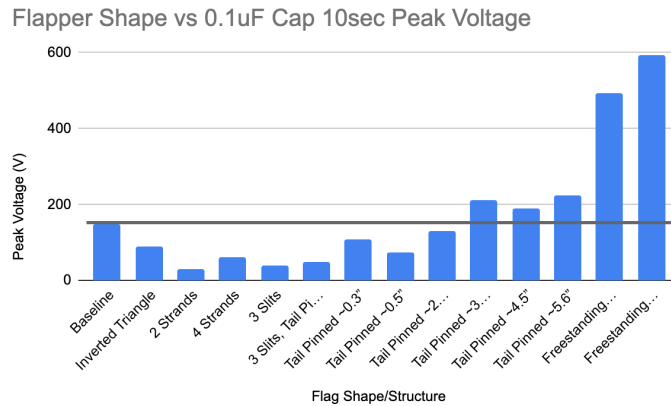


Figure 69. Graph comparison of TENG structured test results.

0.1uF charged for 10 sec

Shape(Nylon)	Peak V	Peak Energy (watts)	Peak Energy (joules)
Baseline shape	149	$1.11 \times 10^{-4}$	0.00111005
Inverted Triangle	88.4	$3.91 \times 10^{-5}$	0.0003911012255
2 Strands	31.092966	$4.83 \times 10^{-6}$	0.00004833862673
4 Strands	61.746233	$1.91 \times 10^{-5}$	0.0001906298645
3 Slits	40.2	$8.08 \times 10^{-6}$	0.00008080604417
3 Slits, Tail Pinned	48.2	$1.16 \times 10^{-5}$	0.0001163607026
Tail Pinned ~0.3°	109	$5.89 \times 10^{-5}$	0.0005890760598
Tail Pinned ~0.5°	74.4	$2.77 \times 10^{-5}$	0.000276558678
Tail Pinned ~2.75°	128.76885	$8.29 \times 10^{-5}$	0.0008290708365
Tail Pinned ~3.75°	213	$2.27 \times 10^{-4}$	0.002269841742
Tail Pinned ~4.5°	188.94473	$1.79 \times 10^{-4}$	0.00178500555
Tail Pinned ~5.6°	225	$2.53 \times 10^{-4}$	0.002534077532
Freestanding Mode	493	$1.21 \times 10^{-3}$	0.01214916807
Freestanding Mode	593	$1.76 \times 10^{-3}$	0.01760831074

Table 15. Chart comparison of TENG structured test results.

Our next test was to adjust the dimensions of the freestanding TENG. We tested three heights for the top layer of the freestanding TENG. The difficult part about this freestanding TENG is that the tail pinning distance and effective layer height correlate heavily. When a pinning distance is large, meaning the flapper is looser, the layer height needs to be high to capture the tall waves. Whereas when the pinning distance is low, meaning the flapper is pulled tighter, lower heights are better for capturing those waves. This is the reason we got some interesting results from testing the freestanding layer heights. We tested heights of 1, 1.5, and 2

inch separation between layers. Similar to the pinning distances, the layer height of 1.5 inches was the worst with 376 volts. And layer heights of 1 inch and 2 inches both produced around 525 volts. These testing results did not yield much useful data but it is interesting to see that there are multiple sweetspots, probably because of the repetitive wave nature of the system.

### 8.3.6 Wind Speed Testing

Finally, we tested blowing wind at different speeds in our model. Early in the year we had reasoned that if parachutes fall straight downward at around 15 to 17 mph but travel at about a 45° angle, then they would feel a wind speed of around 21 to 24 mph or 9.4 to 10.7 m/s. However, wind currents and motion, especially high up, are difficult to calculate. Additionally, the wind up in the sky stores more energy than that of our small hairdryer. For this reason for all tests before this we had the hairdryer on max speed. Using a hand held wind meter we were able to determine that our hairdryer has four speed settings ranging from 7.5 to 12 m/s or 16 to 26 mph at our desired distance. At lower air speeds, around 7.5 to 8.5 m/s the TENG only produced 328 and 334 volts respectively. At a slightly higher speed of around 11 m/s the TENG jumped up to around 511 volts. Throughout all previous tests we had been using the highest wind speed of around 12 m/s.

### 8.4 Final Design and Future Work

For the final design we decided to use a freestanding mode TENG with a 0.1uF capacitor which yielded which is the greatest out of all the combination. We were able to charge the capacitor to 593V in 10 seconds. Giving us an energy of 0.0175 J, with a power of  $1.76 * 10^{-3}$  W. For future work, we would want to place a battery in parallel with the capacitor to allow it to power low-wattage sensors as mentioned previously , as well as being able to incorporate the design within a parachute, since the wind speeds will be much higher, and we can potentially harvest more energy. Making the design more efficient would also greatly improve the performance of the TENG, because as of right now our efficiency is 5.07%.

## Chapter 9: Applications

This chapter discusses the potential uses for the TENG after all of the testing has been concluded. We refer to the power and energy results from the wind and boot TENGs and relate them to electronics that store or use power. Additionally, we mention how these TENGs can be put to use in the military based on the results we received.

### 9.1 Uses for Power

The concept of the project relating it back to the start was to create a TENG that could generate power. After constructing and testing many different TENGs, we obtained insights into how useful the TENG we constructed could be relating to what the military wanted. We looked into many different potential uses for what this energy would go to and how relevant they would be.

#### 9.1.1 Battery Charging

The first idea for this project was to charge a battery with the TENG, either by wind or walking. This has many different potential applications since it could be easily removed once done charging and gone into anything that needed a battery to charge it. This would help soldiers not need to bring additional batteries when in a setting where batteries are not easy to come by.

The smallest common everyday use battery is a AAA battery, which has a 1.5V output, and on average 1200 mAh lifespan. To calculate the energy in a battery, we can use the formula

$$E = Q * V$$

where E is the electrical energy in Joules J, Q is the quantity of electric charge in coulombs C, and V is the voltage potential difference in Volts V. Using the conversion of mAh to charge we use,

$$Q = 1200 \text{ mAh} * \frac{3.6 \text{ C}}{1 \text{ mAh}}$$

which equals 4320 C. Now using the equation for energy we get,

$$4320 \text{ C} * 1.5 \text{ V} = 6480 \text{ J}.$$

Based on the best-performing boot TENG which had an average energy per step to be  $3.7093609219 \times 10^{-6}$  J, it would require 1.7 Billion steps to fully charge this battery. This is unfeasible as it is not possible to charge a battery in any realistic amount of time.

The wind testing on the other hand proved that it had much higher potential. The highest energy output was the freestanding TENG, which had an output of 0.001758245 Joules/second or Watts. The freestanding has its problems, but even the highest with the materials on the same surface had an output of 0.000253125 Joules/second. The freestanding TENG would require 1023.7 hours to charge a AAA battery, and the other TENG would require 7111.1 hours to fully charge the AAA battery. This is better than the boot TENG but it is still not enough to be feasible.

### 9.1.2 Passive Sensors

Another idea of what to do with the energy generated by the TENG was to have passive biosensors on the soldiers to understand their condition. After our meeting at the Natick Soldier Center, our project sponsor Justin Silvia, and other people in the meeting showed their interest in this concept because this would allow health monitoring to check on their physical condition, as well as monitoring their situational awareness. By integrating passive biosensors into the soldier's gear, such as uniforms or wearable devices, commanders and medical personnel can remotely monitor vital signs and physiological parameters in real time. However, as said in the meeting, they do not want to have to change out batteries to constantly check on these things, they want it to be self-powered, so that is why a TENG has the potential to be useful for this scenario.

One sensor that had high interest was an accelerometer. Accelerometers allow for activity monitoring, so it would track the soldier's movements, providing data on their physical activity levels, including walking, running, climbing, or even sudden movements like falls or impacts.

### FUNCTIONAL BLOCK DIAGRAM

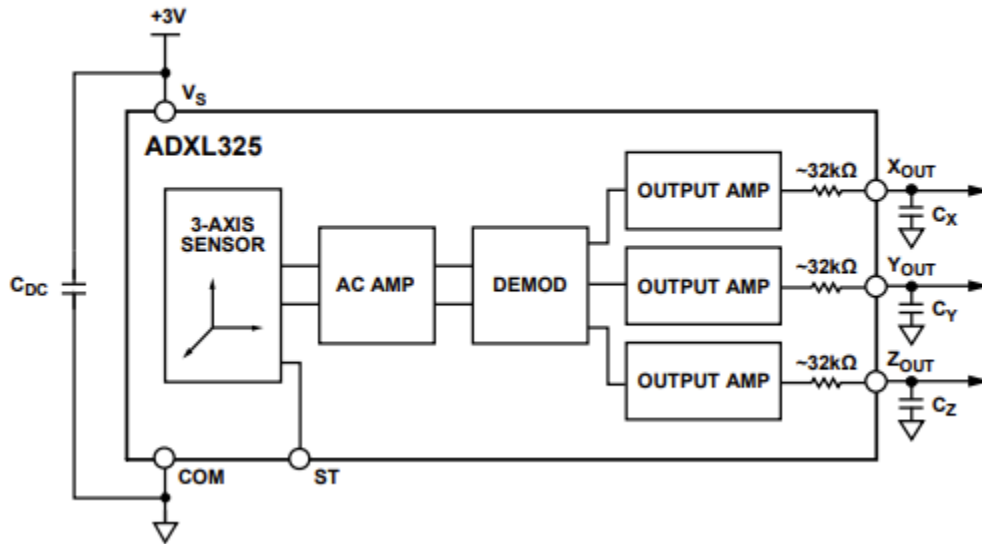


Figure 70. The circuit diagram for an accelerometer [33].

The requirements to run this are in the chart below. The power requirement to run the accelerometer is 1.05mW to keep the accelerometer running. It is unsure of the exact power generated from the boot TENG because that is dependent on the frequency of steps, but with 3.70936092  $\mu\text{J}$  per step, it would need 283 steps per second to meet the requirements. This is not possible, however, this is still much more likely than using this to charge a battery. In the wind application, however, assuming the output tested was constant, the freestanding TENG would be able to power this as it had an average power being 1.758245mW. The other wind TENG had an average power of .253125mW, so it would need to improve 4.148 times.

POWER SUPPLY					
Operating Voltage Range		1.8		3.6	V
Supply Current	$V_S = 3\text{V}$		350		$\mu\text{A}$

Figure 71. The specifications to run the accelerometer sensor [34].

Another sensor that had a high interest was a heart rate monitor. This would allow the monitoring of the soldier's cardiovascular health and exertion levels. This can help assess the soldier's physical condition, indicating whether they are experiencing stress, fatigue, or overexertion. This could be done in multiple ways including a pulse sensor,

photoplethysmography, or an electrocardiograph (ECG). The one with the least power consumption is the ECG with the spec sheet listed below.

## Electrocardiography (ECG) Sensor Data Sheet

### SPECIFICATIONS

- > **Gain:** 1000
- > **Range:**  $\pm 1.5\text{mV}$  (with  $V_{CC} = 3\text{V}$ )
- > **Bandwidth:** 0.5-100Hz
- > **Consumption:**  $\sim 1\text{mA}$
- > **Input Impedance:**  $> 100\text{G}\Omega$
- > **CMRR:** 100dB

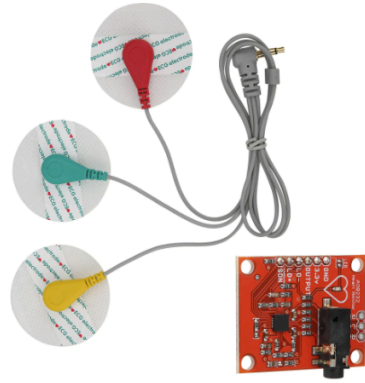


Figure 72. The ECG sensor and the data sheet for it [35].

The requirement to run this would be 3mW of power, which is slightly higher than the required power for the accelerometer.

Another sensor that the military was interested in was a temperature sensor. Temperature sensors are used to evaluate environmental conditions and to help understand troop performance as well as equipment performance. It allows soldiers to adapt their clothing and hydration to maintain peak performance.

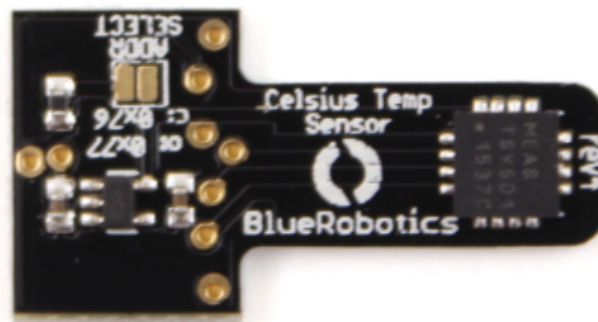


Figure 73. The block diagram for a temperature sensor [36].

Using the spec sheet below, this sensor would require 0.135mW to run. Using the best-performing energy per step TENG, this would need about 36 steps per second to run. Although still not possible to do, this is an option for the future, because using the improvements talked about later in the paper, the power could be increased much more. Both applications for the wind TENG would be able to constantly power this sensor.

POWER SUPPLY					
Supply Range	$V_s$		2.7	5.5	V
Supply Current	$I_{SY}$ (ON)	Unloaded		50	$\mu A$
Supply Current (Shutdown)	$I_{SY}$ (OFF)	Unloaded	0.01	0.5	$\mu A$

Figure 74. The specifications to run the temperature sensor [37].

For the wind application, the military was interested in having a UV sensor attached to the parachute. Too much UV exposure starts to break down the materials used in parachutes, making them a potential safety hazard. So by incorporating UV sensors, military personnel can track UV levels during parachute deployment, to make sure that the equipment is safe to use.

To be able to use this sensor, it requires 1.55mW of power. Comparing this to the results from the wind TENG, the freestanding TENG would just barely be able to run this sensor, while the other would need a slight improvement to run it.

Item	Min	Typical	Max	Unit
Operating Voltage	3.0	5.0	5.1	VDC
Current		0.31		mA

Figure 75. The specifications to run the UV sensor [38].

## 9.2 Energy Comparison

Using triboelectricity is one of many ways of generating passive electricity. In this section, we will compare other options for harvesting energy both for efficiency and for its ability to be used in practical settings.

One other option was harnessing solar energy, either by attaching a panel directly to a soldier's equipment like their ruck or helmet or by strapping on a solar-powered battery pack on a

pocket or strap and having it dangle. To measure energy we can use this formula

$$Energy = Area * Efficiency * Insolation * Time$$

which can be compared directly to the size of our TENG which was 21 square inches. The average efficiency of a solar panel is 20%, and the average insolation of a solar panel on a house is 300 watts per square meter. This could be completely different for military use since it depends on the terrain, so it could vary in how useful it could be. Using

$$Energy = 0.0135484m^2 * 0.2 * 300W/m^2 * 1s = 0.8129J$$

for one second. This is higher than both the wind TENG and the boot TENG, however, it has its drawbacks, as it is harder to implement into soldiers' equipment. Additionally, they are much easier to damage, and if damaged they cannot be fixed, they will need new solar panels.

Another option for harnessing energy would be using piezoelectricity. Piezoelectricity, very similar to triboelectricity, is a way of harvesting electrical energy by putting a mechanical strain on materials. The difference is however piezoelectricity doesn't move electrons through materials, it compresses metal or crystals which generates electricity. To find energy we use the formula

$$E = 1/2 * m * v^2$$

We assume that a quarter of a person's weight goes into each step, and each step is about 15 cm off the ground, meaning the velocity would be 1.714 m/s. Using this we calculate Energy to be

$$.5 * 40kg * 1.714m/s = 34.28 J$$

This however is the same estimation for energy generated from triboelectricity, except, we know from measuring that this is not similar to the results. This has to do with the piezoelectric constant that varies from material to material, but a common material is PZT which has a constant of 200 pC/N. This means that only a small amount of charge is getting through. Since

$$F = m * a$$

we can find that the force in Newtons which is

$$40kg * 9.81m/s^2 = 392.4N$$

If the material is 200 pC/N and there is 392.4N, there is 39.24nC. If that amount of charge gets through, then it is estimated that the Joules measured from the kinetic energy multiplied by the amount of charge would give a better estimate which would be 1.345uJ for one second. This is

an estimation, to find out this would need extensive testing to find out the efficiency of this. That being said, it would be just as easy and safe to implement on a soldier as a TENG.

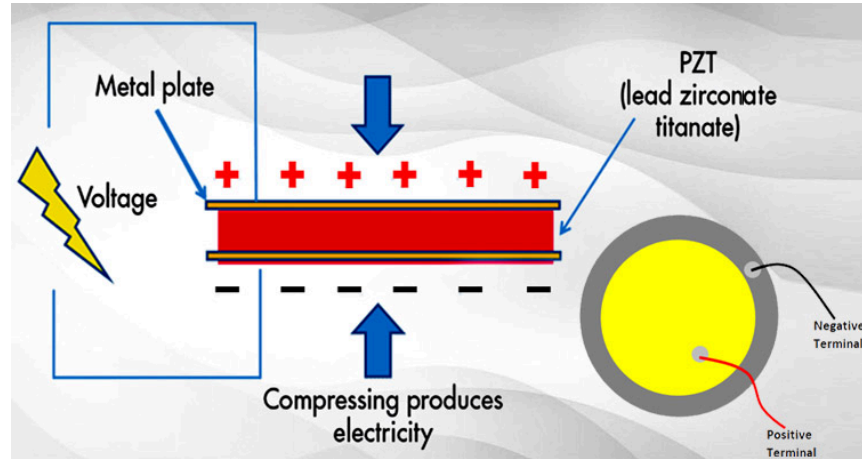


Figure 76. A diagram of how piezoelectricity works [39].

### 9.3 Potential Military Uses

#### 9.3.1 Parachute

Missions involving parachutes in the military have the potential to be efficient sources of energy for soldiers' gear. Wind energy can be converted into electrical energy using the fabric of the parachute as the kinetic energy harvester. The friction created by wind at high altitudes on the parachute can be turned into electrical energy to be used or stored during the mission. High altitude low opening (HALO) jumps would be able to generate a good amount of power for the mission alone. Another approach to adding TENGs to parachutes could be to help track the condition or lifespan of parachutes. Parachutes begin to break down after being exposed to UV light for a long enough period. UV light sensors could be added to the parachute, which would then track how much UV light the parachute receives. From there, units could access this data and better maintain their parachutes and possibly other equipment, reducing accidents while parachuting. One could also install GPS sensors, with the ability to track location, speed, direction, and altitude. This could help soldiers become more proficient at aerial insertions, or it could help headquarters track the mission progress without direct communication with the

soldiers. Any kind of aerial insertion involves high levels of friction between the parachute and wind, making it a reliable form of energy no matter where the soldiers may be deployed.

### 9.3.2 Soft Structures

Temporary shelters like Rapid Deployment Tents could have some kind of wind TENG built into the tent, to harvest energy from the wind while deployed. The wind energy harvested by these TENGs could be used to supply power to lights used within the tent, air conditioning units, or electrical outlets to help charge devices. Having a flag that attaches to the top of the tent would be an efficient way to harvest wind energy, or maybe designing a tube that funnels airflow into one spot to maximize potential energy output. Having different layers on the outside of the tent just to harvest any wind that contacts the tent at any point could be another possible use, adding to the efficiency of the structures. Similar to parachutes, as long as there is wind, then these tents could harvest some energy to help power equipment around the forward operating base. This would cut down the need for batteries, potentially cutting out the use of battery resupplies altogether.

### 9.3.3 Patrolling

Triboelectric energy harvesting has no limit of applications within the military. The main applications we have been focusing on involve patrolling applications. Any mission in which soldiers are moving by foot for any amount of time has the potential to involve triboelectric boot harvesting. Generating energy as one walks would be of help to the soldiers on the mission, as they wouldn't have to rely on using one-time use batteries as much, allowing them to travel further and with less stops for resupply. Equipment like GPS, night optical devices, weapon optics, communication devices, and headlamps would be powered by TENGs, or it could open up the possibility of adding biometric sensors to soldiers in order to help monitor and keep them healthy. It also cuts down on the logistical side of organizing batteries to be sent to patrols constantly. Sending out batteries with food and water every time a unit requests a resupply takes time, and adds one more thing that logistical units would need to consider, plan, and pack for each resupply. It would cut out a resource that would otherwise need to be tracked and replaced during missions, giving soldiers more time to focus on completing the mission. Soldiers utilizing

this technology would make them more self-sufficient, reducing logistical loads on both the patrol and supply chains, but also give them a reliable source of energy to be used. Another option for potential patrolling uses would be to attach wind TENGs to convoys, where the vehicles generate some power just by moving. This would be a great way to keep the vehicles as a reliable source of power for charging any dismounted unit equipment, as previously mentioned before.

# Chapter 10: Broader Impact

## 10.1 Engineering Ethics

This technology upholds all the Engineering Ethical Standards and then some. We worked in conjunction with the U.S. Army to fulfill their goals while following their guidelines. We helped increase the understanding of triboelectric power production by conducting experiments and performing extensive research. Dealing with electricity on the human body can be risky, so we made sure that our prototype was safe for human use and was not going to cause harm to anyone in the process of harvesting energy. Using technology at WPI, we could design a prototype that was safe for use in all kinds of situations. All of our reports about our technology were accurate, and no information was added or withheld to make our report look better. We met with our sponsors once a week at least, to keep them updated with what we were working on and to make sure we weren't going in a direction they did not desire. Lastly, we stayed within our expertise. Using the advice we received, we focused solely on our set objectives, and did not try to wander outside our focus area.

## 10.2 Environmental Impacts

This technology is actively working to reduce the amount of non-renewable energy sources used around the world. The potential impact of this technology is to vastly reduce the amount of batteries used by the U.S military. Additionally, if applied elsewhere this tech has the ability to have much greater impacts such as powering other independent, lower power systems, replacing more batteries and waste. If small independent systems powered themselves and we did not have to run or transfer power to them, the efficiency of the system would be massively increased. Also, these systems would not rely on a central power source that could fail, rendering the system powerless. A boot TENG allows power generation alternatives to fossil fuels in remote places. Though it may seem like an extremely small amount of power, this is an important step towards the pursuit of clean energy.

### 10.3 Economic Impacts

The economical impacts of this technology would be extraordinary. A boot TENG would allow for power generation in areas where maybe costly fossil fuels would have been used. A wind TENG on a parachute would eliminate battery cost of the sensors, as well as reduce waste by keeping more accurate data of the condition of parachutes. While eventually the TENGs would need to be replaced, they would need to be replaced far far less than the current system, batteries. The TENG is made of very cheap materials, one of them being Nylon, which the parachute is already made from. These low material costs improve the economical impacts of this technology even further. While the wind TENG is less efficient than a wind turbine at energy harvesting, for now, the TENG's material and manufacturability costs are exponentially lower.

### 10.4 Societal and Technological Impacts

Societally, a lot of people support renewable energy. People will see the army using green energy and perhaps influence their perception of the military and U.S government for the better. As far as technological impacts, I think the boot TENG technology will open people's eyes to the fact that there are other ways to capture renewable energy other than wind, water, and solar. And for the wind TENG it shows people that there are other ways to capture wind other than a turbine. The impact of new renewable technologies on our society is that it helps us inch closer to solving the energy crisis.

# Chapter 11: Conclusion

Based on the research done in previous years, we were able to build off of the TENGs that were created in years past without a much greater power output. Rather than building a prototype, we spent our time testing with the raw TENG as much as possible to generate the most power. Additionally, we improved on the way to understand the TENG through an electrical perspective, as we understand the energy that can be created as well as the voltage and current which was new. Improving the way of understanding the power in this system puts into perspective the functionality that a TENG could have in a real-world application. In the future, groups will look at the following improvements that we made as a building-off point, rather than starting from scratch. Additionally, following the continuations that we made, which we didn't have time to do, would greatly increase the practicality of the TENG.

## 11.1 TENG Improvements

Over the course of the year, we had many ideas for improving the TENG and some of the tests succeeded and some failed. This section will go into three of the biggest successes that we had during testing, and what went into them to make them work well.

### 11.1.1 Texturing

The introduction of textured triboelectric materials led to one of the biggest improvements in TENG voltage production during the course of this project. Texturing in literature can be a complex and expensive process involving specialized machines and materials. However, due to the lack of access to these machines, this project utilized basic abrasive hand tools and achieved impressive results. Though the texturing processes and implements utilized were very basic in nature, even the worst performing textured TENG nearly doubled the output of the unaltered control TENG. The increases in available contact surface area were a critical part of improving the boot-integrated TENG's performance.

### 11.1.2 Components

One of the changes that resulted in improvements was choosing components that fit into the application. Components with suitable specifications are crucial for ensuring the proper functionality and efficiency of the system.

One example of this is the diode in the diode bridge circuit. The diode we used in our saved testing was the HP2800 Schottky Diode. This diode has 2 major benefits, the first is having a low voltage drop across it, and the second is the picosecond switching speed. Because the TENG changes from positive to negative voltage so quickly, a high switching speed is required to allow proper flow of current to the energy storage device. In previous tests, we had used a few different diodes, and the output would have negative values for voltage, so the diodes in the circuit were not switching fast enough and were discharging the capacitor. Making sure components fit the application you need them for is very important.

Additionally, due to the laboratories in Atwater Kent having a lot of electrical devices, there was a lot of noise due to electromagnetic interference. To combat this, we used a ferromagnetic core which was wrapped around the wires going from the TENG to the circuit. Ferromagnetic material absorbs high-frequency noise and reduces interference.

### 11.1.3 Building Off of Feedback

One improvement we made was not on the manufacturing of the TENG but rather the time management of researching prior to starting tests. Using the results from years past was a way to start at a further point, so we didn't need to start the testing process completely from scratch. In the last 2 years, they did testing on many different circuit designs to rectify the TENGs output. They tested different rectifiers one year and then tested them again the next year. We just looked at what we needed the output to be and chose two circuits that would be able to achieve this. This saved time, so we were able to test more as we didn't spend time doing what was already known. Also, using the testing apparatus that was made by the previous group made it easier to progress. Rather than designing and constructing a new testing rig, we used the one they had made the previous year and then made improvements to it afterward.

## 11.2 Continuation

Although the results were not as hoped for, this project was not a failure. The improvements that were made during the terms of testing yielded great improvement in output power. If instead of starting over with material testing and creating an entirely new way of benchmarking the testing, using the results in this paper, this project can improve greatly. However, there are still many recommendations we have to improve these TENGs to make them have a useful application in the military.

### 11.2.1 Integration with Soldier Equipment

Having the TENG in a prototype is the only way to properly understand how functional this can be in real-world applications. We ran out of time to place the TENG in a boot and get results walking over a long period of time. We recommend getting the TENG into a boot or on a parachute or any other place on a soldier to see the practicality of this, as well as showing the sponsor a real prototype of this.

### 11.2.2 PCB

In order to integrate the TENG with soldier equipment, the circuit requires being put onto a printed circuit board (PCB). PCBs are small, typically green circuits used in the final product for anything containing electronic components. This is important for the improvement of the TENG since it allows for better reliability, and finding out a way to properly integrate this system onto a soldier. With just a standard breadboard, there is no way to properly find out if this can fit a soldier comfortably. Additionally, they take time to outsource or make, so if having a final prototype is a goal, doing this early is important.



### 11.2.5 Sliding Testing

Sliding testing was not thoroughly tested. Originally, we had planned on creating a motor powered machine that could perform a repeated sliding motion with two materials, however, we never finished designing the machine, and therefore weren't able to test the sliding capabilities of our materials. For future endeavors, we would recommend making or designing some sort of machine that can test sliding motions for the materials with added weight pushing the materials together to get a somewhat realistic understanding of how the materials would perform while walking. We tried designing something with a wheel and arm bar, that way we could attach a rotary motor to the center of the wheel, then power the rotation that way. Then attach the arm bar to a peg on the wheel, so that as the wheel rotates, the arm bar slides back and forth with the rotations. As for adding some weight to put some friction on the materials, we thought about just anchoring a plate to the table, while the arm bar had weight on top of it pressing down on the materials. One material would then be attached to the underside of the arm bar, while the other would be fixed to the plate on the table, allowing the arm bar material to move freely with the arm bar, and still be weighed down by the weights and therefore add friction.

### 11.2.6 Surface Modifications

As mentioned in section 11.1.1, the surface texturing and modifications utilized in this project were extremely simple when compared to the methods that can be found in literature. This contrast was a result of many factors, however, the results of this year of testing definitively prove that surface texturing yields impressive increases in output voltage and is worth investigating further. Future projects should invest more time, money, and energy into pursuing this research. Groups should get certification training on the texturing machines present within Professor Rao's laboratory, conduct a more thorough study of both macro- and micro- surface texturing, and determine the most effective patterns for raising TENG efficiency. Additionally, teams may need to conduct additional rounds of material testing, as many types of surface texturing require specific material properties.

### 11.3 Final Remarks

Over the course of the 2023-2024 academic year at Worcester Polytechnic Institute, our group of engineers worked to progress the field of triboelectricity in conjunction with the U.S. Army Combat Capabilities Development Command for future use in the United States military. We explored possible options for energy harvesting using triboelectric nanogenerators such as implementing them into boots to harvest electrostatic energy, or placing them within parachutes or soft structures to harvest the mechanical energy offered by the wind. Triboelectricity has unlimited potential for use in not just the military, but in the search to find alternative energy sources. While this technology is new, there is still much research that needs to be done to fully understand triboelectricity.

## Bibliography

1. ADXL343BCCZ-RL7 Analog Devices Inc. | Sensors, transducers | digikey marketplace. (n.d.-a).  
<https://www.digikey.com/en/products/detail/analog-devices-inc/ADXL343BCCZ-RL7/3542894>
2. All About Circuits. (2018). Introduction to Diodes And Rectifiers | Diodes and Rectifiers | Electronics Textbook. Allaboutcircuits.com.  
<https://www.allaboutcircuits.com/textbook/semiconductors/chpt-3/introduction-to-diodes-and-rectifiers/>
3. *CWB 150*. Inventus Power. (2017).  
[https://inventuspower.com/wp-content/uploads/2017/10/Inventus-Power\\_CWB-150\\_Data-Sheet.pdf](https://inventuspower.com/wp-content/uploads/2017/10/Inventus-Power_CWB-150_Data-Sheet.pdf)
4. Diode bridge. (2023, December 18). In *Wikipedia*.  
[https://en.wikipedia.org/wiki/Diode\\_bridge](https://en.wikipedia.org/wiki/Diode_bridge)
5. *ECG sensor with ECG cable and electrodes AD8232*. indiamart.com. (n.d.).  
<https://www.indiamart.com/proddetail/ecg-sensor-with-ecg-cable-and-electrodes-ad8232-20592992848.html>
6. Eckstrom, J., Eller, F., Holohan, K., Honnavalli, Y., Shaw, E., & Silvia, J. (2023, September). Natick Soldier Systems Center Interview. Personal.
7. EDU34450A 5 1/2 digit digital multimeter user's guide (English, French, and Spanish) | keysight. (n.d.).  
<https://www.keysight.com/us/en/assets/9921-01392/user-manuals/EDU34450A-Digital-Multimeter-Users-Guide.pdf>
8. Empowering innovation | microchip technology. (n.d.-c).  
<https://ww1.microchip.com/downloads/aemDocuments/documents/APID/ProductDocuments/DataSheets/MCP1640-Family-Data-Sheet-DS20002234E.pdf>
9. Fan, F., Lin, L., Zhu, G., Wu, W., Zhang, R. and Wang, Z. *Transparent Triboelectric Nanogenerators and Self-Powered Pressure Sensors Based on Micropatterned Plastic Films*. Nano Letters 2012 12 (6), 3109-3114. DOI: 10.1021/nl300988z

10. Fagerholm, P., Hess, K., Kean, C., Postans, K., Woodruff, J. (2022). Energy harvesting for the U.S. Army. Digital WPI.
11. Ferrecchia, A., Hyers, K., MacPherson, K., Morissette, K. (2023). Boot Insole-Based Triboelectric Power Generation in Military Applications. Digital WPI.
12. File:SEG DVD 430 - Printed circuit board-4276.jpg. (2022, December 10). *Wikimedia Commons*. Retrieved 23:12, April 21, 2024 from [https://commons.wikimedia.org/w/index.php?title=File:SEG\\_DVD\\_430\\_-\\_Printed\\_circuit\\_board-4276.jpg&oldid=713872445](https://commons.wikimedia.org/w/index.php?title=File:SEG_DVD_430_-_Printed_circuit_board-4276.jpg&oldid=713872445).
13. Grove - UV sensor. (n.d.-d). [https://www.mouser.com/datasheet/2/744/Seeed\\_101020043-1217466.pdf](https://www.mouser.com/datasheet/2/744/Seeed_101020043-1217466.pdf)
14. *How does a piezoelectric generator work? – types and characteristics*. Components101. (n.d.). <https://components101.com/articles/how-does-a-piezoelectric-generator-works-types-and-characteristics>
15. KG, B. G. & Co. (n.d.). *Keysight DSOX1204A*. Batronix. <https://www.batronix.com/shop/oscilloscopes/Keysight-DSOX1204A.html>
16. Mao, Y., Zhang, N., Tang, Y., Wang, M., Chao, M., & Liang, E. (2017). A paper triboelectric nanogenerator for self-powered electronic systems. *Nanoscale*, 9(38), 14499–14505. <https://doi.org/10.1039/c7nr05222g>
17. McCutcheon, A., Nguyen, N., Scholz, E., Serven, R., Tess, S. (2021). Triboelectric energy generation. Digital WPI.
18. *Nett Warrior (NW)*. Program Executive Office Soldier. (2019). <https://www.peosoldier.army.mil/Equipment/Equipment-Portfolio/Project-Manager-Soldier-Warrior-Portfolio/Nett-Warrior/>
19. Niu, S., & Wang, Z. L. (2015). Theoretical Systems of Triboelectric nanogenerators. *Nano Energy*, 14, 161–192. <https://doi.org/10.1016/j.nanoen.2014.11.034>
20. PCB for celsius fast-response,  $\pm 0.1^{\circ}\text{C}$  temperature sensor. Blue Robotics. (2024b, April 24). <https://bluerobotics.com/store/sensors-cameras/sensors/celsius-sensor-pcb-r1/>
21. *Photonic Professional GT2*. Nanoscribe.com. (2022). <https://www.nanoscribe.com/en/products/photonic-professional-gt2/>

22. *Pixdro inkjet printing*. Inkjet Printing | SUSS MicroTec. (n.d.).  
<https://www.suss.com/en/products-solutions/inkjet-printing>
23. Rashwan, Ola. *Micro Surface Texturing for Friction Control*. (2013). Electronic Theses and Dissertations. 4869. <https://scholar.uwindsor.ca/etd/4869>
24. *Special operations soldiers test new parachute automatic activation device*.  
www.army.mil. (2022, April 5).  
[https://www.army.mil/article/255282/special\\_operations\\_soldiers\\_test\\_new\\_parachute\\_automatic\\_activation\\_device](https://www.army.mil/article/255282/special_operations_soldiers_test_new_parachute_automatic_activation_device)
25. *Squad Power Manager™ SPM-622*. Galvion. (2019).  
<https://www.galvion.com/products/squad-power-manager-spm-622>
26. Stew Smith, C. (2022, January 6). *Ask stew: What is a ruck?*. Military.com.  
<https://www.military.com/military-fitness/army-fitness-requirements/what-is-a-ruck-great-question>
27. Storen. (n.d.). *T8 extreme GTX regular: Winter military boots: Garmont tactical*.  
Garmont Tactical USA.  
<https://garmonttactical.com/product/21448647/t-8-extreme-gtx-regular>
28. Storr, W. (2022a, February 21). *Rectification of a single phase supply*. Basic Electronics Tutorials. <https://www.electronics-tutorials.ws/power/single-phase-rectification.html>
29. Swagatam. (2019, February 4). *How an accelerometer works*. Homemade Circuit Projects. <https://www.homemade-circuits.com/how-accelerometer-works/>
30. The four fundamental modes of the TENG. (a) the vertical... | download scientific diagram. (n.d.-e).  
[https://www.researchgate.net/figure/The-four-fundamental-modes-of-the-TENG-a-The-vertical-contact-separation-mode-b-The\\_fig1\\_300366751](https://www.researchgate.net/figure/The-four-fundamental-modes-of-the-TENG-a-The-vertical-contact-separation-mode-b-The_fig1_300366751)
31. Thomson, L. (2020, August 6). *Harvesting energy as you move: The Future of Wearable Technology*. AZoNano. <https://www.azonano.com/article.aspx?ArticleID=5536>
32. *Transformer simulation: Virtual testing for open and short circuits*. EMWorks Blog. (2024, April 21).  
<https://www.emworks.com/blog/transformers/transformer-simulation-perform-open-short-circuit-tests-easily-inside-solidworks>

33. *U.S. Army Multicam Molle II large rucksack W/ frame used.*

GRANDPOPSARMYNAVY. (n.d.-b).

<https://grandpopsarmynavy.com/products/u-s-army-multicam-molle-ii-large-rucksack-w-frame>

## Appendix A: Supplemental Material Testing Graphs

Below, a selection of graphs used to make the Figures of Chapter 6 are included. The Figures of Chapter 6 include the same information as the below graphs, but are condensed for brevity. The following graphs are included for clarification purposes.

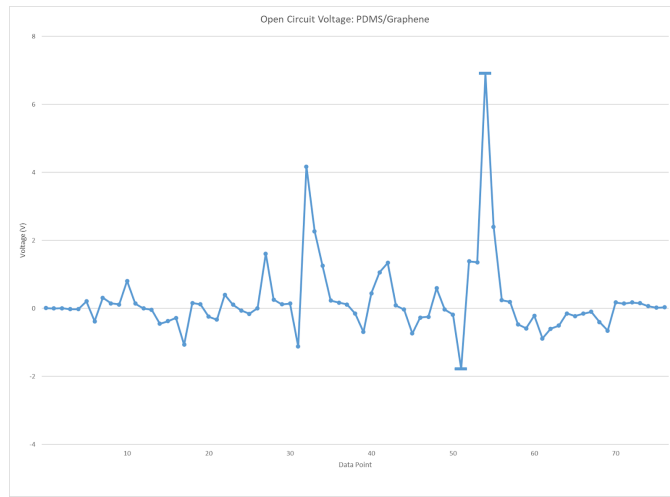


Figure A1. Graph showing the open circuit voltage of the TENG made from PDMS and graphene during the first round of testing.

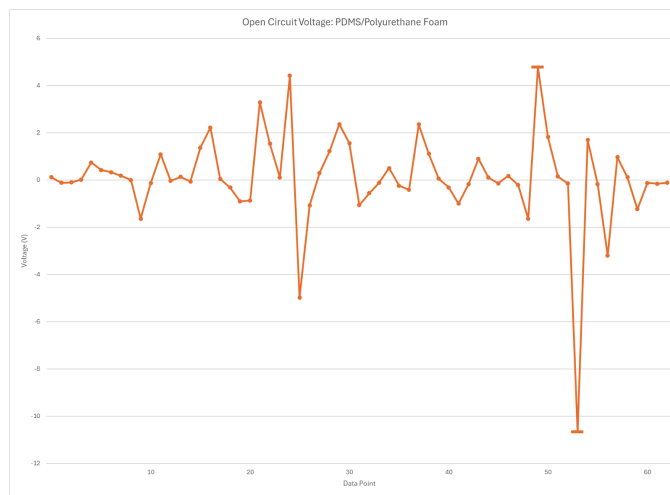


Figure A2. Graph showing the open circuit voltage of the TENG made from PDMS and polyurethane foam during the first round of testing.

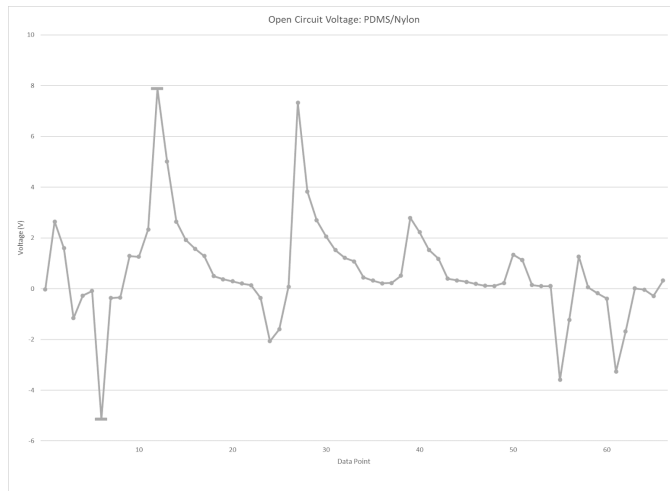


Figure A3. Graph showing the open circuit voltage of the TENG made from PDMS and nylon during the first round of testing.

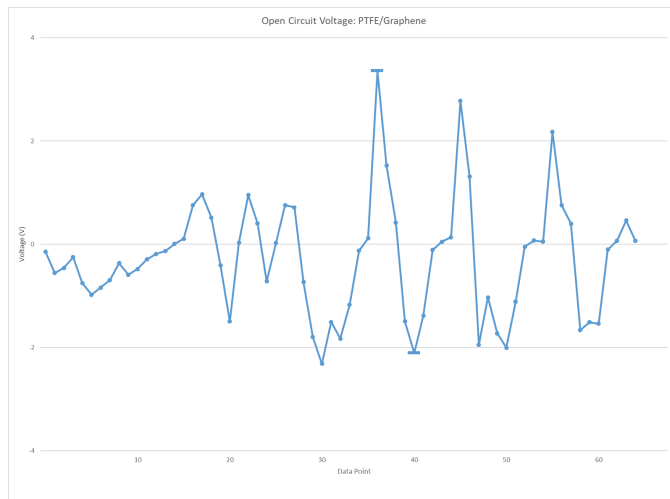


Figure A4. Graph showing the open circuit voltage of the TENG made from PTFE and graphene during the first round of testing.

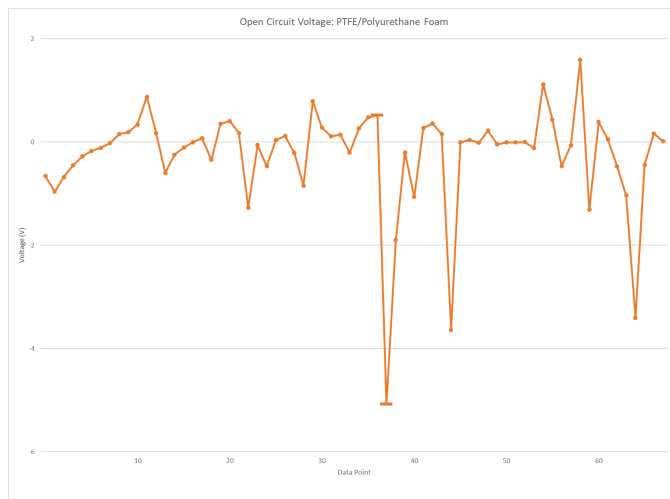


Figure A5. Graph showing the open circuit voltage of the TENG made from PTFE and polyurethane foam during the first round of testing.

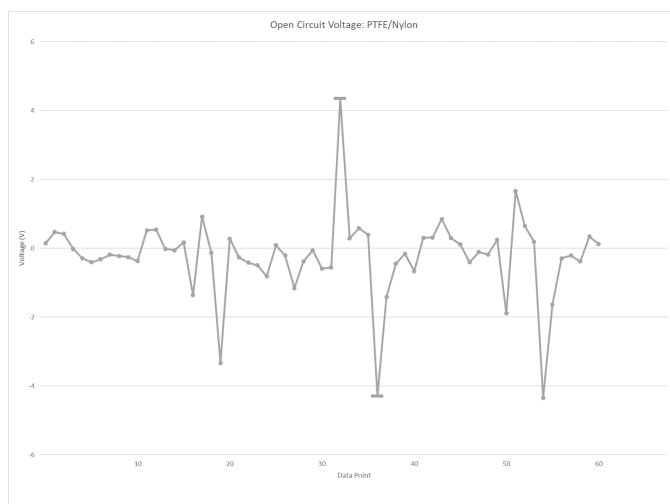


Figure A6. Graph showing the open circuit voltage of the TENG made from PTFE and nylon during the first round of testing.

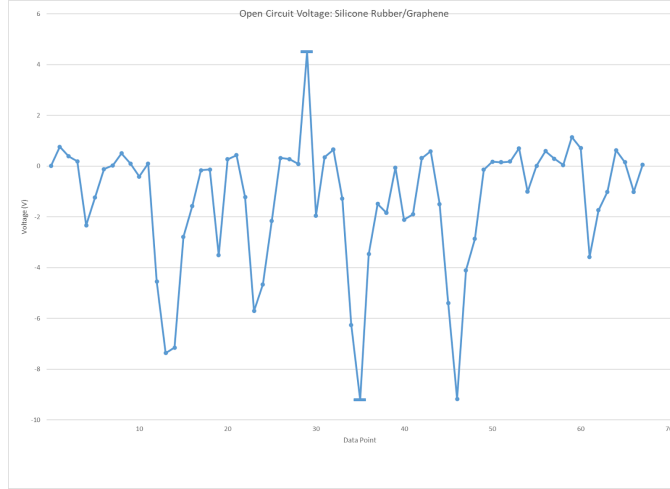


Figure A7. Graph showing the open circuit voltage of the TENG made from silicone rubber and graphene during the first round of testing.

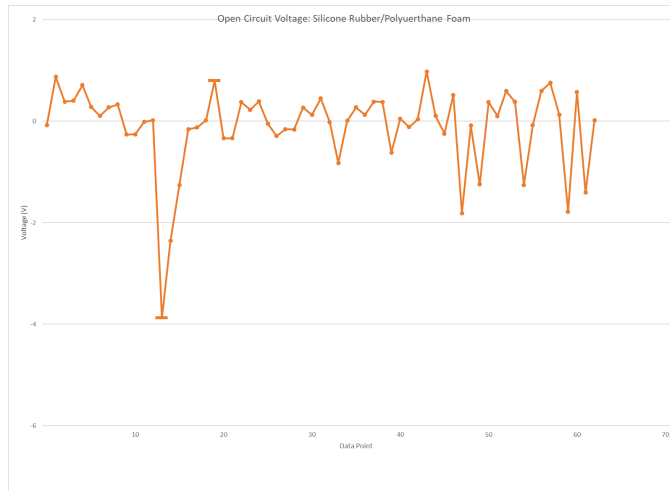


Figure A8. Graph showing the open circuit voltage of the TENG made from silicone rubber and polyurethane foam during the first round of testing.

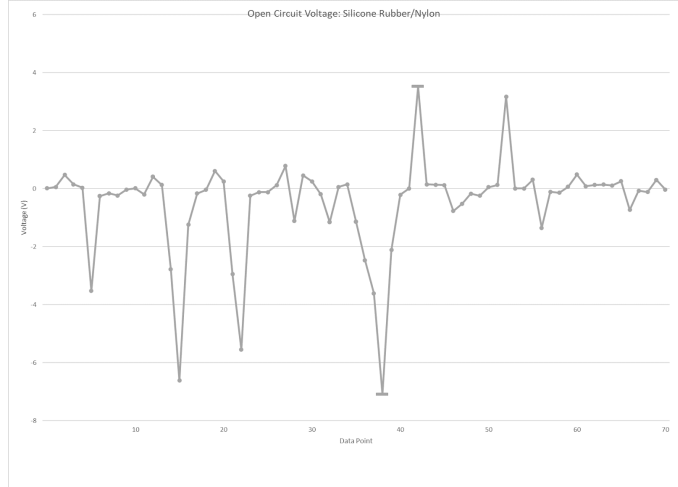


Figure A9. Graph showing the open circuit voltage of the TENG made from silicone rubber and nylon during the first round of testing.

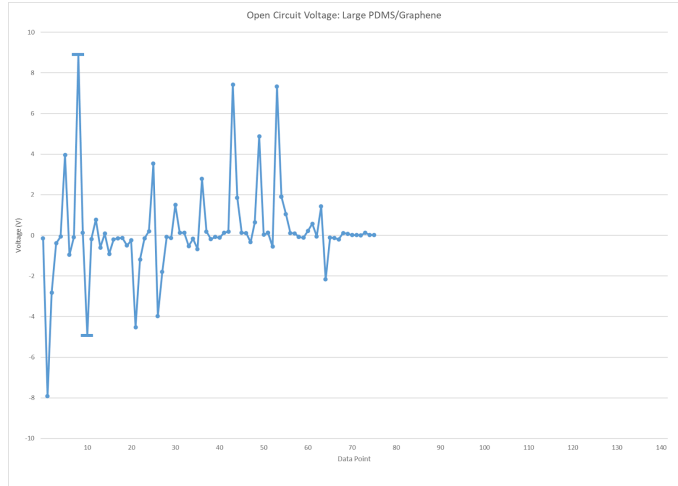


Figure A10. Graph showing the open circuit voltage of the TENG made from PDMS and graphene during the second round of testing.

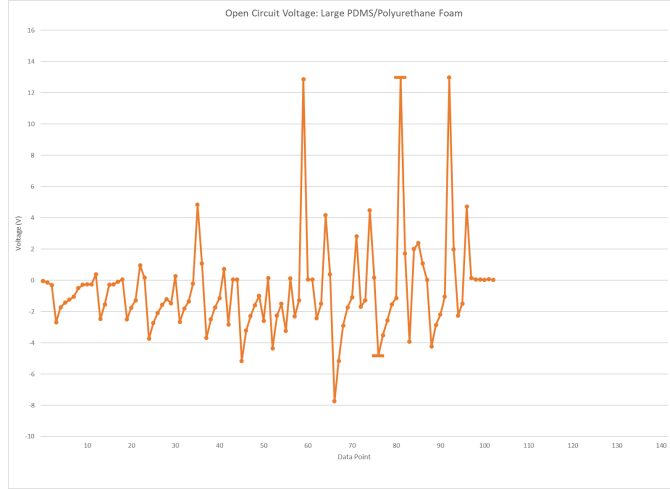


Figure A11. Graph showing the open circuit voltage of the TENG made from PDMS and polyurethane foam during the second round of testing.

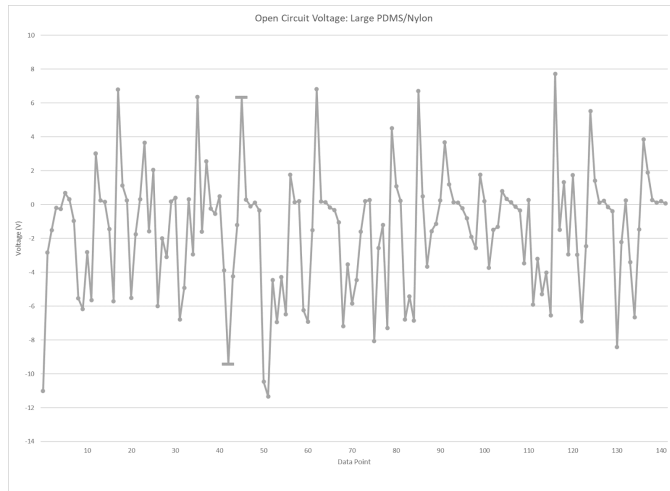


Figure A12. Graph showing the open circuit voltage of the TENG made from PDMS and nylon during the second round of testing.

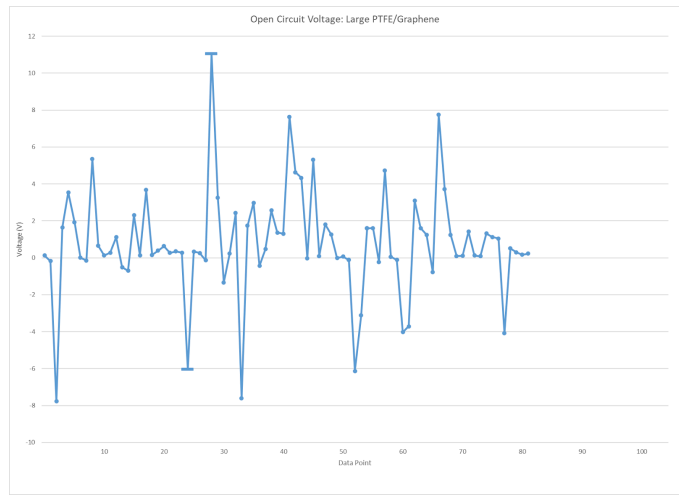


Figure A13. Graph showing the open circuit voltage of the TENG made from PTFE and graphene during the second round of testing.

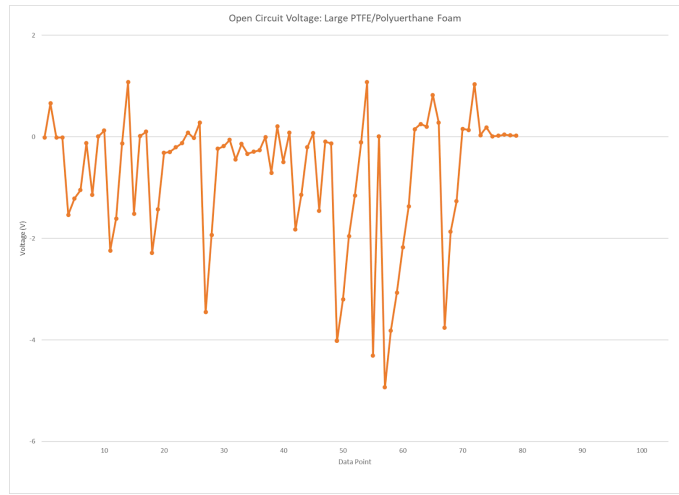


Figure A14. Graph showing the open circuit voltage of the TENG made from PTFE and polyurethane foam during the second round of testing.

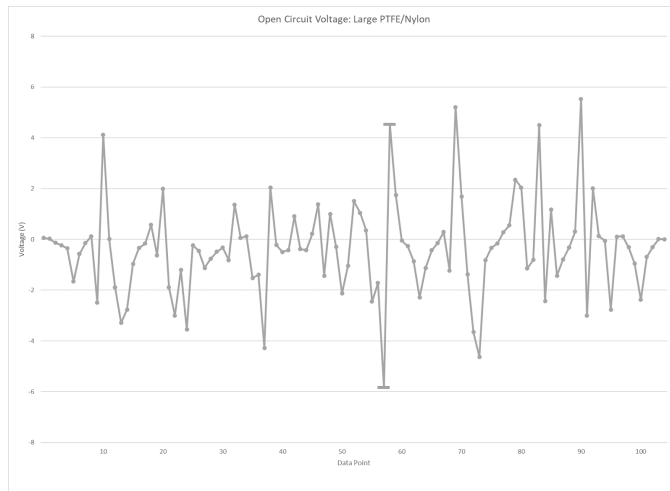


Figure A15. Graph showing the open circuit voltage of the TENG made from PTFE and nylon during the second round of testing.

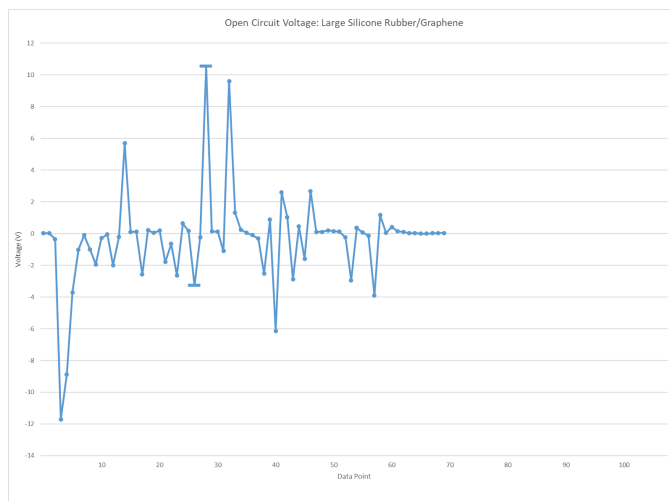


Figure A16. Graph showing the open circuit voltage of the TENG made from silicone rubber and graphene during the second round of testing.

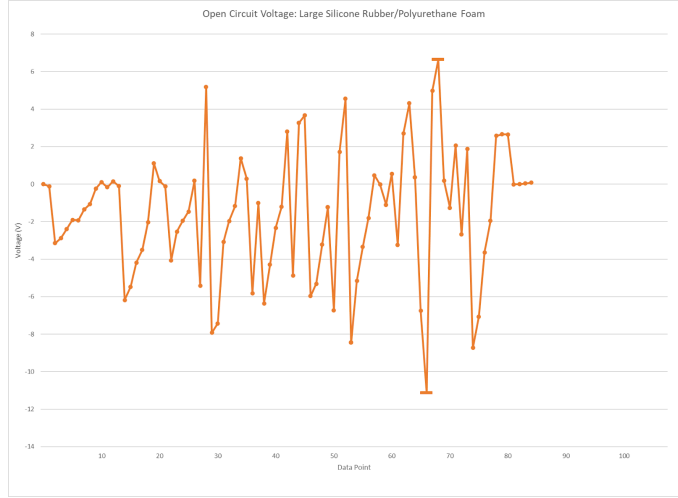


Figure A17. Graph showing the open circuit voltage of the TENG made from silicone rubber and polyurethane foam during the second round of testing.

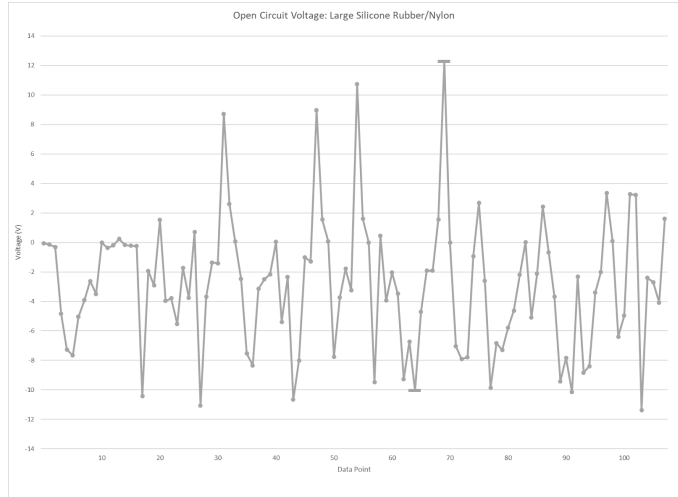


Figure A18. Graph showing the open circuit voltage of the TENG made from silicone rubber and nylon during the second round of testing.

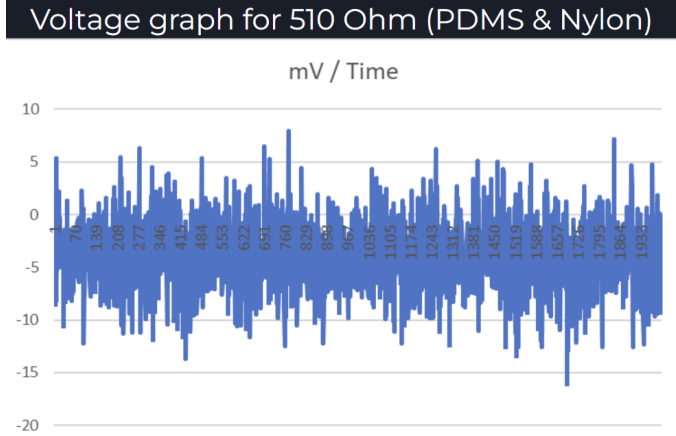


Figure A19. Voltage produced by a PDMS TENG at 510Ω resistance.

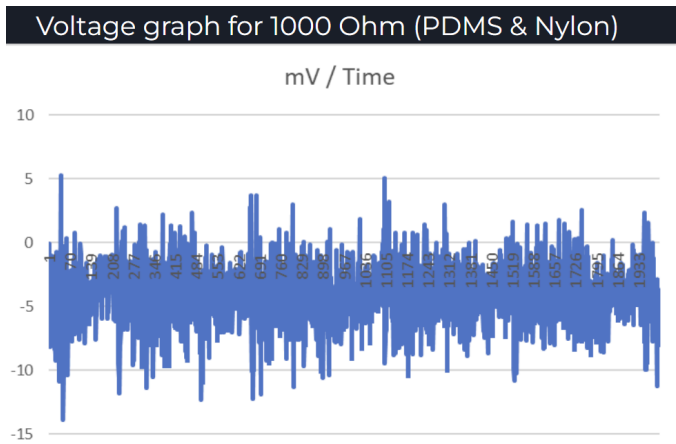


Figure A20. Voltage produced by a PDMS TENG at 1000Ω resistance.

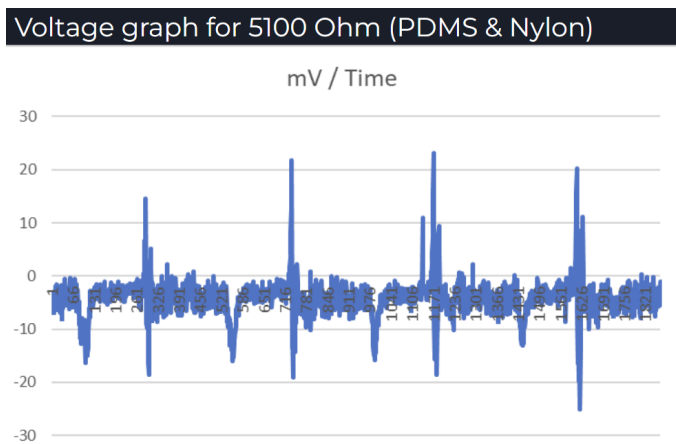


Figure A21. Voltage produced by a PDMS TENG at 5100Ω resistance.

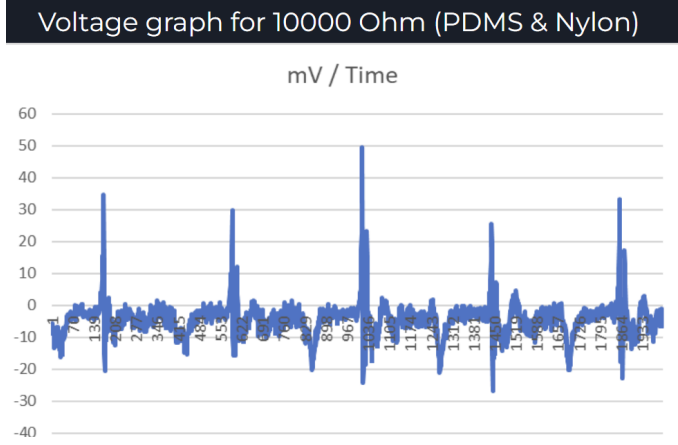


Figure A22. Voltage produced by a PDMS TENG at 10000Ω resistance.

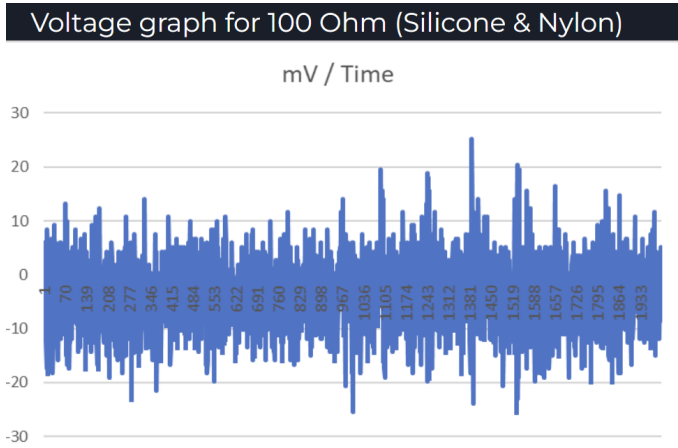


Figure A23. Voltage produced by a silicone rubber TENG at 100Ω resistance.

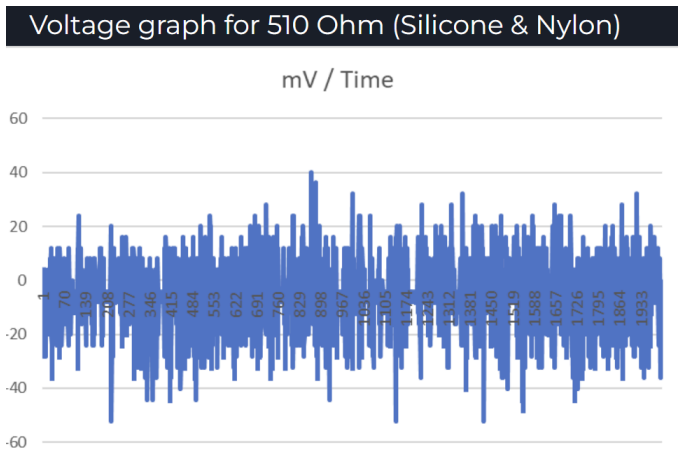


Figure A24. Voltage produced by a silicone rubber TENG at 510Ω resistance.

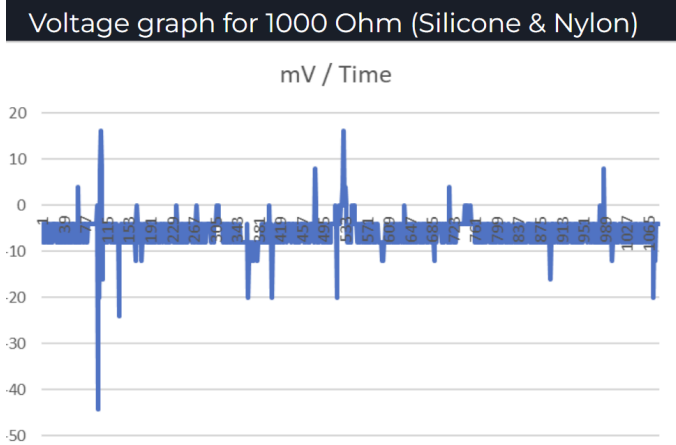


Figure A25. Voltage produced by a silicone rubber TENG at 1000Ω resistance.

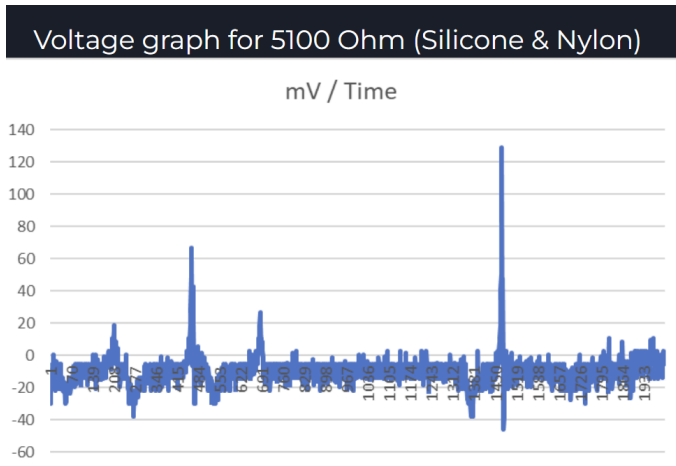


Figure A26. Voltage produced by a silicone rubber TENG at 5100Ω resistance.

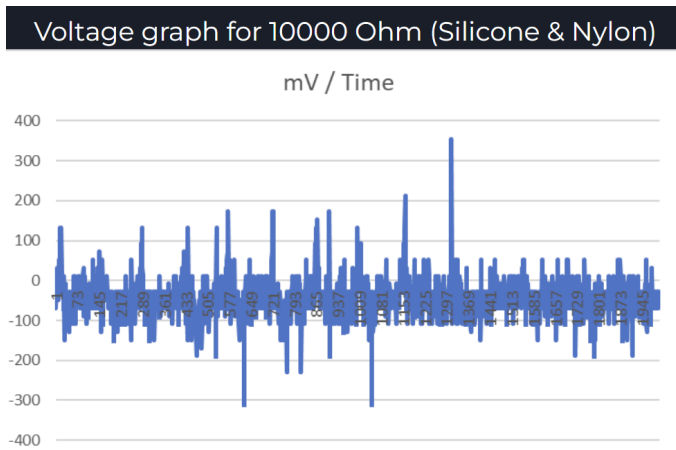


Figure A27 Voltage produced by a silicone rubber TENG at 10000 $\Omega$  resistance.